SURFACE WATER AND GROUNDWATER INTERACTION MECHANISM: PLAICHUMPHOL IRRIGATION PROJECT AS A STUDY AREA

Miss Pwint Phyu Aye

กลไกปฏิสัมพันธ์น้ำผิวดินกับน้ำใต้ดิน: พื้นที่ศึกษาในโครงการชลประทานพลายชุมพล

น.ส.พวิน พยู อาย

วิทยานิพนธ์นี้เป็นส่วนหนึ่งของการศึกษาตามหลักสูตรปริญญาวิศวกรรมศาสตรดุษฎีบัณฑิต
สาขาวิชาวิศวกรรมแหล่งน้ำ ภาควิชาวิศวกรรมแหล่งน้ำ
คณะวิศวกรรมศาสตร์ จุฬาลงกรณ์มหาวิทยาลัย
ปีการศึกษา 2561

Thesis Title	SURFACE WATER AND GROUNDWATER INTERACTION MECHANISM: PLAICHUMPHOL IRRIGATION PROJECT AS A STUDY AREA
By	Miss Pwint Phyu Aye
Field of Study	Water Resources Engineering
Thesis Advisor	Associate Professor SUCHARIT KOONTANAKULVONG, D.Eng.

Accepted by the Faculty of Engineering, Chulalongkorn University in Partial Fulfillment of the Requirement for the Doctor of Engineering

.... Dean of the Faculty of Engineering
(Associate Professor Supot Teachavorasinskun, D.Eng.)

DISSERTATION COMMITTEE

.... Chairman
(Associate Professor Tuantan Kitpaisalsakul, D.Eng.)

.... Thesis Advisor
(Associate Professor SUCHARIT KOONTANAKULVONG, D.Eng.)

.... Examiner
(Assistant Professor Sunthorn Pumjan, Ph.D.)

.... Examiner
(Assistant Professor Anurak Sriariyawat, Ph.D.)

.... Examiner
(Pongsak Suttinon, Ph.D.)

.... External Examiner
(Emeritus Professor Tawatchai Tingsanchali, D.Eng.)

จุฬาลงกรณ์มหาวิทยาลัย

CHULALONGKORN UNIVERSITY

พวิน พยู อาย : กลไกปฏิสัมพันธ์น้ำผิวดินกับน้ำใต้ดิน: พื้นที่ศึกษาในโครงการชลประทานพลายชุมพล. (SURFACE WATER AND GROUNDWATER INTERACTION MECHANISM: PLAICHUMPHOL IRRIGATION PROJECT AS A STUDY AREA) อ.ที่ปรึกษาหลัก : รศ. ดร.สุจริต คูณธนกุลวงศ์

โครงการชลประทานพลายชุมพลเป็นพื้นที่ชลประทานหนึ่งที่พึ่งพาทั้งน้ำชลประทานและน้ำบาดาลมานาน เกษตรกรในพื้นที่ทำการเกษตรทั้งปี น้ำบาดาลเป็นแหล่งน้ำสำรองที่สำคัญ โดยเฉพาะในช่วงหน้าแล้ง เป้าหมายของงานวิจัยนี้ต้องการทำความเข้าใจต่อกลไกปฏิสัมพันธ์ของการเติมน้ำสู่ชั้นน้ำบาดาลจากผิวดินและจากแม่น้ำและพารามิเตอร์ เพื่อวิเคราะห์กลไกการปฏิสัมพันธ์ระหว่างน้ำผิวดินและน้ำใต้ดินในการพัฒนาแบบจำลองน้ำบาดาลในพื้นที่

การศึกษาได้พัฒนาแบบจำลองน้ำใต้ดินทั้งระดับภูมิภาคและพื้นที่เพื่อตอบเป้าหมายดังกล่าวและทำการสอบเทียบแบบจำลองดังกล่าวโดยใช้ข้อมูลช่วงปี 1993-1997 และตรวจสอบจากข้อมูลช่วงปี 1998-2003 โดยเทียบกับระดับน้ำที่มีการวัด ซึ่งแสดงผลการจำลองของระดับน้ำใกล้เคียงกับข้อมูลวัด ค่าพารามิเตอร์ปฏิสัมพันธ์ทั้งจากผิวดินและแม่น้ำมีการวัดภาคสนามด้วยเซนเซอร์ความชื้นในดิน และค่าการซึมในแม่น้ำเพื่อประเมินอัตราการเติมน้ำจากผิวดิน และจากแม่น้ำ โปรแกรมไฮดรัส ๑ มิติ ถูกใช้เพื่อวิเคราะห์หาอัตราการซึมลึก และเครื่องวัดการซึมน้ำในแม่น้ำ ใช้วัดอัตราการซึมของน้ำแม่น้ำกับน้ำบาดาลตามแนวแม่น้ำ ค่าพารามิเตอร์ที่วัดได้ทำการเทียบกับค่าพารามิเตอร์ที่ได้จากการสอบเทียบจากแบบจำลองน้ำใต้ดินที่พัฒนาในพื้นที่

ปริมาณและรูปแบบของการปฏิสัมพันธ์ระหว่างน้ำผิวดินและน้ำใต้ดินได้จากการวิเคราะห์สมดุลน้ำจากแบบจำลองน้ำใต้ดินที่พัฒนาขึ้นในพื้นที่ และพบว่า น้ำบาดาลจากพื้นที่ต้นน้ำเป็นแหล่งน้ำไหลเข้าหลักในพื้นที่ศึกษาและมีปริมาณ ๑๓.๒ ล้านลบมต่อวัน ขณะที่น้ำบาดาลไหลออกจากพื้นที่ศึกษาทางท้ายน้ำมีปริมาณ ๔.๒๘ ล้านลบมต่อวัน การซึมของน้ำจากแม่น้ำเป็นแหล่งน้ำไหลเข้าอันดับสองและมีปริมาณ ๓.๑๕ ล้านลบมต่อวัน แต่การซึมของน้ำบาดาลสู่แม่น้ำสุทธิมีปริมาณ ๔.๒๘ ล้านลบมต่อวันโดยเฉลี่ย การเติมน้ำจากผิวดินสู่ชั้นน้ำบาดาลมีปริมาณ ๐.๒๕ ล้านลบมต่อวัน การไหลเติมจากแม่น้ำสู่ชั้นน้ำบาดาลเกิดขึ้นในพื้นที่ต้นน้ำมีปริมาณ ๒๓๘๕ ลบมต่อวัน และชั้นน้ำบาดาลออกสู่แม่น้ำในพื้นที่ปลายน้ำในปริมาณ ๑๔๕๓ ลบมต่อวัน โดยสรุปแหล่งเติมน้ำหลักของระบบน้ำบาดาลในพื้นที่ศึกษามาจากชั้นน้ำบาดาลในเขตต้นน้ำ และการเติมน้ำจากแม่น้ำ

เพื่อแก้ปัญหาขาดแคลนน้ำในพื้นที่ศึกษาในอนาคต ควรมีการจัดการน้ำบาดาลให้มีความเข้มข้นขึ้น เพื่อให้สามารถรักษาระดับน้ำบาดาลในระดับที่เหมาะสม ก่อนเข้าช่วงหน้าแล้ง

สาขาวิชา	วิศวกรรมแหล่งน้ำ	ลายมือชื่อนิสิต ....
ปีการศึกษา	2561	ลายมือชื่อ อ.ที่ปรึกษาหลัก ....

Pwint Phyu Aye : SURFACE WATER AND GROUNDWATER INTERACTION MECHANISM: PLAICHUMPHOL IRRIGATION PROJECT AS A STUDY AREA. Advisor: Assoc. Prof. SUCHARIT KOONTANAKULVONG, D.Eng.

The Plaichumphol Irrigation Project is an irrigation area which depends on both irrigation water and groundwater for long time. Farmers in that area have their cultivation almost whole year. Therefore groundwater supply is a major alternative source especially in dry periods. The aims of this study are to understand the interactions and parameters of land and river recharge, to analyse the surface water and the surface water and groundwater interaction mechanism via development of local groundwater model.

For this purpose, groundwater flow model (GMS) was used to develop regional and local groundwater models. The model was calibrated from 1993-1997 and verified from 1998-2003 using the peizometric heads observed. The results of showed that simulation values were closed with observed data. The proper interaction parameters: land and river were measured in the field using soil moisture sensor and seepage meter to investigate land recharge and estimate river conductance. HYDRUS-1D software package was used to analyse deep percolation rate and seepage meter was modified to measure the flow along the river. The values of these interaction parameters were used to check with the calibrated interaction parameters from the local groundwater model developed.

The interaction volume and patterns between surface water and groundwater were analysed from flow budget via developed local groundwater simulation. Groundwater flow from the upstream boundary area into the aquifer is the main input to the aquifer system with 13.2MCM/day and the downstream boundary outflow is about 4.18MCM/day. The river recharge to the aquifer is the second input and equals to 3.15MCM/day while the river gain is 4.28 MCM/day in average. Land recharge to the aquifer is 0.25MCM/day. The net of the aquifer recharge (river gain) to the river at upstream is 2,385m^3/day and river loss to the aquifer at downstream is 1,493m^3/day. The main sources of groundwater input are from upstream boundaries and river recharge.

To counter with water shortage in the area in the future, more intensive groundwater management is necessary to keep groundwater level at the appropriate level before the dry season.

Field of Study:	Water Resources Engineering	Student's Signature ....
Academic Year:	2018	Advisor's Signature ....

ACKNOWLEDGEMENTS

TABLE OF CONTENTS

LIST OF FIGURES

LIST OF TABLES

LIST OF ABBREVIATIONS

DGR	Department of Groundwater Resources
GMS	Groundwater Modelling System
GW	Groundwater
K	Hydraulic Conductivity
LGM	Local Groundwater Model
MCM	Million Cubic Meter
MSL	Mean Sea Level
PIP	Plaichumphol Irrigation Project
RGM	Regional Groundwater Model
RID	Royal Irrigation Department
S_c'	Specific Capacity
SW	Surface Water
T'	Transmissivity
UCP	Upper Central Plain
USGS	United States Geological Survey

CHAPTER I: INTRODUCTION

1.1 Background problem

In the last decades, water demand has increased due to the rapid development in the economy in Thailand. Thai people, farmers, normally used rain and flood water for their cultivation especially paddy. Upper Central Plain (UCP) was the important agricultural area of Thailand with potential groundwater sources. The groundwater resource had been used as a major source for rural domestic water and a supplementary source for agricultural use in this past 20 years due to the rise of rice price and the irrigation shortage in the dry season (from October to April) (Koontanakulvong and Panot (2003)). The local farmers replaced the groundwater to cultivate the crop, especially paddy to match with their requirements. Although a number of canals had been built in the Upper Central Plain, the canal cannot distribute an irrigation system. As there are many irrigation projects in Upper Central Plain which are not capable to provide a sufficient amount of water to farmers. They used groundwater about 715MCM/year for their agriculture (Suthidhummajit and Koontanakulvong (2017)). The groundwater usages grew up in speed and caused by the water scarcity from surface water distribution in these areas. It may cause impacts to groundwater resources and economic development in the future. Hence, there is a need to assess the groundwater interactions and groundwater potential in order to accomplish both surface water and groundwater properly.

Because of the spatial and temporal distribution of rainfall and insufficient water, at present, the water allocation for Plaichumphol Irrigation Project area PIP is based from the ratio of water storage from Bhumiphol and Sirikit Dams (called as two main dams) whether additional water could be made available reliance on the level of the dam storages. The local farmers used groundwater in PIP area 143MCM/year (74MCM in the dry season and 69MCM in the wet season (Bejranonda et al. (2008)). However, the amounts are not enough for their cultivation in this area. Thus, river interaction is an important issue for groundwater potential assessment and water allocation in this area.

1.2 Research significance

In the Upper Central Plain (UCP) area, the annual groundwater flow budget from the previous study was 1.237MCM/day from land recharge and 0.21MCM/day in river recharge. The river-aquifer interaction gave an average annual recharge of 337MCM resulting from the hydraulic properties of the river bed materials. Total inflow boundary is 587MCM/year derived from the available head distribution along the boundaries and the outflow is 56MCM/year. These flow numbers were used to improve regional groundwater model. Referred to the past study (Suthidhummajit and Koontanakulvong (2017)), the groundwater flow in the regional area is mostly affected by land recharge and river recharge, hence this study is focused on these two interaction parameters.

At present, water shortage is partially solved by using groundwater as supplementary in this study area. To use groundwater sustainability, groundwater system management needs more understanding of the interaction between surface water and groundwater reserve.

This study showed the role of interactions which help to understand more on the groundwater system and groundwater reserve in this area by patterns, volumes, locations. Both the groundwater model and field measurement were conducted to estimate the interaction parameters and simulate the groundwater system in finer grid size than the past study. By understanding groundwater reserve and groundwater balance, groundwater resources can be used appropriately, sustainably and helped to solve water shortage in the area.

1.3 Objectives of the study

The main objective of this study is to analyse the mechanism of surface water and groundwater interaction. The specific objectives are;

1. to understand the interactions of land recharge and river recharge in the regional area
2. to analyse the surface water and groundwater interaction parameters with groundwater model from field investigations

3. to analyse the interactions mechanism between groundwater and surface water in the Plaichumphol Irrigation Project (PIP) used as a study area with local groundwater model.

1.4 Scope of work

The scope of the study area is the Upper Central Plain (Regional area) and Plaichumphol Irrigation Project (local area) (see Chapter 3).

This study used groundwater flow model (GMS-MODFLOW) (see Appendix III) to simulate groundwater flow conditions in both regional and local areas during the period 1993-2003 and HYDRUS-1D was used to simulate the vertical deep percolation (see Appendix V) during April 2016 to February 2018 using field measurements for calibration and verification. Seepage meter was used to estimate river recharge analysis (see Appendix VI) and field measurement was done on 23-28 January 2018. Surface water and groundwater interaction mechanism was analysed from the groundwater flow budget and river interaction patterns in seasonal: rainy (April to September) and dry (October to March) and water year (drought, dry, normal, and wet) patterns from well calibrated/verified groundwater model simulation results. The detailed scope of study will discuss in Chapter IV, section 4.1.

1.5 Limitations

This study is based on primary and secondary data from past studies. The constants a and b are used from the empirical formula of Koontanakulvong and Panot (2003) to estimate hydraulic parameter distribution. The regional groundwater model was redeveloped from the previous study (Suthidhummajit and Koontanakulvong (2017)). Kriging method was used to interpolate the hydraulic conductivity for layer 1 while zoning method from the previous study was used for Layer 2. The calibrated observed water level and parameters from the regional model were used to develop the local groundwater model to estimate the interaction mechanism for Layer 1only. In local model development, parameters in layer 2 are fixed with no change due to the limited data and limited effect to the groundwater interaction. The field measurement data, land recharge and river recharge were used to check with the calibrated values from the developed local groundwater model.

1.6 Thesis content

This thesis is divided into six chapters. Chapter I describes the related problems facing in this study area, the significance of the research, the aim of this study, the scope of work and the detailed structure of research.

Chapter II presents a literature review on hydraulic parameter estimation, groundwater flow model (GMS), application of geostatistic method in groundwater modelling system, previous works in the study area (Upper Central Plain (Regional) and Plaichumphol Irrigation Project (Local)) to check consistency and continuity of existing studies and their results, groundwater and surface water interaction mainly focus on recharge parameter estimation such as land recharge and river recharge and finally considered the missing gaps from the literature review.

Chapter III provides a brief explanation of the study area conditions (both regional and local areas and primary and secondary) used in the study including geography, climate, hydrogeology, data used and site locations for field data measurements.

Chapter IV consists of research's design, including the study approach, study method used, and preliminary mathematical material which serves the purpose of setting up the framework for the study.

Chapter V presents the research's results including the regional groundwater model improvement in which hydraulic parameter was estimated via the geostatistical method and piezometric heads were applied in local groundwater model development. The goal of this study was to analyse the interaction mechanism between surface water and groundwater, especially recharge parameters. To do this, recharge parameters; land and river were measured in the field and checked the data with the model results and finally, the water budget was estimated from the local groundwater model by patterns, water years and locations (up, mid, down streams).

This study ends with Chapter VI summarizing the principal findings and outlines the research's more general contributions and concludes discussing the research's limitations and proposing future research.

CHAPTER II: LITERATURE REVIEWS

The goal of this chapter is to review the research concerned and to find the gaps and needs for research. The references from the literature review include parameter estimation, groundwater flow model, geostatistic methods application to groundwater MODFLOW model, Previous works in study area; both regional (Upper Central Plain, UCP) and local (Plaichumphol Irrigation Project, PIP), groundwater and surface water interactions, field measurements: land recharge analysis, soil moisture sensor and river recharge analysis by using seepage meter and river hydraulic conductivity.

2.1 Hydraulic parameter estimation

Many techniques are available to calculate transmissivity by using time-drawdown aquifer tests. There are numerous different approaches for estimating transmissivity from specific capacity such as analytical, semi-analytical, and empirical. The suitable technique for relating specific capacity to transmissivity depends on wells construction, pumping rates, and the accuracy of the applied technique (Taher (2018)). Several relationships between transmissivity and the specific capacity measured in the same well have been also established by several authors.

Logan (1964) studied aquifer hydraulic properties. In his study, transmissivity is determined from aquifer pumping test and specific capacity is calculated from the pumping rate divided by the change in water level. It normally has the units of m^3/h per meter of the drawdown. He mentioned that there was a generally good correlation between good performance and aquifer yield unless the well is inefficient and a great drawdown occurs than otherwise reflects the aquifer properties. It is beneficial to develop a relationship between specific capacity and transmissivity where no pumping test results exist. Transmissivity can be derived from the more abundant specific capacity information. The theoretical relationship between specific capacity and transmissivity is linear on a log scale. Some authors have also developed empirical or observed relationships between specific capacity and transmissivity (Driscoll (1986)).

Mace (2001) investigated an empirical and geostatistical approaches for transmissivity estimation from specific capacity. Richard et al. (2016) investigated the possibility and reliability of estimating the transmissivity using numerous available specific capacity data and compared with other existing relationships. The resulting of their empirical equation has a correlation coefficient of 0.66.

2.2 Groundwater flow model

Groundwater flow model, MODFLOW, is useful to predict aquifer response in terms of groundwater level (head) and groundwater fluxes into and out of an aquifer. Groundwater model derived from Darcy's law is used to calculate the rate and movement of groundwater through the aquifer (Freeze (1971)).

Roy et al. (2015) studied the impact on water flow fields due to deviations in river stage using groundwater modelling to assess the safe yield. Short and long period pumping test have been done at different sites. The suitable hydrogeological approaches were employed to estimate the values of aquifer parameters such as specific yield (Chulalongkorn (2010)), transmissivity (T) and hydraulic conductivity (K). They developed a hypothetical aquifer-stream water interaction system using GMS software. The results showed that a model represented hydraulic head variations which indicate how surface water could affect the groundwater system due to changes in the river stage.

Suthidhummajit and Koontanakulvong (2017) used MODFLOW to analyse the flow budget and conjunctive use pattern of surface water and groundwater mechanism under the climate change scenario in Upper Central Plain. Their study showed that the average land recharge was 0.9MCM in wet season and 0.01MCM in dry season. The river recharge was different from land recharge, and it renewed to the aquifer is 0.77MCM/day in the wet season but it received water from the aquifer is -1.54MCM/day in the dry season. The average groundwater pumpage of 2.0MCM/day was very high in the dry season. For these reasons, the average groundwater level reduced. However, the conjunctive use pattern in the future showed that the ratio of groundwater use decreases even the groundwater pumping increases. They concluded that the water use in the future depend more on new sources of surface water or need more demand side management measures.

Tuan and Koontanakulvong (2018) estimated the river conductance values along Saigon River, Vietnam to analyse the interaction between river recharge and groundwater reserve. Geostatistical tools in GMS were applied to simulate hydraulic conductivity distribution, conductance calibration, water balance, and river recharge. Recharge rate is used as an input data from rainfall. Their result for groundwater modelling, hydraulic conductivity estimation of riverbed can be applied for future groundwater modelling.

2.3 Geostatistical method application

Kitanidis and Vomvoris (1983) examined the inverse problem in groundwater modelling (steady state) and one-dimensional simulation from a geostatistical viewpoint. The estimated field is even, while small-scale variability is statistically defined. The quality of measurements improved, the procedure duplicates more features of the original field. The results showed to be rather unresponsive to deviations from assumptions about the geostatistical assembly of the field.

Hoeksema and Kitanidis (1984) approached the geostatistical method to estimate transmissivity from head and developed for two-dimensional steady flow. Their study illustrated the geostatistical approach can be a useful tool in the iterative advance. The results showed that the usefulness of piezometric head measurements in improving log-transmissivity estimates in regional aquifer studies depending on the accuracy on these measurements as well as the accuracy of the assumed model.

Long and Koontanakulvong (2017) analysed groundwater balance and river interaction in the Pleistocene aquifer of the Saigon River Basin, South of Vietnam by stable isotope analysis and groundwater modelling. They used land and river recharges as a combination of isotope analysis and groundwater modelling and estimated water balance for the groundwater model. Geostatistics was used to generate hydraulic conductivities. Precipitation, temperature and river stage data were used as input data. Their study showed that the river recharge rise with the same proportion of groundwater conception as a major role in groundwater balance.

2.4 Previous works in the regional area (Upper Central Plain, UCP)

Koontanakulvong and Panot (2003) used MODFLOW model to summarise the groundwater model methodology and determined the parameter applies to the

complex groundwater system with limited data constraint of the North part of Lower Central Plain, Thailand. The results showed that the calibrated model provided acceptable results with the error of 1-4m during 12-year records. The model also provided flow characteristics, water balance of inflow-outflow, recharge which can be used as a basic data for groundwater management planning in that area. However, they suggested that the more accurate model needs more reliable input parameters on both method and data estimation of the parameter is still required.

Bejranonda et al. (2006) used groundwater flow modelling, MODFLOW, to investigate the conjunctive use patterns of the surface and groundwater. The results showed that the conjunctive use pattern significantly varies with the surface water situation, season, aquifer characteristics and irrigation–rainfed area. According to their simulation results, they discussed for the groundwater level where the groundwater is abundantly extracted, the level would possibly let-down by about 10m in a drought year.

Bejranonda et al. (2007) investigated the conjunctive use patterns for different seasons by field surveys and groundwater flow modelling in the Upper Central Plain, using the MODFLOW model. Groundwater use is a main input parameter in that study as agricultural use, domestic use and industrial use. The estimated seasonal and long-term SW-GW balances showed the GW flow model as strong seasonal interaction of surface water and groundwater. Conjunctive use pattern significantly varies with the surface water situation, season, aquifer characteristics and irrigation-rained area.

Bejranonda et al. (2013) studied the dynamic interaction of surface water and groundwater as controlling tools for optimal conjunctive water use policies in the Central Plain, Thailand. A groundwater model was applied to understand the impact of the irrigation behaviour that determines the seasonal and multi-annual water availability in the irrigation area. The numerical results indicate the irrigation canals recharge to the aquifer during both the dry and wet season, small flows from the aquifer to the canals occur only during the wet season. Their analysis showed further that the groundwater potential in the conjunctive use pattern during periods of surface water shortage is not fully exploited by the farmers.

Suthidhummajit and Koontanakulvong (2017) developed the regional groundwater model with 10sq.km grid size to understand the impact of climate change in the Upper Central Plain. The aquifer was defined as a two-layer aquifer, where the depth varies between 40m-100m is upper, semi-confined layer and 100-300m is lower, confined layer. The western, eastern and northern boundaries of the groundwater model was defined as specific inflow boundaries (total 587 MCM/year) derived from the available head distribution along the boundaries which are an impermeable body of consolidated rock and were defined. The southern boundary was set as an outflow boundary. The land recharge rate was estimated based on the amount of rainfall and soil type of each area (7 soil types). The hydraulic conductivity and specific storage were estimated from pumping test data. The hydraulic conductivity in that area was in the range 0.5-200m/day. In his study, 143 wells data were used to compute the groundwater level and hydraulic conductivity was interpolated by zoning for both layer1 and layer 2. They suggested that the farmers are the main groundwater users in this region with 715MCM/year. The water inflow-outflow for the year 2003 illustrated that the total inflow amounts are 1.45MCM/day and outflow is 0.15MCM/day. The aquifer contributed an average 12% of the annual aquifer-recharge into the river (river gain) in the wet season, but is recharged from the rivers (river loss) in the dry season with 42% of the total recharge. The groundwater use pattern varies significantly with the water availability situation as farmers are attempting to compensate during drought years and an cumulative quantity of groundwater had to make up for the scarcity of surface water.

2.5 Previous works in the local area (Plaichumphol Irrigation Project, PIP)

Bejranonda et al. (2008) studied the interaction between streamflow and groundwater toward the conjunctive use management and focused on water use and allocation in the irrigation area by using groundwater flow model, MODFLOW, to determine the potential of conjunctive use. The model results showed that streamflow was an important source of recharge to maintain groundwater level beneath the cultivated area; therefore the farmers were able to access groundwater resources from their own wells. They suggested that the sustainable water allocation required the

combination of surface water and subsurface-water supply towards comprehensive management.

Koontanakulvong et al. (2014) studied the climate change impact on the irrigation system and farmers' response at Plaichumphol Irrigation Project. They focused on water shortage and groundwater pumping aspects in the designated dry year, i.e., period 1 type (1993-1995) or serious-serve-extreme year and period 2 types (1998-2000) or normal-serve-normal year. The simulation used the change in rainfall and temperature to evaluate the impacts on irrigation. In water condition as period type 1, water supply reduces in the wet season. Water demand rises in the dry season. Water shortage increases in the wet season and decrease in the dry season. Groundwater pumpage progresses in the wet season and slightly decrease in the dry season. In water condition as type 2, water supply will increase in the wet season and the dry season. Water demand increases in the wet and the dry season. Water shortage decreases in the wet and the dry season. Groundwater pumpage decreases in both wet and dry season. They suggested that farmers needed to alter to new paddy variety that uses less water, changes cropping pattern, modifies to flood-resist paddy variety, changes to other plants that consume less water.

Koontanakulvong and Suthidhummajit (2015) studied the role of groundwater to mitigate the drought and as an adaption to climate change in the Plaichumphol Irrigation Project, in the Nan Basin, Thailand to evaluate the effect on groundwater recharge and to determine the role of groundwater to mitigate the drought situation by applying MODFLOW and using the bias-corrected MRI-GCM data. They determined GW flow movement and recharge parameter to examine the relationship of recharge rate with climate condition (temperature) and assess the impact on GW recharge in this area. They found that the recharge decrease and GW level decrease in both near and far futures.

2.6 Groundwater and surface water interaction

Interaction between surface water and groundwater are complex (Sophocleous and Marios (2002)) and challenging to observe and measure (Winter (1998)). To understand these interactions in relation to climate, landform, geology, and biotic factors, a sound hydrogeological framework is required. Groundwater-river water

interaction has received a lot of attention in recent decades. Hydrogeologists and surface water hydrologists traditionally approached the interface between surface water and groundwater from their specific viewpoint. Winter and Rosenberry (1995) and Winter (1999) provided a related approach, concentrating on the hydrologic conditions related to various types of surface waters beds. Sophocleous and Marios (2002) summarized the fundamental concepts and suggestions of groundwater–river water from a hydraulic-hydrogeological viewpoint. Rosenberry and Labaugh (2008), as well as Kalbus et al. (2006), overviews the field techniques to estimate the fluxes between surface water and groundwater at different scales.

Sophocleous and Marios (2002) mentioned that the groundwater flow pattern is controlled by the water table and also the distribution of hydraulic conductivity in addition to topographic and geologic effects. Groundwater moves along flow paths that are organized in space and form a flow system which is affected by climate (precipitation being the source of recharge). Based on their relative position in space, Toth (1963) recognizes three distance types of flow systems: local, intermediate and regional which could be covered on one another within a groundwater basin. Water in a local flow system flows to a nearby discharge area, such as a pond or stream. Water in a regional flow system explorations a more distance than the local flow system and often releases to the major rivers, large lakes or to oceans. A middle flow system is characterized by one or more topographic highs and lows located between its recharge and discharge area.

Kalbus et al. (2006) reviewed the measuring methods for surface water and groundwater interactions to provide an outline of the methods that are the current state of the art for measuring interactions between SW-GW. They focused on the estimation of water fluxes at the river-aquifer interface. They grouped the methods into (1) direct measurements of water flux; (2) heat tracer methods; (3) methods based on Darcy's Law; and (4) mass balance approaches due to the investigations of interactions between GW-SW have various backgrounds in the different disciplines of hydrology. They defined the various attitudes and techniques to measure the interaction between SW-GW with their limitations and uncertainties. A multi-scale approach combining multiple techniques can considerably reduce uncertainties and constrain estimates of fluxes between groundwater and surface water.

Baskaran et al. (2009) investigated the groundwater-river interactions using environment tracers to know the stream-aquifer connectivity in the river catchment. to better understand groundwater-surface water interactions in the catchment. Their study showed that recharge of the alluvial aquifers by surface water occurs by bank infiltration, with diffuse recharge during high rainfall events more dominant farther away from the river.

Brunner et al. (2010) focused on the effect of conceptual assumptions on the simulation of the interaction between losing streams and groundwater using MODFLOW. They mainly point out the relevant for gaining streams. The results showed that (1) Neglecting negative pressure gradients mains to an under estimation of the infiltration flux; (2) because river are assigned to only one grid cell, the infiltration flux under a river is uniform while in reality, this is only true for disconnected systems; (3) the size of the single grid cell a river is assigned to influences the infiltration flux; and (4) the vertical discretization of the aquifer affects the infiltration flux.

2.6.1 Land recharge analysis

Several techniques are accessible to analyse recharge, however, selecting appropriate techniques is often difficult. The goal of the recharge study is important because it may require space/time scales of the recharge estimate. Techniques based on surface water and unsaturated zone data provided estimation of potential recharge, whereas based on groundwater data generally estimates of actual recharge (Scanlon et al. (2002)).

Soil water balance model has been applied to evaluate drainage for the paddy field since 1960 (Baier and Robertson (1966), Baier (1972), Reddy (1983)). The soil moisture change was measured by the gravimetric technique, electrical-resistance, heat-diffusion, absorption, tension-metric, penetration, radioactive. The disadvantage of the method is required a lot of data for calibration and verification in spatial and time (Kumar (1997), Simmers (2013)).

Numerous researchers have applied successful zero flux plane method to estimate the groundwater recharge (Wellings (1984), Cooper et al. (1990), Tsujimura et al. (2001), Khalil et al. (2003), Khalil et al. (2006)). However, the method

unsuccessful to estimate the soil water during periods when rainfall exceeds saturated hydraulic conductivity. Moreover, this method requires the experimental determination of the unsaturated hydraulic conductivity-moisture content relationship which consumes a lot of field data in a regional scale.

One-dimensional soil water flow model has often used to predict the water flux through the unsaturated zone; such as UNSAT-H (Fayer and Jones (1990)) and HYDRUS Simunek et al. (2005) have been widely adopted to predict recharge estimates using the basis of Richards' Equation. This models were applied successfully to evaluate coefficients of groundwater recharge by the precipitation (Yeh et al. (2007)), estimate average mean annual groundwater recharge (Cao (2011)), analysis the impact of different thickness and lithology of vadose zone to groundwater recharge (Liu et al. (2011)).

Groundwater level fluctuation method is ease to use. The disadvantage is one well cannot be representative for the whole basin. The method cannot interpret for a steady rate of recharge and difficulties relate to identify the cause of water level fluctuations and calculate a value for specific yield (Johansson (1988)).

A hybrid water fluctuation approached to recharge estimation (Sophocleous and Marios (1991)) by associating water table with specific precipitation events and by combining the recharge estimates from the soil water balance analysis with the resulting water table rises. One can achieve reliable effective storativity values for each recharge study site. The site-calibrated effective storativity value can be used to translate each major water table rise into a corresponding amount of groundwater recharge. The method is reliable for estimating natural groundwater recharge in relatively flat areas with a shallow water table (< 10m).

The tracers can be precisely identified in very low amounts and concentrations which do not disturb the hydrologic system under investigation (Moser and Rauert (2005)). Numerous of researches showed that the advantage of radioactive in groundwater recharge investigation such as identify leak zone in reservoir (Guizerix (1983)), evaluate the meltwater infiltrated to the soil and discharge to stream channels (Dincer et al. (1970)), date groundwater with residence times (Vogel et al. (1970)), restrict and measure the seepage flow in dams (Drost (1989)). As simple detection in the borehole, short half-lives (five years ages), and no sorption, the environmental

nuclides methods are useful in application for a direct measurement of the water movement in the unsaturated zone and thereby of the groundwater recharge rate (Sharma and Gupta (1985), Seiler (1998), Moser and Rauert (2005)). However, this technique shows some promise for problems of mixing of water of different origins. The survey work is necessary to evaluate the phenomena with the usefulness of a radioactive tracer (Aggarwal et al. (2005)).

In summary, soil water balance method is facing a difficult task in runoff and evapotranspiration in a regional scale. Zero flux plane method is a challenge on determine zero flux plane depth under saturated condition. Hybrid water fluctuation method and groundwater level fluctuation method is facing special storage and steady recharge estimation. Chemical and radio method get problems of mixing of water of different origins, they can use an evaluation process under clear the mechanism of groundwater recharge. One-dimensional soil water flow model is the popular method to estimate land recharge in the point scale.

2.6.1.1 Soil moisture

Soil moisture is a significant parameter in the atmospheric water cycle of land and atmosphere interaction (Raju (2017)). Lu et al. (2010) estimated the groundwater recharge to investigate the effects of irrigation and water table depth on groundwater recharge. A one-dimensional unsaturated flow model (HYDRUS-1D) was used to calibrate field data of climate, soil moisture, and groundwater level. They founded that a weakness of unsaturated flow modelling was the need for long-term data about climate, irrigation practices, and soil physical parameters.

Kojima et al. (2016) developed a low-cost soil moisture profile probe using thin-film capacitors and a capacitive touch integrated circuit. The developed sensor captured dynamic changes in soil moisture at a different depth, with a period required after sensor installation for the contact between capacitors and soil to down. The results showed that the influence of the individual sensor differences, however, the developed sensor could detect large differences and the different magnitude of changes in soil moisture. They suggested that the advanced sensor made more reasonable to farmers as it requires low financial investment and it can be utilized for decision making in irrigation.

Li et al. (2017) studied the modelling of soil water management and water balance in a relocated rice field experiment with reduced irrigation and evaluated using HYDRUS-1D model. Measured and simulated results indicated that water percolation was the main track of water losses from the transplanted paddy fields, and recommended that long and high standing water increased water percolation.

2.6.1.2 Deep percolation

Deep percolation is the flow of soil moisture by gravity below the effect of the root zone. It is an important factor in the filling of groundwater and scheme of surface drainage. There are two methods available for estimation or measuring the deep percolation: 1) the water balance method and 2) method of concurrent measurement of moisture and soil suction at various depths.

Water balance method is the measurement of soil humidity at the root region, evaporation and transpiration and also measurement of rain and irrigation depth. Several people estimated the deep percolation using the water balance method (Phillips (2007), Kaveh et al. (2015), Allison et al. (1994)).

To estimate groundwater recharge, deep percolation must be monitored below the root zone where it would be constant (Slavich et al. (1995)). Percolation could be estimated below the root zone to extend form 0-0.8m. Estimated deep percolation were obtained at a depth of 2.0m using the water balance and chloride mass balance modelling methods since water content and chloride data were collected to this depth.

Willis et al. (1997) estimated deep percolation under irrigation on two soils to assume groundwater recharge. They used three methods; (1) water balance; (2) Darcy flux calculations; and (3) chloride mass balance modelling. The results of the water balance designated that deep percolation extreme in the growing season, following initial wetting of the soil, when the crop had a low leaf area index. Results using Darcian flux equations were highly variable and unreliable to estimate deep percolation. The chloride mass balance model was used to estimate the magnitude of potential annual groundwater rise and reliable for estimation of deep percolation and thus groundwater recharge can be obtained using either the water balance or chloride mass balance techniques. Slavich et al. (1990) also described that the results

calculated using a water balance closely approved with those calculated using a chloride mass balance model.

2.6.2 River recharge analysis

Groundwater recharge shows major spatial and temporal variability as a significance of variations in climatic situations, land use, irrigation and hydrogeological heterogeneity (Arnold et al. (2000)).

An increasing rate of exchange between streams and groundwater has led to the use of seepage meters in stream channels (Murdoch and Kelly (2003)) However, the data obtained are often extremely variable because the original design and application were intended for lake and estuary environments, where issues of current and scour are generally insignificant.

2.6.2.1 Seepage meter

Measurements of groundwater seepage rates into surface water bodies are constructed using manual "seepage meter". Lee and Robert (1947) designed a seepage meter consisting of one close of 55-gaon (208 liters) steel drum that is close-fitting with a sample of the container and a plastic collection bag. The drum forms a hollow which is inserted open end down into the sediment-water seeping through the sediment will transfer water trapped in the chamber forcing it up through the port into the top plastic bag. The variation of water volume in the bag over a measured time interval provides the fluctuation. A seepage meter involves a container that is pressed into the bottom of the stream or river. Attached to the cylinder is a reservoir of water; the rate at which water within the cylinder enters is determined by changes in reservoir volume. This method is inexpensive and easy to apply (Scanlon et al. (2002)).

Lee et al. (1978) described the use of two simple inexpensive devices that enable students to measure the flow of groundwater and to demonstrate for themselves some of the basic principles of hydrogeology. The devices are known as the tiny piezometer and the seepage meter. Seepage meters and small piezometers are inserted in the sediment of shallow areas in the streams, a few hours; the devices can be mounted, monitored, and removed. Information on the direction and rate of groundwater flow can be achieved.

Hatch et al. (2006) determined streambed seepage rates using time series thermal data based on quantifying changes in phase and amplitude of temperature variations between pairs of subsurface sensors. In their study, they used heat as a seepage tracer. The benefits of using heat as a tracer in groundwater systems have been recognized for decades and there is particular interest in applying thermal methods to assess SW-GW interactions. Seepage meters have reached the following general conclusions (Taniguchi et al. (2002)): 1) many seepage meters are desired because of the natural spatial and temporal variability of seepage flow rates (Shaw and Prepas (1990a;b)). 2) the resistance of the flow tube (Fellows and Brezonik (1980)) and bag (Shaw and Prepas (1989), Belanger and Montgomery (1992)) should be minimized to the degree of the possible to prevent artifacts; 3) use of a cover for the collection bag may reduce the effect of surface water movement due to waves, currents or streamflow activity (Libelo and Macintyre (1994)); and 4) a seepage meter detection limit should be applied (Cable et al. (1997)).

2.6.2.2 River hydraulic conductivity

Song et al. (2009) determined the vertical hydraulic conductivity of riverbed using the grain-size analysis methods which is important in the analysis of water quantity exchange and solute transfer between a stream and its sediments. They used empirical methods to calculate the K value of streambed from grain-size distribution data of sediments. They suggested the K value from grain-size distribution derives from the formula (Shepherd (1989)) for channel sediments are close to vertical K. Streambed sediments can be hypothesized that smaller conductance values must be used in the estimation of vertical K for general soil samples.

Cousquer et al. (2017) estimate river conductance to improve surface-subsurface model calibration. They used head-dependent flux boundary condition to know the flow from stream to aquifer with a river conductance. The river conductance was estimated from physical parameters and measured in the field. Parameters are taken into account: (1) the anisotropy of the aquifer hydraulic conductivity; (2) the size of river cells in the regional model grid. The global sensitivity analysis highlighted the importance of parameters and justified their consideration.

2.7 Summary of literature review

In summary, most of the prior research in this study area focused on the groundwater conjunctive use and groundwater management for climate change.

In the previous, hydraulic parameter (hydraulic conductivity) was estimated from pumping test data by zoning for both layers 1 and 2 with 10sq.km grid size. The model should be redeveloped with smaller grid size (2sq.km) to simulate river interaction better and used the more well data (259) to be smooth and interpolated the piezometric head for layer 1 via geostatistic method for each point to be smooth for each grid. The improved groundwater levels can then be used as a boundary condition to develop local groundwater model accuracy.

Based on the review, recharge parameters (land and river) estimation were focused to complete the goal of this research in order to determine the interaction mechanism. For this purpose, the field measurement on interaction parameters including soil moisture sensor applications and seepage meter measurement were needed to be conducted and checked with the local groundwater model's results. Then the flow budget can be estimated from the local groundwater model to determine the interaction between surface water and groundwater. Finally, the surface water and groundwater interaction mechanism can then be determined via patterns/water year/locations and recommended for groundwater management and local people.

CHAPTER III: STUDY AREA

Interactions between surface water and groundwater have a significant impact on the water quantity and quality of the hydrological zones. Groundwater and land recharge rates are also controlled by piezometric heads from the regional groundwater flow system. This study used the regional area (Upper Central Plain) and the local area (Plaichumphol Irrigation Project, PIP) to understand flow budget and groundwater and surface water interaction mechanism. This chapter describes first hydrological factors such as area conditions, climate, topography, hydrogeology and also groundwater utilization in the study areas and second describes the field measurements area and conditions.

3.1 General conditions of the study area

In this study, the regional area (Upper Central Plain, UCP) and the local area (Plaichumphol Irrigation Project, PIP) were used as a study area to investigate the interaction mechanism between surface water and groundwater. The regional area was used to improve regional groundwater model by parameter estimation, and these model results are used as boundary conditions for the local groundwater model with smaller grid size. Plaichumphol Irrigation Project was used to develop the local groundwater model to estimate interaction parameters (land recharge and river recharge) and to analysis interaction mechanism from model results.

3.1.1 Regional area (Upper Central Plain, UCP)

The regional study area, Upper Central Plain, means Northern part of Chao Phraya Plain, covering the areas of Uttaradit, Sukhothai, Phitsanulok, Kampangphet, Pichit, and Nakornsawan Provinces as shown in Figure 3.1. It is composed of five basins that are Lower Ping Basin, Lower Yom Basin, Lower Nan Basin, Upper Sa-Gae-Grang Basin, and Upper Chao Phraya Basin Bejranonda et al. (2006). Total area coverage is 48,000km^2 (29,991,700 rais). There are two main rivers namely, the Yom and the Nan rivers which flow parallel from North to South and join at Ban Gei Chai, Amphor Chumsang, Nakornsawan province. In addition, there is Ping River which flows from west side of the area and joins with the Yom and Nan rivers at Amphor

Paknampho, Nakornsawan province. They become the Chao Phraya River which continuously flows to the Central Plain.
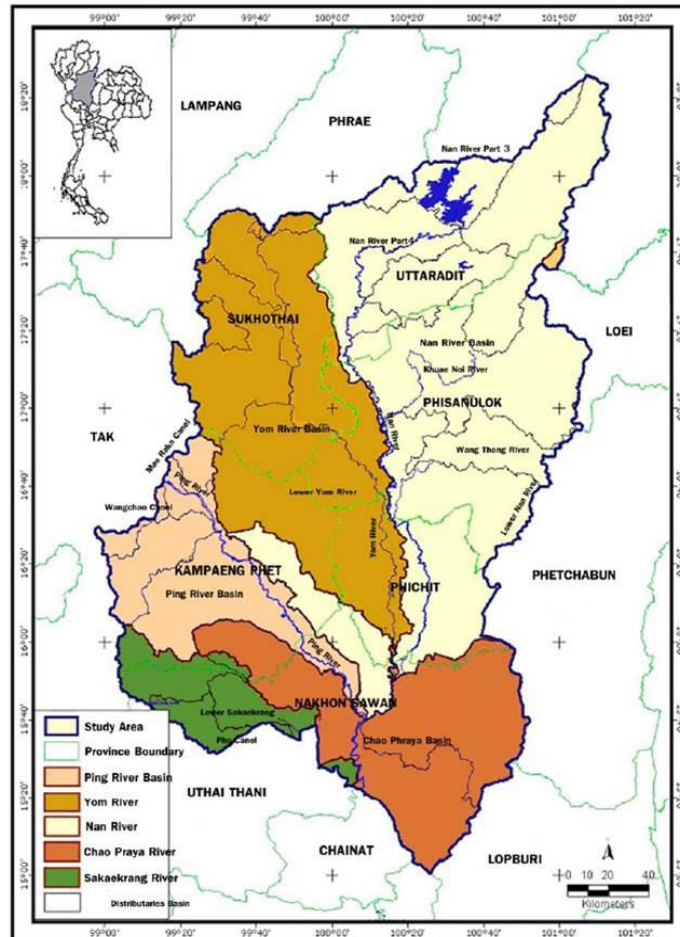
Figure 3.1 Upper Central Plain (Regional area)

3.1.2 Local area (Plaichumphol Irrigation Project, PIP)

The local study area, Plaichumphol Irrigation Project (PIP), is situated in the lower northern region of Thailand, approximately 400 km away from Bangkok. The total project area is 273,000 rai (436km^2) and irrigation areas of 211,476 rai (338km^2). The boundary of the study area, Plaichumphol Irrigation Project, is shown in Figure 3.2. The main rivers in the study area are the Yom River in the west and the Nan River in the east which are parallel flow from North to South.
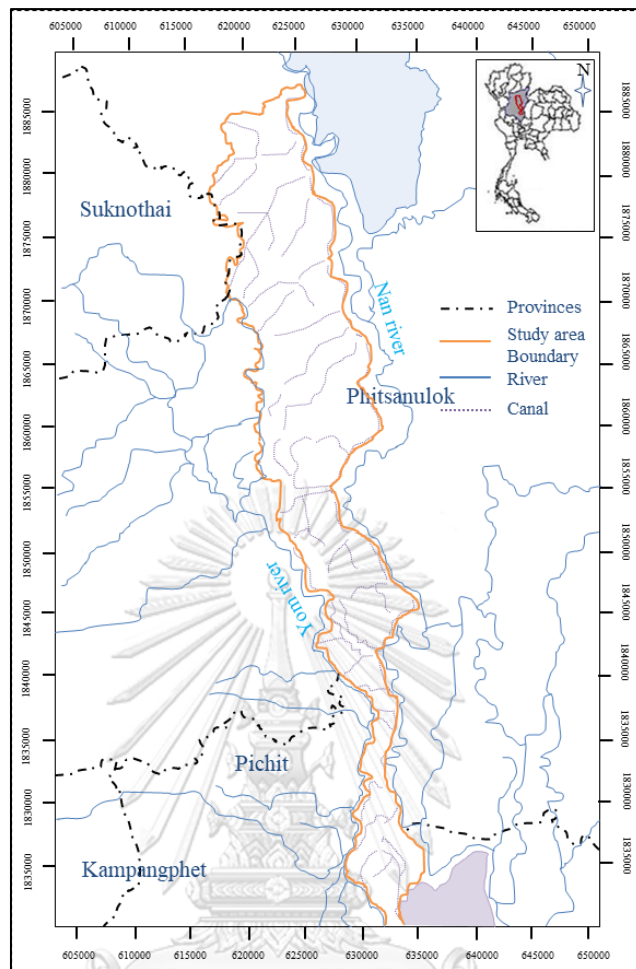
Figure 3.2 Plaichumphol Irrigation Project (Local area)

3.2 Topography

The boundary of the Upper Central Plain, UCP covers the areas of Uttaradit, Sukhothai, Phitsanulok, Kampangphet, Pichit and Nakornsawan Provinces. The average height is approximately 40-60 meters above mean sea level (MSL). The areas consist of sediments which were changed from erosion and decay of rock, then accumulated and generate as plain, terrace and swamp as shown in Figure 3.3. According to geographic conditions, the upper half and middle part of Plaichumphol Irrigation Project, PIP is the highland, where the eastern and north-eastern parts are tables consisting of high mountains and fertile alluvial valley as shown in Figure 3.4. The lower half is Yom and Nan river basins. The area consists of solid rocks which include sedimentary, metamorphic and igneous rocks of various ages.
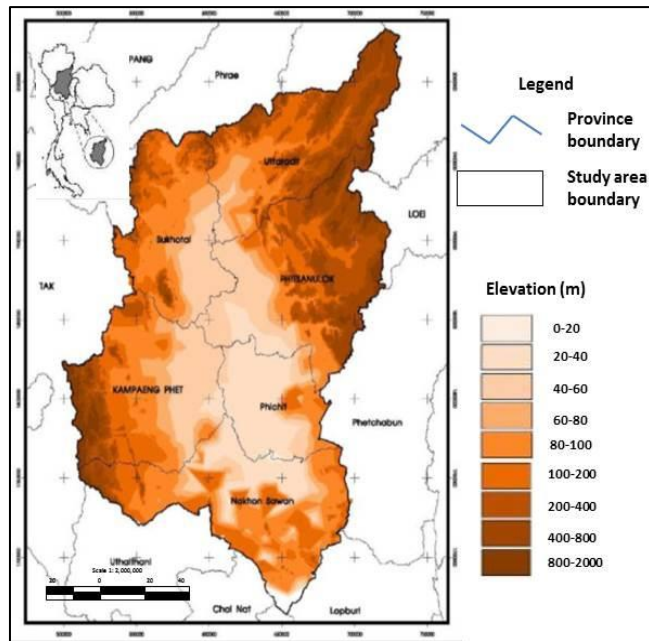
Figure 3.3 Topography and boundary of the Upper Central Plain (Regional)
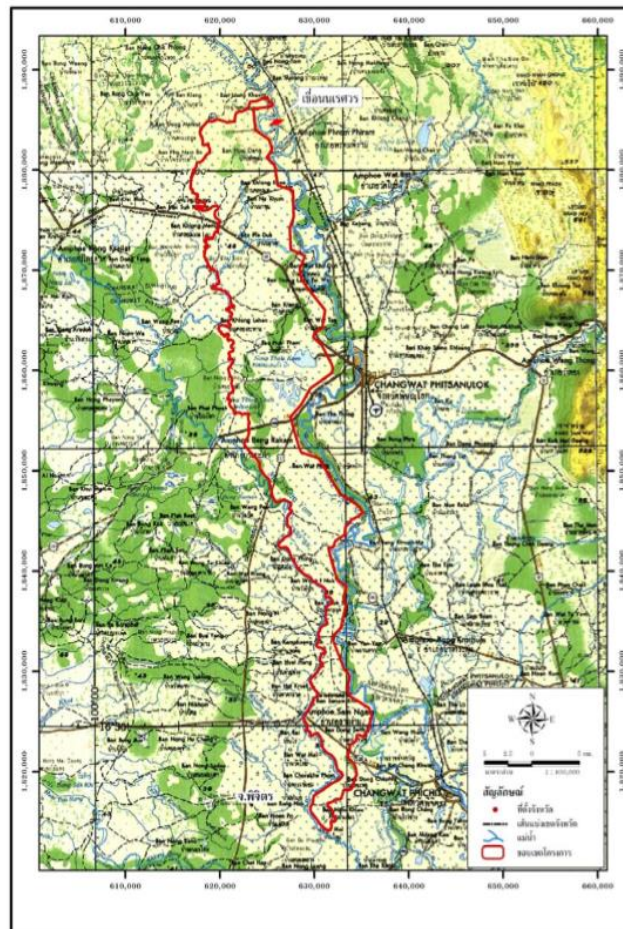
Figure 3.4 Topographic map of Pliachumphol Irrigation project

3.3. Climate

During the rainy season from April to September, annual rain is 81% and less than 19% during the dry season from October to March. Average annual rainfall is between 900 to 1700 mm/year. Pan evaporation ranges from 1400 to 2000 mm/year with the lowest evaporation in August and the highest in February. The humidity is generally varying from 70% to more than 80% in the wet season. The temperature varies between 27°C in the coolest month (January) and 32°C in the hottest month.

The Irrigation Project (PIP) area is affected by the southwest monsoon and northeast monsoon. Besides there are a number of depressions and typhoon from South China Sea from time to time which make seasons in the area. The highest temperature is in April and lowest temperature is in December. The highest relative humidity is in August, and the lowest is in March. The highest average wind velocity is in March and April while the lowest is in January. The highest evaporation rate is found in April and the lowest is in January. The precipitation during rainy season (May-October) cover 90 % of the average annual precipitation while the rest 10 % is between summer (November-April). The intense precipitation is between August-September. From the meteorological station in Phitsanulok Province during 1993-2003, the climate condition in the study area can be summarized in Table 3.1. Figure 3.5 shows the monthly rainfall data by water year (wet, normal, dry, and drought) during the study period (1993-2003).

Table 3.1 Climate parameters

Climate Parameter	Monthly average data	Annual average data
Temperature (°C)	23.4 – 30.7	27.7
Wind Velocity (knot)	0.9 – 2.1	-
Evaporation (mm)	109.8 – 186.8	1,647.6
Humidity (%)	61 – 86	74.4
Precipitation (mm)	107.7 – 152.4	993.6 – 1,692.6
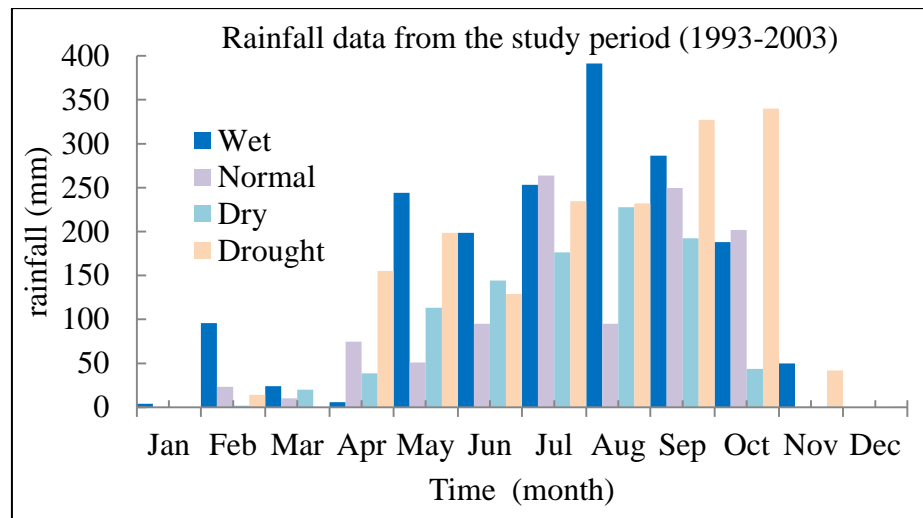
Figure 3.5 Monthly rainfall data by water year

3.4 Aquifer characteristics

A two-layer aquifer was defined vertically in this study both regional and the local, whereby the thickness of the upper, semi-confined layer varies between 40-100m and lower, confined layer between 100-200m (Bejranonda et al. (2006)) as shown in Figure 3.6. The high terrace deposits, the low terrace deposits, recent flood plain deposits and bed rocks are the main hydrogeological characteristics of regional area, while the western and eastern areas were impermeable consolidated aquifers, composed of granite and volcanic rocks. The southern part is partially blocked by impermeable rocks and forms a narrow through the mountains in the east and in local area, recent flood plain and low terrace deposit are mainly composed as shown in Figure 3.7 (Chulalongkorn (2010)).
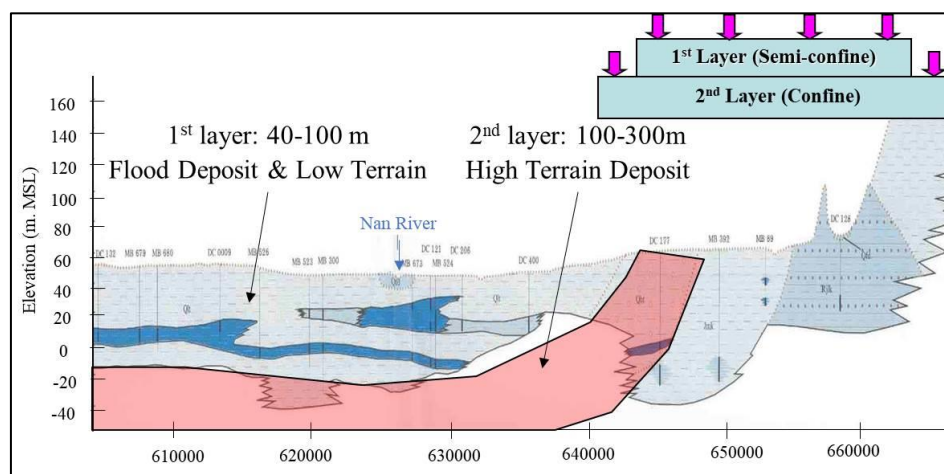
Figure 3.6 Two layers aquifer conceptual model (vertical view)
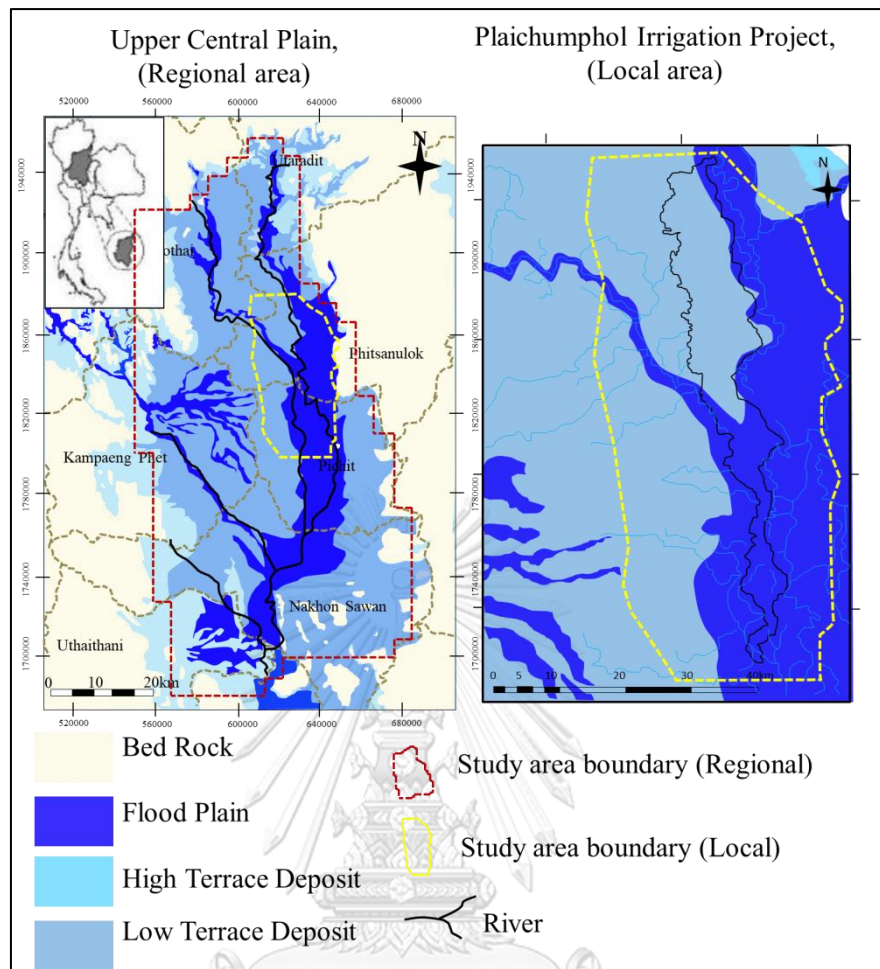
Figure 3.7 Aquifer characteristics of study area (plain view)

3.5 Data usage

The study used secondary and primary data collected from the government agencies and the others were surveyed and additionally collected in the field. There are 34 monitoring wells in Plaichumphol Irrigation Project (PIP) but the data recording is stopped since 2000. Groundwater level data were collected from existing monitoring wells. A new 5 observation wells network was set up near the river on April 2016 to create fitting water level profile(s) included active the serviceable existing observed wells in the site. There are two water stations: Y16 and Y17 along the Yom River and four stations; N27A, N68, N5A, and N74 along the Nan River (Figure 3.8) for surface water profile and groundwater boundaries for groundwater modelling. Groundwater interaction was conducted to determine the recharge to shallow aquifers in PIP. The overall data usages in this study are shown in Table 3.2.
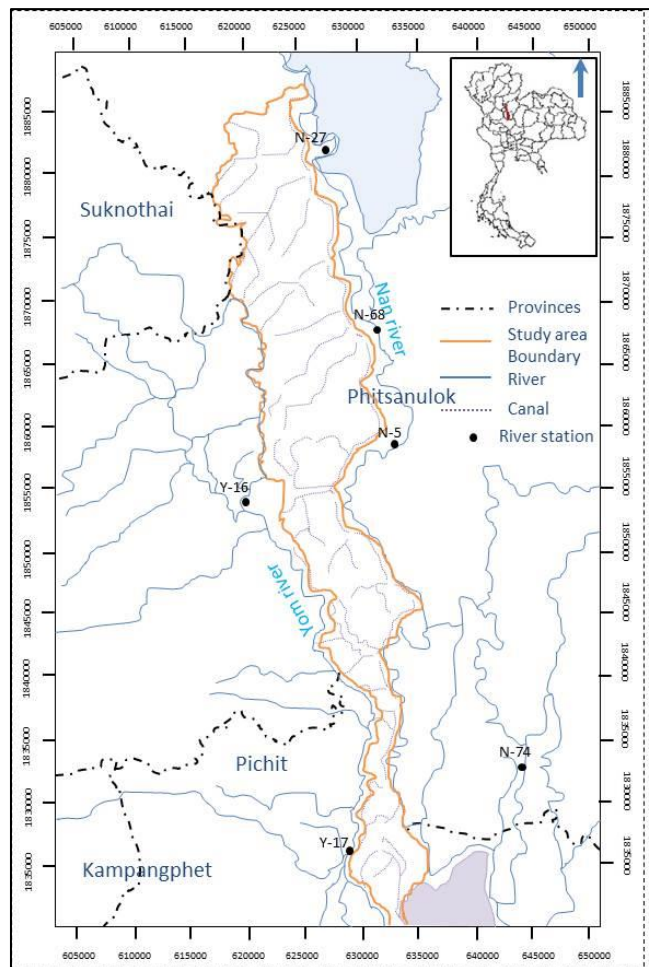
Figure 3.8 River stations along Yom River and Nan River in the study area

3.6 Monitoring wells

3.6.1 Regional area (Upper Central Plain, UCP)

The pumping data were confirmed from the past study results and groundwater levels were computed from the redeveloped regional groundwater model. Regional groundwater model was developed with smaller grids (2sq.km) and redeveloped by accumulating more wells data and applied the geostatistical methods to estimate the parameter distribution (Aye and Koontanakulvong (2018)). The bore logs data of 259 observation wells (Figure 3.9) were used to estimate hydraulic conductivity distribution from parameter i.e. transmissivity and specific capacity.

Table 3.2 Data used in the study area

No.	Data	Sources	Description
1	Topography	Thai Military Map Department (2003)	Map scale 1:50,000
2	Monthly rainfall data	Thai Meteorological Department and Royal Irrigation Department (1993-2003, 2017)	Digital files
3	Monthly evaporation	Thai Meteorological Department (1993-2003, 2017)	Digital files
4	The main stream	Thai Meteorological Department (2003)	Digital files
5	Aquifer characteristics	Conjunctive use project on the upper Chao Phraya basin (2006)	Groundwater parameter
6	Irrigated area boundary	Royal Irrigation Department	Digital files
7	Well log data	Royal Irrigation Department (1993-2006)	Digital files
8	Result of pumping test and groundwater parameter	Conjunctive use project on the upper Chao Phraya basin and Groundwater Department (1993-2003) (259 wells)	Digital files
9	Observation wells	Plaichumphol Irrigation Project (PIP) (2016-2018) (38 wells)	Digital files
10	Well level(MSL)	Plaichumphol Irrigation Project (PIP) (2016-2018)	Self-measuring
11	River stage	Royal Irrigation Department 8stations (1998-2016)	Digital files
		5 stations (2016-2018)	Self-measuring
12	Soil sample	4 samples (2017)	Self-measuring
13	Soil moisture	5 stations	Self- measuring
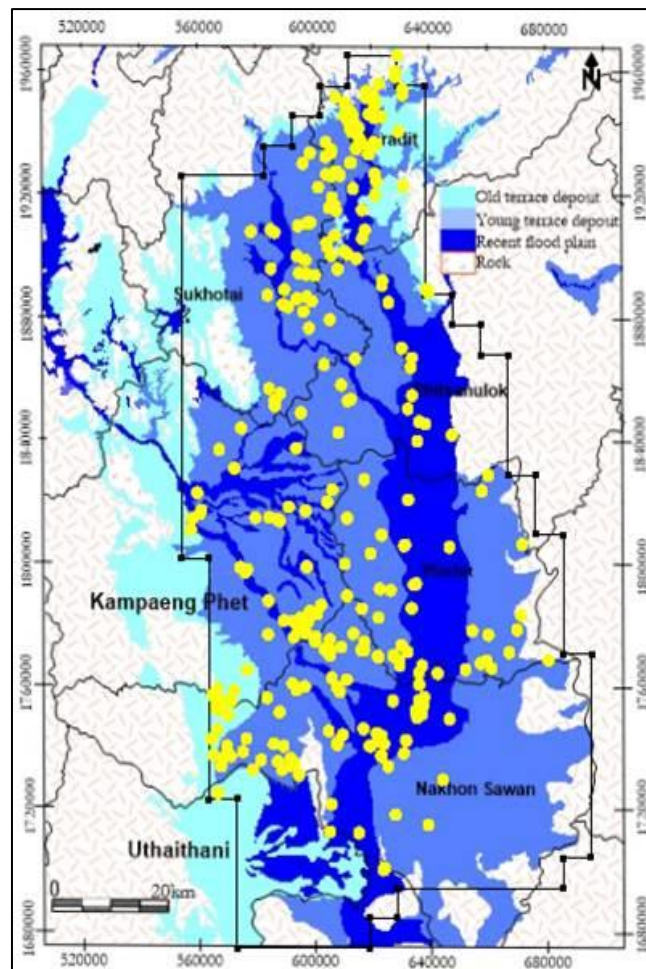
Figure 3.9 Maps showing the well locations in regional area

3.6.2 Local area (Plaichumphol Irrigation Project)

The irrigation area of the PIP is the area which depends on both irrigation water and groundwater for a long time. Farmers in the PIP area have their cultivation almost the whole year, therefore groundwater supply is another major source of water for their cultivation. Groundwater is used as supplementary of irrigation water and it could be assured and safe their water demands. In this study, PIP, there are 34 observation wells to be used for calibrations as shown in (Figure 3.10).
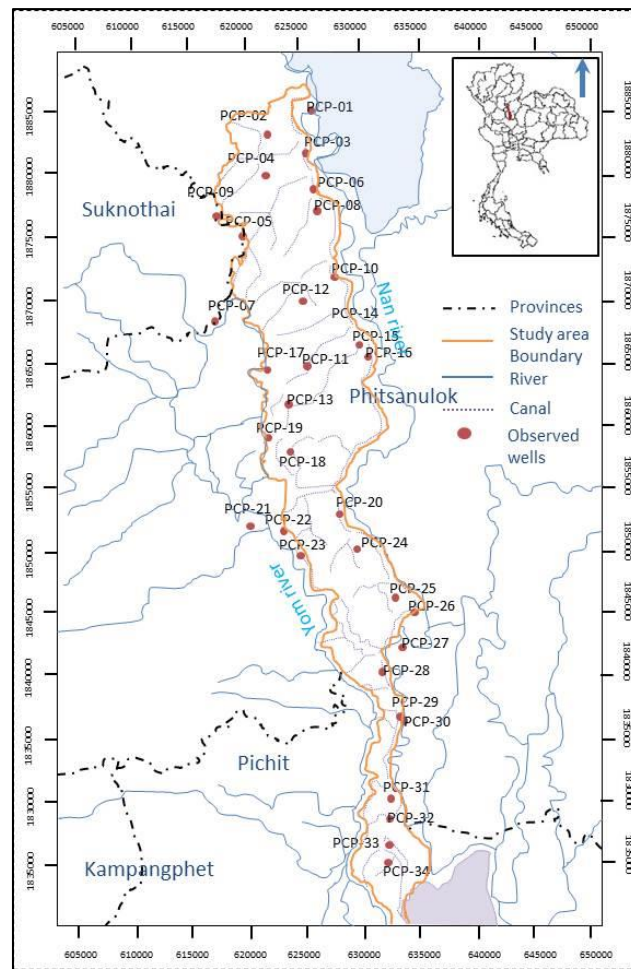
Figure 3.10 Map showing the location of observation wells

3.7 Groundwater use

The Upper Central Plain is a large plain, very suitable for agriculture, as water resources are normally plentiful. Farmers tend to grow rice more, which can be achieved through increased irrigation using both surface and also more groundwater, putting more pressure on the available water resources in the region. The major groundwater use in this area is by agriculture, namely, for rice and some sugar cane in the western section of the study area. According to Koontanakulvong and Panot (2003), the average use of groundwater in a normal year is 134MCM/day. The average capacity per well is $41m^3$/hour, whereas the average pumping rate per well is 79 m^3/day (Bejranonda et al. (2006)) in Upper Central Plain. Table 3.3 described the water demand and water situation from 1993-2003 (Suthidhummajit and Koontanakulvong (2017)). In average the ratio of groundwater use and surface water

use were 0.12 and 0.63 respectively. In a drought year, the ratio of groundwater use was highest (0.13-0.17) and the lowest was in a wet year (0.06-0.09).

Table 3.3 Water demand, water use pattern and water situation in 1993-2003

Year	Water Demand (MCM)	GW ratio	SW ration	Water year
1993	3,885	0.12	0.63	Dry
1994	4,617	0.1	0.53	Drought
1995	3,775	0.09	0.68	Wet
1996	4,757	0.08	0.74	Wet
1997	4,873	0.12	0.66	Normal
1998	4,701	0.13	0.52	Normal
1999	4,535	0.17	0.64	Drought
2000	4,588	0.14	0.67	Normal
2001	4,804	0.08	0.64	Wet
2002	5,445	0.07	0.63	Wet
2003	6,159	0.06	0.63	Wet
Average	4,740	0.12	0.63	

3.8 Field measurement

Field measurements of river water level, land recharge, and river seepage were conducted in Plaichumphol Irrigation Project area to investigate and compare the parameters with the model results.

3.8.1 River water level

The river water level was measured along rivers (Yom and Nan) from April 2016 to February 2018 as shown in Figure 3.11. This measurement was done to

investigate the interaction between river and groundwater and to check the river recharge parameter.

3.8.2 Soil moisture test (land recharge)

Field experiment for soil moisture test was conducted at the paddy's irrigation plot from the mid rainy season till the end to raining season from August to November in 2017 (108days). The experimental site was located in the Rice Water Use Experimental Station 2 of Royal Irrigation Department at Amphoe Phom Piram (17°2′0″N, 100°12′7″E) in the north-western part of Phitsanulok Province, Upper Central Plain, Thailand as shown in Figure 3.11. The experimental study plot is 20 x 25 square meters where the experimental station was testing the wet-dry irrigation scheme to save water where minimum irrigation water was filled to the plot as necessary. Automated profile soil moisture measurements at an hourly time step are collected from the soil surface to 4m depth. This study was carried out by developing a field sensor system to monitor soil moisture under irrigation field and to understand deep percolation characteristic in the unsaturated zone for land recharge estimation in groundwater modelling.

3.8.3 Seepage meter (river conductance)

Seepage measurement was conducted to measure the flow of water between groundwater and surface water along the rivers (Nan River and Yom River) at Phitsanulok Province, Northern Thailand. This study was carried out during 23rd to 28^{th,} 2018 (rainy (wet) season) to know discharge and recharge from river seepage to analyze interaction mechanism and to compare and check the local groundwater model (flux). During the field trip, the flux discharge from groundwater to river was measured at two stations along Yom River and three stations along Nan Rivers as shown in Figure 3.11. The test was processed at the right river bank and main channel river bed.
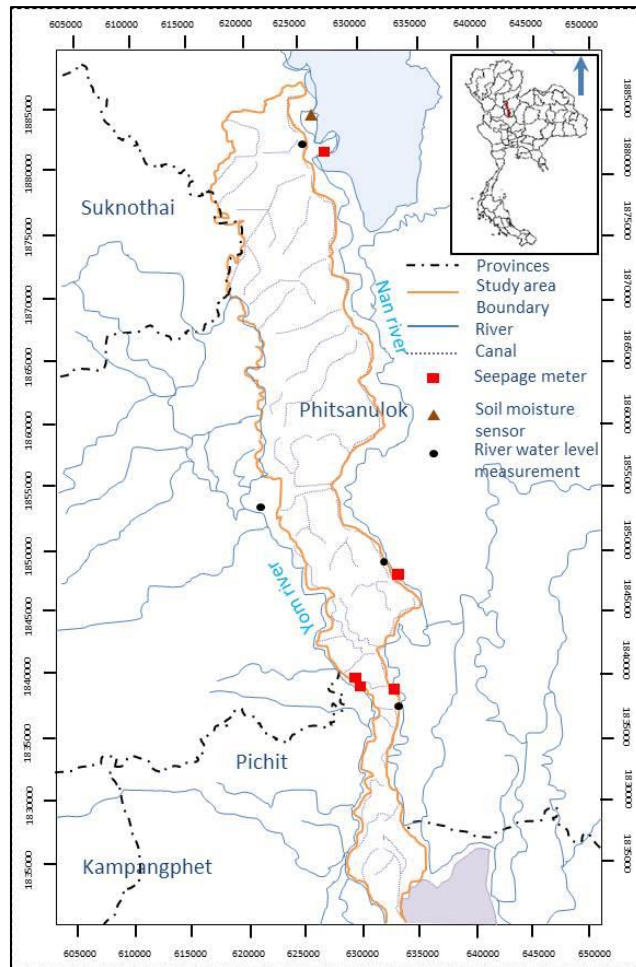
Figure 3.11 Field measurement locations for recharge parameters and river stations

จุฬาลงกรณ์มหาวิทยาลัย

CHULALONGKORN UNIVERSITY

CHAPTER IV: METHODOLOGY AND THEORIES USED

This chapter introduces the methods and theories used to analyse the surface water and groundwater interaction mechanism in Plaichumphol Irrigation Project (PIP) as a case study area. Study approach and methods are briefly discussed in this chapter. It explains the improvement of boundaries condition of groundwater modelling and describes how data collected from the field investigation. Step by step methodologies is described to achieve the objectives of the study and explained the equations used as follow.

4.1 Detailed scope of work

First, regional groundwater model was redeveloped from the previous study (Suthidhummajit and Koontanakulvong (2017)) especially for layer 1 to understand the interactions of land recharge and river recharge in the regional scale and to be used as boundary conditions for local groundwater model. More well data (269 wells) were used to evaluate the hydraulic parameter i.e. hydraulic conductivity and interpolate in each point dataset using geostatistics method (Kriging) to be smooth for smaller grid size (2sq.km) than the previous model grid (10sq.km). For layer 2, hydraulic conductivity distribution was used zoning of previous study because interaction occurs in layer 1.

Second, local groundwater model was developed in both steady-state and transient state in 400sq.m grid size. Boundary conditions were determined based on the hydrogeology, geology, and piezometry of the aquifer of the calibrated regional groundwater model. Interaction parameters were estimated during the model calibration, and the interaction mechanism was analysed from the model results during the study period (1993-2003). The interaction volume and patterns between surface water and groundwater were analysed from water balance via developed local groundwater model.

In the same time, field measurements on land recharge and river seepage were carried out to estimate land recharge rate and river hydraulic conductance and to analyse interaction mechanism and compare with the developed local groundwater model. Field measurement was done from April 2016 to February 2018 to analysis the

land recharge and river flux and interaction parameters to know the interaction mechanism. The river water level was measured from April 2016 to February 2018 to check the river recharge parameter. Land recharge analysis was done on August 2017 to February 2018 and river recharge analysis was done on 23-28 January 2018.

Finally, flow budget data from a developed local groundwater model were analysed to explain the sw-gw interaction pattern and volume of both time and space distribution.

4.2 Study approach and methodology

4.2.1 Study approach

The main approach is to analyse the interaction mechanism of surface water and groundwater interaction pattern and volume in Plaichumphol Irrigation Project area via groundwater model. A major obstacle to this task is to develop the local groundwater model for Plaichumphol Irrigation Project area. To solve this problem, regional groundwater model was redeveloped from the previous study (Suthidhummajit and Koontanakulvong (2017)) to be used as boundary conditions for the local groundwater model.

This study redeveloped his model by creating small grid size (2sq. km) to grasp more sw-gw interaction especially for river grid and adding more well data (259). Due to the smaller grid size, hydraulic conductivity was interpolated by geostatistic methods for each grid. The redeveloped groundwater level was used to set up the boundary conditions in the local groundwater model.

With the limited well data, proper parameter estimation method was applied for the groundwater modelling to understand the GW-SW interaction mechanism and parameter distribution. Appropriate interaction parameters i.e. land recharge and river recharge were measured in the field and local groundwater model (400 sq. m grid size) was developed to understand the surface water and groundwater interactions mechanism and to check the model's interaction parameters with the field observed data.

Land recharge parameter was calibrated with13 observed well data far from the river out of total 34 wells data and river conductance was calibrated with well data near Nan River; upstream (5wells); mid-stream (8wells) and downstream (3wells) and

near Yom River; mid-stream (3 wells) and downstream (2wells). Pumping rate was readjusted overall wells data of the study. The groundwater flow budget and river interaction patterns were analysed in seasonal and water year from well calibrated/verified groundwater model simulation results of the developed local groundwater model.

Table 4.1 shows the types of the water year in the period between 1993 and 2003 (Koontanakulvong (2002)). The surface water and irrigation water were provided by the total storage of the Bhumibol and Sirikit reservoirs on January 1st to define the situation of surface water availability, specifically: severe year (drought), serious year (dry), normal year (normal), and extreme year (wet).

Table 4.1 Types of water year (from 1993- 2003) and reservoir storage of the Bhumiphol and Sirikit Dams

Water year	Reservoir storage (MCM)	1993	1994	1995-1996	1997-1998	1999	2000	2001-2003
Severe year (drought)	< 4,200		√			√		
Serious year (dry)	4,200-8,500	√						
Normal year (normal)	8,500-12,500				√		√	
Extreme year (wet)	> 12,500			√				√

4.2.2 Study methodology

The data obtained for this study were reviewed from previous studies and collected the historical data such as rainfall, evaporation, observed groundwater level, pumping test data, etc.

First, pumping test data were analysed to determine yield/drawdown characteristics of a well and hydraulic parameters of the aquifer such as specific capacity (S_c) and transmissivity (T). To increase the accuracy of defining this

parameter, the equation describing the relation between transmissivity and specific capacity (yield divided by drawdown; m^2/d) was derived as Equation 2. The proper parameter estimation from wells data was applied and the geostatistical method was used to estimate the hydraulic conductivity distribution and which are compared with hydrogeological characteristics.

Secondly, this study required the regional groundwater model (RGM) to be used as boundary conditions for the local groundwater model (LGM). Therefore, RGM was redeveloped from the previous study (Suthidhummajit and Koontanakulvong (2017)) with smaller grid size (2sq.km) and redeveloped by adding more well data (259) from estimated hydrogeological parameters i.e. hydraulic conductivity. Improvement of regional groundwater model calibration and verification was checked by the error with the previous study and the piezometric head was used as boundary conditions for the local groundwater model.

Thirdly, local groundwater model was developed with grid size (400sq. m) to understand the sw-gw interaction mechanism more precisely. Minor adjustment between land recharge and river conductance was calibrated to match with the nearby observed data. Land recharge rate is adjusted based on soil type, and river conductance is based on river bed materials and slopes. Pumping wells are also adjusted by seasonal and zoning, though, with the same amount of annual pumping as the previous study.

Fourthly, the field measurements of soil moisture via sensor system and seepage meter were conducted to investigate land recharge and river conductance. HYDRUS-1D package was applied to simulate water movement with soil hydraulic parameter for calibration and verification to understand the deep percolation characteristics in the unsaturated zone for local groundwater model. Seepage meter was used to find river conductance from the river bed to verify the river loss and gain. The calibrated seepage values (conductance) from the developed local groundwater model were checked by comparing with data from field measured and other studies as well.

Finally, the groundwater flow budget from the local groundwater model was used to determine interaction mechanism by volume of interaction functions and patterns. The general framework of the study is shown in Figure 4.1.
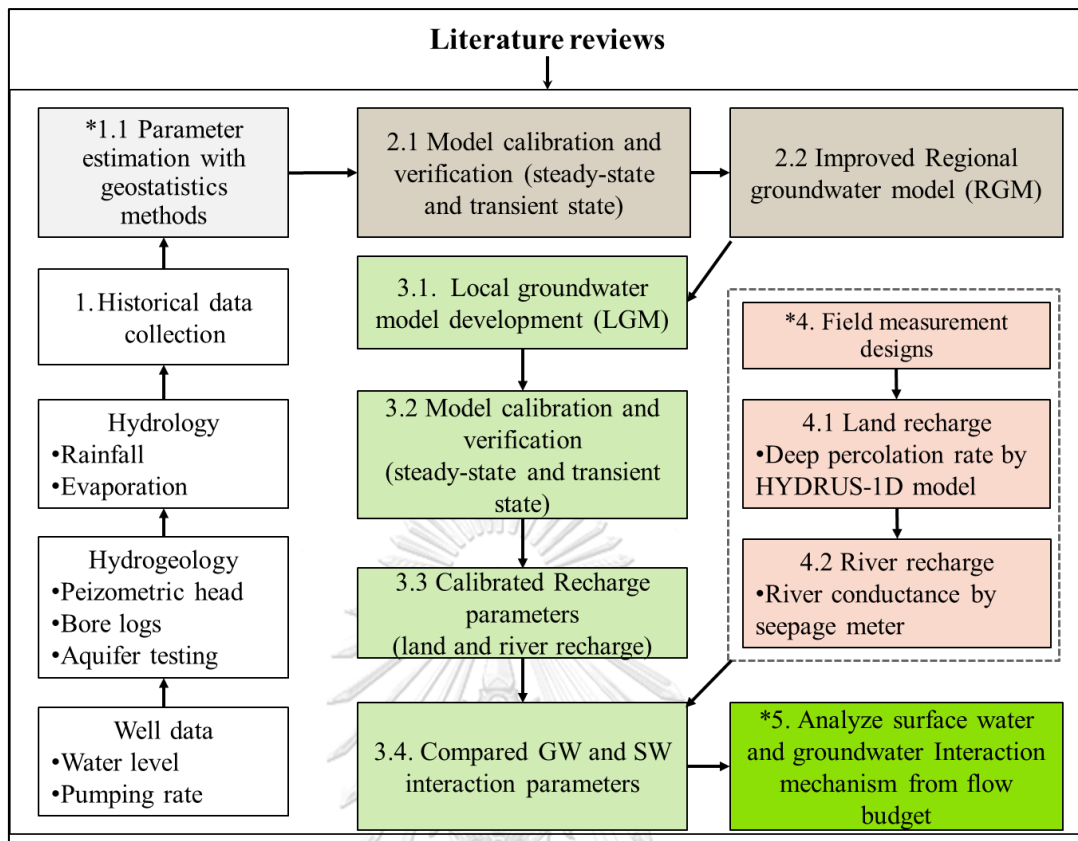
Figure 4.1 Framework of the study
(* refers to the journal paper publications)

4.3 Theories used

As background theories, this study used the theories and techniques including parameter estimation using empirical formula, groundwater flow model, geostatistic methods application, one-dimensional soil water flow model for soil moisture sensor, seepage meter measurement for river conductance, water balance analysis, river loss and gain for interaction mechanism and error estimations. The groundwater modelling system (GMS) was used to analyse the flow budget and boundary conditions to identify the interaction mechanism. HYDRUS-1D software package was used to estimate land recharge with Arduino sensor and seepage meter was installed to estimate the river recharge using river conductance.

4.3.1 Groundwater flow model

Groundwater flow modelling was accomplished using MODFLOW within the Groundwater Modelling System (GMS) version 10.1. MODFLOW is the finite-difference groundwater flow modelling program written by the United States

Geological Survey, which is a computer code to develop a numerical representation that is the groundwater model of the hydrogeological environment at a field site. Groundwater flow model domain into a series of rows, columns, and layers which defines a unique set of grid blocks (model cell) to represent the distribution of hydrogeological properties and hydrologic boundaries within the model domain.

To develop a groundwater model, the properties and boundaries to the cells were assigned to create a set of the finite-difference equation that it solves to calculate the hydraulic head at the centre of each model cell. This program was used to simulate the flow of groundwater through the aquifer and to predict aquifer fluxes into and out of an aquifer. The three-dimensional movement of groundwater of constant density through porous earth material may be described by the partial differential equation.

$$\frac{\partial}{\partial x}\left[K_{xx}\frac{\partial h}{\partial x}\right]+\frac{\partial}{\partial y}\left[K_{yy}\frac{\partial h}{\partial y}\right]+\frac{\partial}{\partial z}\left[K_{zz}\frac{\partial h}{\partial z}\right]+W=S_s\frac{\partial h}{\partial t} \qquad (1)$$

Where,

- K_{xx}, K_{yy} and K_{zz} refer the values of unsaturated hydraulic conductivity along the x, y and z coordinate axes and are function of space
- h is the potentiometric head (hydraulic head)
- W is a volumetric flux per unit volume representing sources and/or sinks of water
- S_s is the specific storage of the porous material and is function of space and
- t is time.

The Equation, together with a specification of flow and head conditions at the boundaries of the aquifer system and specification of initial head conditions, constitutes a mathematical representation of the groundwater flow system.

4.3.2 Parameter estimation

4.3.2.1 Aquifer transmissivity and specific capacity

Aquifer transmissivity is normally determined from aquifer pumping tests. Because of its abundance and cost-effectiveness, specific capacity is used to estimate the transmissivity of an aquifer. An empirical relationship for the study area is determined by linear regression of the log-transformed information. Several authors

had also developed the empirical or observed relationship between specific capacity and transmissivity from the short term pumping test data with adequate accuracy (Logan (1964), Driscoll (1986), El-Naqa (1994), Hamm et al. (2005), Rotzoll et al. (2007)). The hydraulic properties of the aquifer, namely, transmissivity and specific capacity, were estimated from historical wells recorded data by using this equation and are expressed as:

$$T' = a\left(S_c'\right)^b \tag{2}$$

$$S_c' = \frac{Q}{\Delta s \times l} \tag{2.1}$$

Where,

- Q is discharge (m³/hour)
- Δs is drawdown (m)
- l is screen length of the well (m)
- T' is transmissivity (m/hour)
- S_c' is specific capacity (m/hour) and
- a , b are constants.

4.3.2.2 Hydraulic conductivity

Hydraulic conductivities are generated from the aquifer data and optimized the hydraulic conductivities in steady state with known observed piezometrics. The hydraulic conductivity (K) is defined as transmissivity (T) divided by the saturated thickness of the aquifer (D).

$$K = \frac{T}{D} \tag{3}$$

The estimating of hydrological parameter distribution, in particular, hydraulic conductivity was examined in geostatistical frameworks (Natural Neighbour, Inverse Distance Weight, and Kriging) and selected the appropriate methods. Then, the regional groundwater model was computed with best geostatistical interpolation (Kriging).

4.3.3 Geostatistic methods

4.3.3.1 Inverse distance weight method (IDW)

IDW is a method of low computational costs that depends on the number of point samples as well as prediction points. The predicted value corresponds to a weighted average of the sample data points. The weight assigned to each sample depends in an inversely proportional way, to the distance that separates it from the un-sampled sites. Its characteristics are outlined in detail in (Shepard (1968), Bartier and Keller (1996)).

It explicitly implements the assumption that things are close to one another (Figure 4.2). It assumes each measured point has a local influence that diminishes with distance. It weights the points closer to the prediction location greater than those fathers away, hence the name inverse distance weighted. Weight of each sample point is an inverse proportion to the distance (Kitanidis and Vomvoris (1983)). Inverse distance weight is given by

$$W_i = \left(\frac{1}{(d_i)^p} \right) / \sum_{i=1}^{n} \left(\frac{1}{(d_i)^p} \right) \qquad (4)$$

Where

- d_i is the distance between the estimated point and the sample and
- p is an exponent parameter.
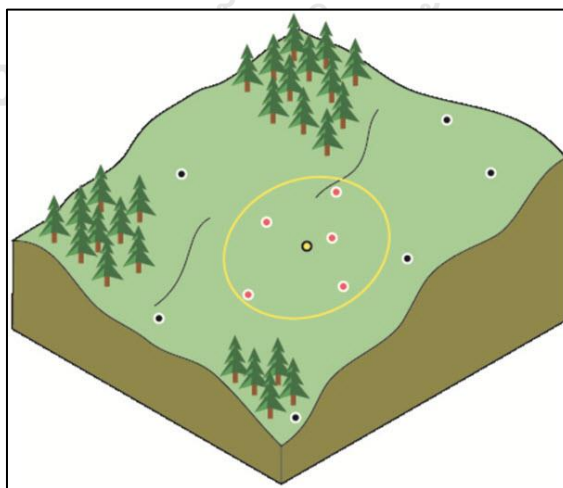
Figure 4.2 The Inverse Distance Weighting (IDW) interpolations technique

4.3.3.2 Natural neighbour method (NN)

Based on the natural neighbour coordinates, Robin Sibson developed a weighted average interpolation technique that the named natural neighbour interpolation (Sibson (1981)).

$$G(x, y) = \sum_{i=1}^{n} W_i f(x_i y_i) \qquad (5)$$

Where

- $G(x, y)$ is the NN estimation at (x, y);

- n is the number of nearest neighbours used for interpolation;

- $f(x_i y_i)$ is the observed value at $(x_i y_i)$; and

- W_i is the weight associated with $f(x_i y_i)$. The weights W_i are calculated by finding how much of each of the surrounding areas is taken when inserting (x, y) into the tessellation.

4.3.3.3 Kriging method

Kriging is one of the important geostatistical techniques which have been applied to many hydrogeological problems for estimation and sampling purposes. This algorithm is basically a statistical interpolation technique (Figure 4.3). Kriging technique is an exact interpolation estimator used to find the best linear unbiased estimate. This feature offers a measure of the estimation accuracy and reliability of the spatial distribution of the variable. Errors in this method are independence from variable and dependent to spatial location and it causes to predict the best location sampling is possible. Variogram relationship based on the measured points is as follows:

$$\gamma(h) = \frac{1}{2n(h)} \sum_{i=1}^{n(h)} \left[z(x+h) - z(x) \right]^2 \qquad (6)$$

Where

- $\gamma(h)$ is the variogram for a distance (lag) h between observations $z(x)$ and $z(x+h)$

- $n(h)$ is the number of pairs of observations which are at distance h

- $z(x)$ and $z(x+h)$ are the values of the variable at point x and at a point of h from point x.
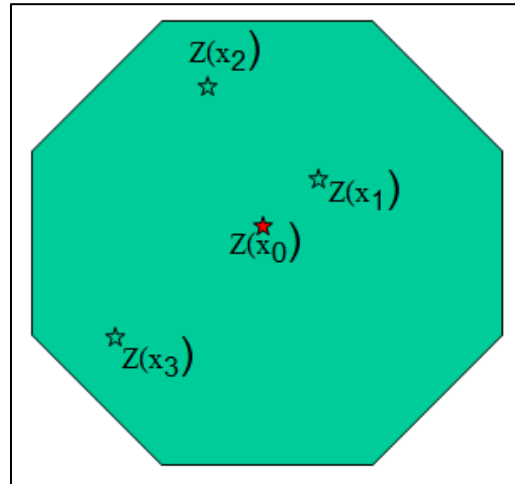
Figure 4.3 Kriging interpolating technique

The variogram is a three-dimensional function of direction and a measure of how quickly things change on the average. The underlying principle is that, on the average, two observations closers together are more similar than two observations farther apart. There are two independent variables (the direction θ, the separation distance h) and one dependent variable (the variogram value γ(θ, h)). When the variogram is specified for kriging, the sill, range, and nugget were given and specified the anisotropy information.

4.3.4 Recharge parameter estimation via field measurement

4.3.4.1 Land recharge analysis

Groundwater recharge is estimated using an improved daily soil moisture balance based on a single soil water store in Phitsanulok Province. Soil water content is essential in controlling the soil processes involving the physical, chemical, and biological processes of the soil system (Brevik et al. (2015)). In general, these processes that take place in soil strongly depend on the quantity and composition of water. In the case of the water infiltration process, soil water content dictates that water flows across the soil surface, reaches the soil profile, or finally, percolates to recharge aquifers, which is essential to understand the hydrological cycle (Cerdà (1999)). Infiltration is the movement of water into the soil from the surface by

downward or gravitational flow (Thompson et al. (2010)). It is the feedback between the infiltration of water from precipitation and the water use characteristics of the particular vegetation community that ecologically predominates in an area that determines the moisture state of the soil in the root zone (Sandvig and Phillips (2006)).

Numerical modelling has often been used this function to predict the water flux through the unsaturated zone: such as UNSAT-H (Fayer and Jones (1990)), and HYDRUS (Šimůnek (2005)). HYDRUS-1D is used in the study. It has been widely adopted to predict recharge estimates using the basis of Richards' Equation. These models were applied successfully to evaluate coefficients of groundwater recharge by the precipitation (Yeh et al. (2007)), estimate average mean annual groundwater recharge (Cao (2011)), analysis the impact of different thickness and lithology of vadose zone to groundwater recharge (Lu et al. (2011)). One–dimensional soil water flow model is as follow:

$$\frac{\partial \theta}{\partial t} = \frac{\partial}{\partial z}\left[\left(K(h)\frac{\partial h}{\partial z}\right) + \frac{\partial}{\partial h}\left(K(h)\right)\right] - S(h) \tag{7}$$

Where

- θ is the volumetric water content, by time (t)
- z is the vertical ordinate assumed to be 0 at the soil surface directed upward,
- K is the unsaturated hydraulic conductivity,
- h is the pressure head, and
- S is a sink term to account for root water uptake.

4.3.4.2 Unsaturated soil hydraulic properties

To solve the equation (7), estimation of the relationships of the soil water retention $\theta(h)$ and unsaturated hydraulic conductivity $K(h)$ are required. The van Genuchten–Mualem model (Mualem (1976)) was used to describe the soil water retention $\theta(h)$, and the hydraulic conductivity $K(h)$, and effective saturation S_e, curves which are given by follows:

$$\theta(h) = \begin{cases} \theta_r + \dfrac{\theta - \theta_s}{\left[1 + |\alpha h|^n\right]^m} & h > 0 \\ \theta_s & h \geq 0 \end{cases} \left(m = 1 - \dfrac{1}{n}\right) \qquad (8)$$

$$K(h) = K_s S_e^{\frac{1}{2}} \left[1 - \left(1 - S_e^{\frac{1}{m}}\right)^m\right]^2 \qquad (9)$$

$$S_e = \frac{\theta - \theta_r}{\theta_s - \theta_r} \qquad (10)$$

Where,

- θ_r and θ_s are residual and saturated water content (m^3/m^3) respectively,
- α is the inverse of the air-entry value (or bubbling pressure),
- n is a pore-size distribution index,
- K_s is the saturated hydraulic conductivity and
- S_e is the effective saturation.

For αh, the functional form of (Feddes et al. (1974)) was adopted using HYDRUS-1D. The monitoring of deep percolation from the field measurement, by using soil moisture sensor system developed provided more understandings of deep percolation characteristics, percolation rate and overall water balance of deep percolation system in the soil.

4.3.4.3 Percolation simulation

The percolation rate are computed for each node N according to (Šimůnek (2005)) from the HYDRUS-1D model.

$$q_N^{j+1} = -K_{N-\frac{1}{2}}^{j+1} \left(\frac{h_N^{j+1} - h_{N-1}^{j+1}}{\Delta x_{N-1}} + 1\right) - \frac{\Delta x_{N-1}}{2} \left(\frac{\theta_N^{j+1} - \theta_N^j}{\Delta t} + S_N^j\right) \qquad (11)$$

Where,

- θ is the volumetric water content (m^3/m^3)
- K is the unsaturated hydraulic conductivity (m/day^{-1})
- h is the pressures head (m)
- S is a sink term (day^{-1})
- Δt is time calculation (day)

- Δx is grid size

- j is time step

- N indicate the position node in the finite difference mesh

4.3.4.4 Land recharge coefficient

Land recharge coefficient (k) can be approximated by using the following equation.

$$\frac{R}{P} = k\frac{(P-ET)}{P} \tag{12}$$

Where,

- R is recharge rate (cm/day)

- P is precipitation (cm/day)

- ET is evapotranspiration (cm/day)

- k is land recharge coefficient

4.3.4.5 River hydraulic conductance

In groundwater modelling, the flow across riverbed is represented by the following equation (Mcdonald et al. (1988)):

$$Q_{riv} = C_{riv} \times (h_{riv} - h) \tag{13}$$

Where,

- Q_{riv} is the flow between the river and the aquifer, taken as positive if it is directed into the aquifer (m^3/day),

- C_{riv} is the hydraulic conductance of the river-aquifer interconnection,

- h_{riv} is the head of the river water level (stage) (m) and

- h is the head of groundwater (m).

4.3.4.6 River hydraulic conductance coefficient

Calculating the flow between river and aquifer is done using a coefficient that represents the streambed conductance as shown in Figure 4.4 (McDonald et al. (1988)). This coefficient, termed C_{riv} in equation 12, estimated from streambed deposits properties.

$$C_{riv} = \frac{KLW}{M} \tag{14}$$

Where

- K is the unsaturated hydraulic conductivity of the bed material (m/day),
- L defines the length and the river cell for the calculation node (m),
- W is the total width of interaction layer (m) and
- M is the thickness of aquifer (m)

This equation is used to find the conductance C_{riv} from seepage and the flow rate of river loss and gain equation from that hydraulic conductance.
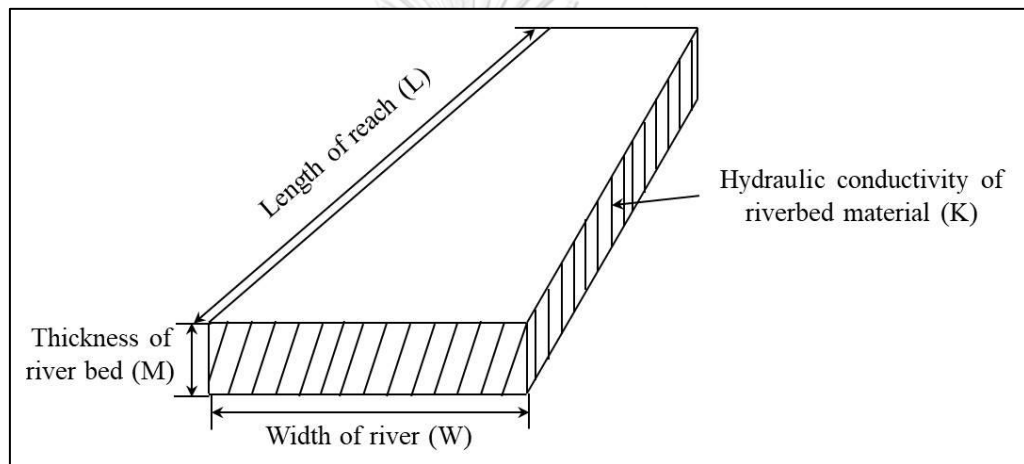
Figure 4.4 Idealization of streambed conductance in an individual cell

4.3.5 SW-GW interaction mechanism

Surface water and groundwater are best addressed in water management with simulation models that can represent the interactions between these two flow regimes including land recharge and river recharge. Land recharge is the sum of positive values of the change in soil water, once the soil water content exceeds the field capacity of the soil and the flow by passing the soil water store. The river and groundwater interaction mechanism were analysed from the flow budget of groundwater model and river loss and gain regime.

4.3.5.1 Water balance analysis

The groundwater balance analysis was done to check the water storage inflow into the aquifer and outflow form the aquifer using the inflow-outflow equation.

$$I - O = \frac{\Delta V}{\Delta t} \qquad (15)$$

Where,

- I is inflow (m^3/day)during time Δt
- O is outflow (m^3/day)during time Δt
- V is change in water volume (m^3)

4.3.5.2 River loss and gain

Interaction between the river and groundwater is primarily determined by the relation between river surface water and groundwater levels, surface water absorption from rivers and raised bogs occurs in sites where the top of the first aquifer is at a lower level than that of the surface water. Depending on the cross-section structure, the volume of filtration losses (-) and condition for groundwater flow along the layers, a scheme of free or backed surface water filtration is formed. River Loss and Gain equation is used to check the flow Q between the river and aquifer;

$$\sum_{i=1}^{n} Q = \sum_{i=1}^{n} \left(Q_{up} - Q_{down} \right) \qquad (16)$$

Where,

- n is the number of observation wells
- Q is river loss or gain,
- Q_{up} is river discharge in upstream and
- Q_{down} is river discharge in downstream.

4.3.6 Error estimations

A calibration criterion for both the steady-state and transient simulations was employed to match simulated heads with observed head. The model calibration was accomplished by analysing the models' performance specified by statistical goodness-of-fit measures mean error, the mean absolute error (MAE), root mean squared error of head (RMSE), and Nash-Sutcliffe coefficient (NSE). MAE and RMSE are valuable because they indicate the error in the units of the constituent of interest which aids in analysis of the results. Nash-Sutcliffe efficiency (NSE) is a normalized statistic that

determines the relative magnitude of the residual variance compared to the measured data variance (Nash and Sutcliffe (1970)) and described as follows:

$$MAE = \left| \frac{1}{n} \sum_{i=1}^{n} \left(h_i^{obs} - h_i^{sim} \right) \right| \tag{17}$$

$$RMSE = \sqrt{\frac{1}{n} \sum_{i=1}^{n} \left(h_i^{obs} - h_i^{sim} \right)^2} \tag{18}$$

$$NSE = 1 - \left[\frac{\sum_{i=1}^{n} \left(h_i^{obs} - h_i^{sim} \right)^2}{\sum_{i=1}^{n} \left(h_i^{obs} - h^{mean} \right)^2} \right] \tag{19}$$

Where,

- n is the number of observation wells,
- h_i^{obs} is the observed head (m),
- h_i^{sim} is the simulated head (m) and
- h^{mean} is the mean of observed data.

The relative degree of the calibration residual measured form the mean observed head water determined by NSE (Nash and Sutcliffe (1970)) using a set of criteria;

- Very good (0.75< NSE ≤1.00),
- Good (0.65< NSE ≤ 0.75),
- Satisfactory (0.50< NSE ≤ 0.65) and
- Unsatisfactory (NSE ≤ 0.50) as defined by Moriasi et al. (2007)

CHAPTER V: STUDY RESULTS

The overall goals of this chapter comprised of three parts. First, the hydraulic parameter was estimated from wells data using empirical formula and distributed by the geostatistic method to improve the regional groundwater simulation. Second, local groundwater model was developed and checked the results with estimated interaction parameters from field measurements such as land recharge via soil moisture sensor and river recharge via seepage meter. Finally, groundwater flow budget was analysed and estimated the interaction mechanism, pattern and volume by water year, season and up-mid-down streams. The detailed results of the study are as follows.

5.1 Hydraulic parameter estimation

The intention of this section is to estimate the parameter, in particular, hydraulic parameter i.e. transmissivity (T′) and specific capacity (S_c′). The proposed parameter and its distribution under limited available well data can be extended to regional groundwater model application. The short pumping well data collected were screened and used empirical formula (Equation 2) to estimate transmissivity (T′) and specific capacity (S_c′).

5.1.1 Relationship of transmissivity (T') and specific capacity ($S_c^{'}$) from well data

From the proposed equation 2, specific capacity (yield divided by drawdown, m^2/d) and transmissivity relation was suggested by Logan (1964) with constants (a=1.22, and b=1.385). This equation describing the relation between specific capacity and transmissivity was derived as T′=2.5(S_c′)$^{0.01}$ (Koontanakulvong and Panot (2003) in the Central Plain area) and used to find the relationship between specific capacity and transmissivity from 259 historical well records. The theoretical relationship between transmissivity (T′) and specific capacity (S_c′) is linear on a log scale utilizing log-log regression analysis as shown in Figure 5.1. These transmissivity values will be used as initial values in the parameter optimization and distribution in the next step.
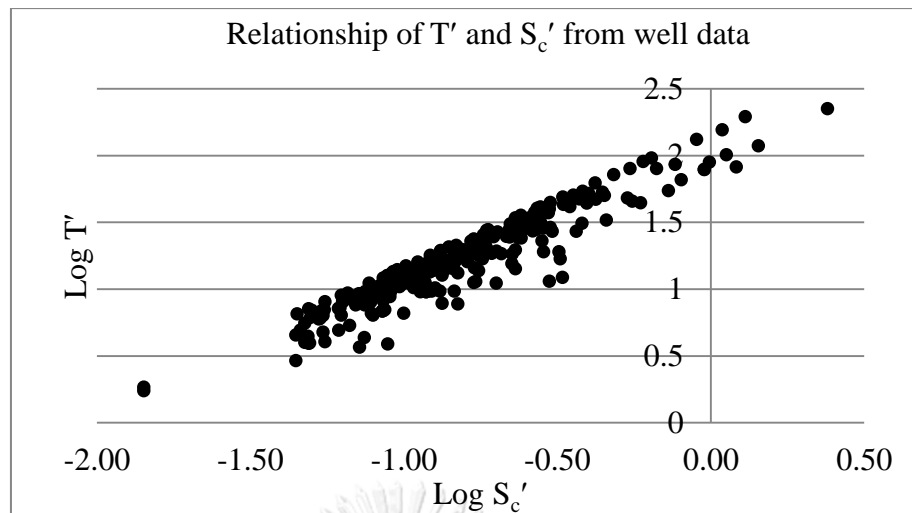
Figure 5.1 Relationship of T' and $S_c{}'$ from well data records

5.1.2 Transmissivity estimation

The transmissivity derived from both pumping test data and 259 well data with the hydrogeological map (separated into old (high) terrace deposit, young terrace deposit and recent flood plain deposit), deposit type range from 0.5 m^2/h to 2m^2/h in the high terrace deposit, 2m^2/h to 50 m^2/h in the low terrace deposit and 50m^2/h to 150m^2/h in the flood plain deposit (Aye et al. (2017)) are plotted. When the values are mapped into the hydrogeological map, it shows fairly good correlated with the deposit types as shown in Figure 5.2. The values from the previous study (Suthidhummajit and Koontanakulvong (2017)) along the flood plain area are >50m^2/h while the value range from 10-50 m^2/h in the low terrace deposit area.

This study found the relationship of specific capacity and transmissivity and its distribution were then estimated from the derived relationship. The transmissivity distribution corresponds with hydrogeological characteristics of the study area and also corresponds with aquifer deposit type. The hydraulic conductivity can be estimated from wells data records and used as initial values for parameter optimization in groundwater modelling.

5.1.3 Estimation of hydraulic conductivity distribution

The scattering of hydraulic conductivity for layer 1 estimated using various geostatistic methods; Inverse Distance Weighting method (IDW), Natural Neighbour method (NN), and Kriging method (equations 4, 5, and 6) to interpolate the scatter

point in groundwater flow model (GMS). Because of the flow budget of the previous study (Suthidhummajit and Koontanakulvong (2017)), the interaction occurs only in layer 1 and layer 2 is also not so much influence in this area. The zoning method from the previous study was used to interpolate for layer 2. The process of geostatistic methods application will discuss in Appendix I. The generated a new dataset was compared with the original dataset and find the error using equations (17, 18, and 19). The good method based on their error was selected to estimate the hydraulic conductivity distribution.
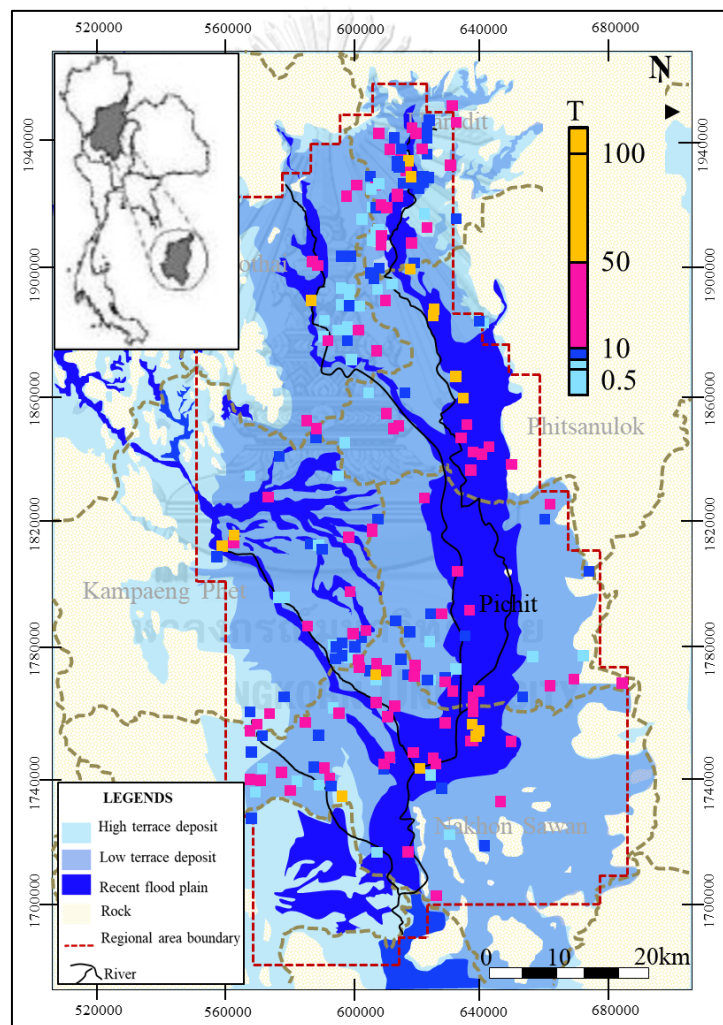
Figure 5.2 The distribution of derived transmissivity.

Table 5.1 shows the results of the error for each method. A result of the Kriging method shows better than other methods. The Kriging method is selected based on this performance to interpolate hydraulic conductivity in the groundwater model.

Table 5.1 Comparison among methods for hydraulic conductivity distribution

Estimation methods	Min	Max	ME	MAE	RMSE	NSE	Performance
Inverse distance weight (IDW)	-35.55	44.39	-0.52	8.99	12.42	0.13	2
Natural neighbour (NN)	-37.07	47.10	0.09	9.15	12.79	0.08	3
Kriging	-30.26	38.16	-0.26	8.31	10.62	0.80	1

5.1.3.1 Data analysis

Kriging is a necessary tool in geostatistic field and based on the hypothesis that the parameter being interpolated. Before interpolating a scatter point set using the Kriging option, a model variogram is defined. A variogram consists of two parts: an experimental variogram and a model variogram.

The experimental variogram is computed by calculating the variance of each point in the set with respect to each of the other points and plotting the variances versus distance between the points. Once the experimental variogram is computed, a model variogram is defined as the next step. A model variogram is a simple mathematical function that models trend in the experimental variogram. A detail variogram data analysis refers to Appendix I.

After testing several types of theoretical variogram, the one that proved to have the best fit to the experimental variogram was Gaussian type which represents very smoothly varying properties. Gaussian simulation is similar to indicator kriging that generates a set of equally probable results which display heterogeneity and are conditioned to values at scattering points.

It can be seen in Figure 5.3, the shape of the variogram indicated that at 2km separation distances, the variance in interpolation is small. In other words, points that are close together have similar interpolated values. After a certain level of separation, the variance in the interpolate values becomes somewhat random and the model variogram flattens out of a value corresponding to the average variance.
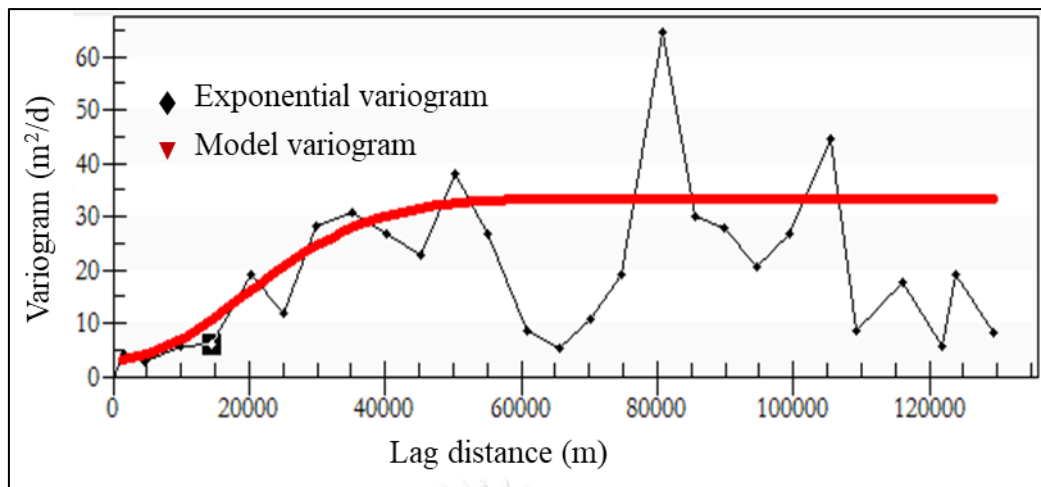
Figure 5.3 Experimental variogram and fitted Gaussian model for hydraulic
conductivity

5.1.4 Distribution of estimation error from the application of Kriging

The hydraulic conductivity distribution was estimated using the Kriging method and confirmed to the hydrogeological map. The hydraulic conductivity value in the river is from 20m/d to 30m/d while in mountains are from 10m/d to 20m/d. Figure 5.4 shows the distribution of hydraulic conductivity which shows the value along the river (flood plain deposit) is higher than the value far from the river (low terrace deposit). It means that the pattern similar to the pattern of the hydrogeological map.

Kriging method can be applied to interpolate hydraulic conductivity distribution. The hydraulic conductivity in the plain is found to be higher than in the mountainous area which is corresponded with hydrogeological characteristics. Estimated hydraulic conductivity distribution by using geostatistical methods (Kriging) is better represented by the mean error. The estimated hydrogeological parameter distribution improved the quality of groundwater modelling in the study area.

5.2 Regional groundwater model improvement

The aim of this task was to improve the regional groundwater model from the previous study to be used as boundary conditions for local groundwater model development. For this purpose, the regional model was redeveloped with smaller grid size and new parameter estimation from 259 well data as specific capacity (S_c'),

transmissivity (T′) and hydraulic conductivity (*K*) (Aye and Koontanakulvong (2017)) and compared with observed data.
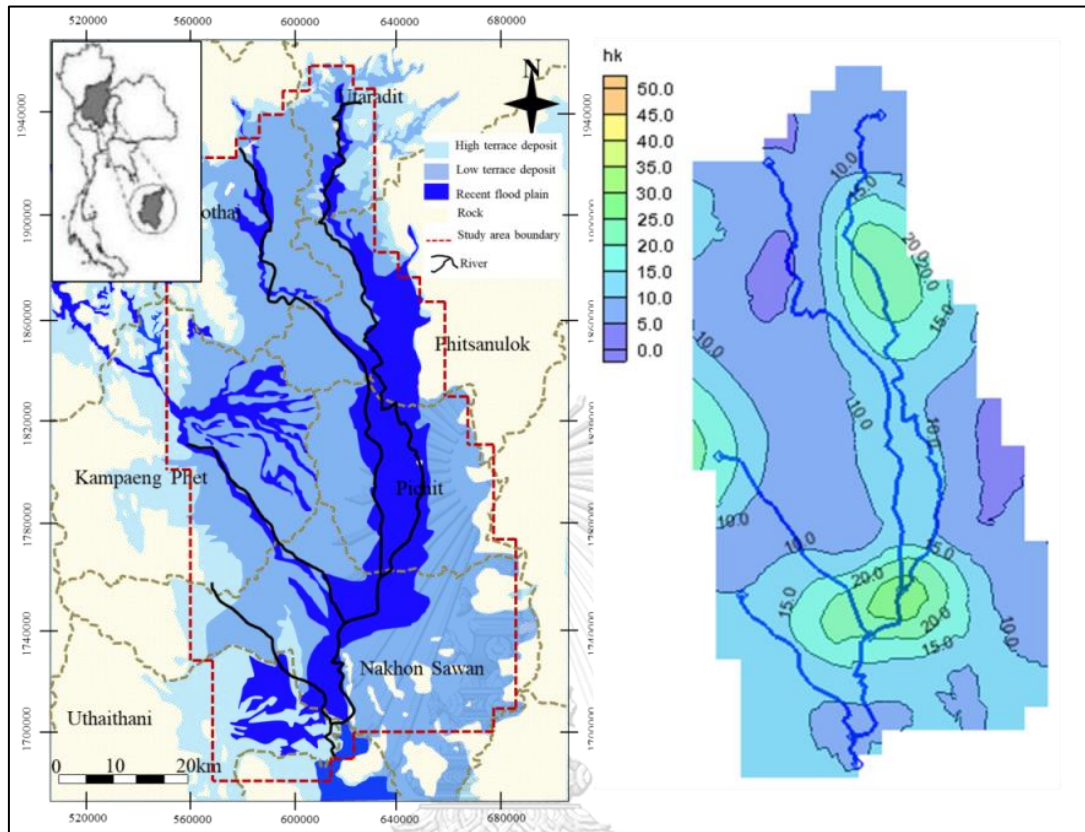
Figure 5.4 Hydraulic conductivity distributions with the Kriging method

The 3D block-centred grid model representing the groundwater basin was created for both layer 1 and 2 (Figure 5.5) which has a uniform grid size of 2 sq.km of the previous GW model grid size 10sq.km, resulting in a model grid of 152 rows and 93 columns, the total number of nodes are 14136 elements in the layer. There are more than 16597 active cells, covering a model area of $47,986 km^2$. The grid is aligned N-S and E-W. The boundary condition is defined as the western, eastern and northern borders of the model where it assumed as an impermeable body of the consolidated rock.
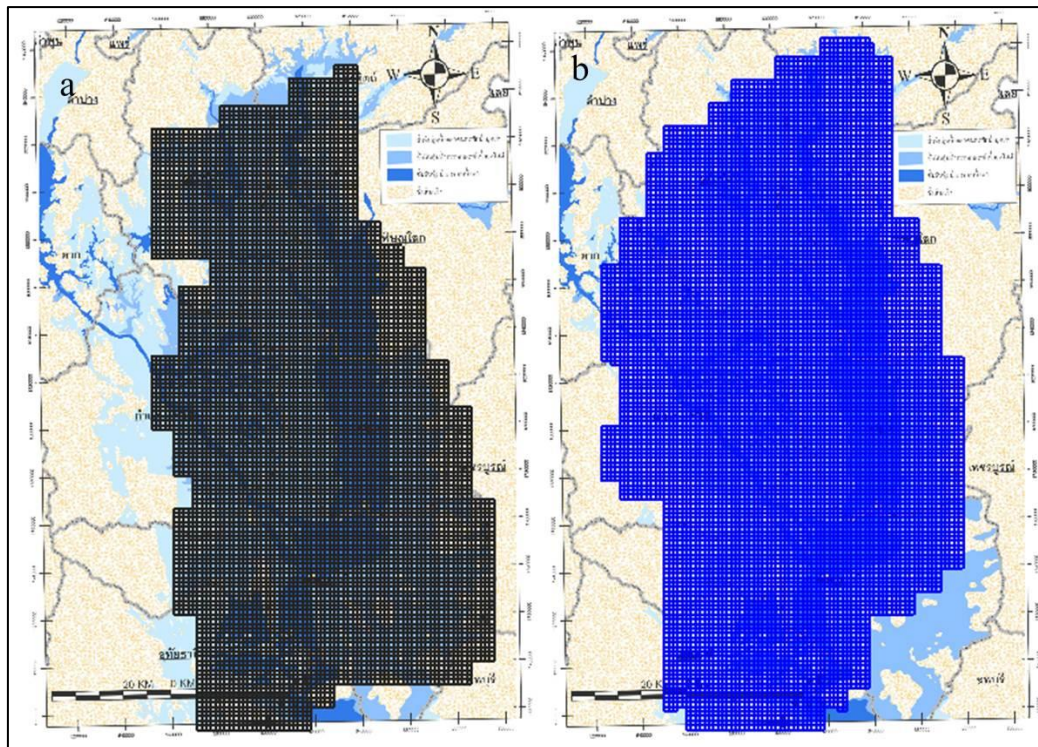
Figure 5.5 Model grid design of Regional groundwater model: a) layer 1; b) layer 2

Distribution of hydraulic conductivity estimated various methods of geostatistics and Kriging method is selected to interpolate in zoning in the groundwater model according to a good performance (Aye and Koontanakulvong (2018)). River water level, recharge rate, observed groundwater level, and boundary conditions were used (Flow in is $257,576m^3/d$; Flow out is $-111,000m^3/d$) from the previous study (Suthidhummajit and Koontanakulvong (2017)) as input data in this study. The input data for regional groundwater model improvement refers to Appendix II. The boundary conditions and model parameters are computed and assigned to the proper cells. The boundary is used to identify specific head boundaries and gave the head at boundaries.

5.2.1 Model calibration

Groundwater flow model (MODFLOW) was used to simulate groundwater flow conditions in the study area during the period 1993-2003. Model calibration is the procedure whereby model parameter structure and input parameter values are adjusted and refined to provide the best match between measured and simulated values of hydraulic heads and flows. The model was calibrated under both steady state and

transient state flow conditions. The calibration result data output from the groundwater model refers to Appendix III.

5.2.1.1 Steady-state model calibration

A steady-state model was calibrated in the 1993 study period with the data from predevelopment time. The input parameters were calibrated as point observations in a groundwater model until the output from the model matches an observed set of data. Each point dataset represents the locations in the study area where the value has been observed. In this case, the points correspond to observation wells and values are the elevation of the groundwater table (the head). Meanwhile, GMS automatically interpolates the computed solution of the observation points and the model outputs the computed values at the observation points. The results of calibration model showed that simulation values were closed with observation data in steady state after optimization as shown in Figure 5.6.
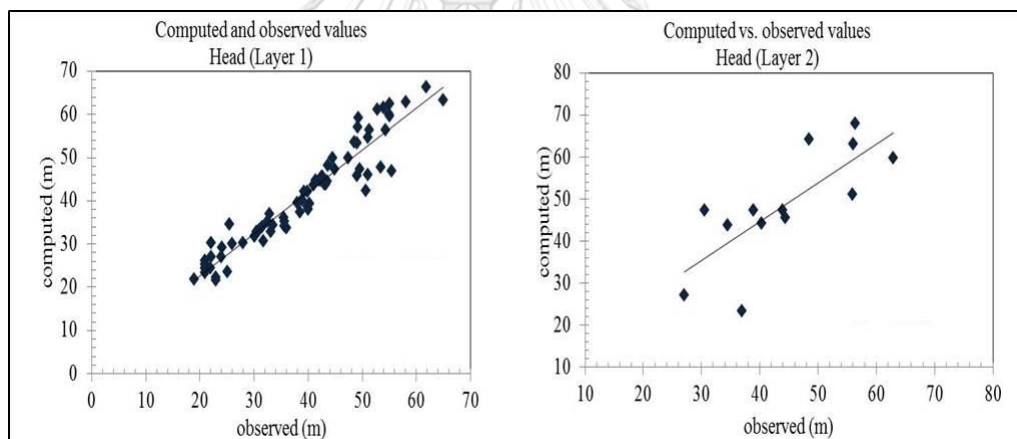
Figure 5.6 Comparison of computed and observed piezometric heads in steady state

5.2.1.2 Transient state model calibration and verification

The transient period is from 1993 to 2003, divided into annual stress period. Pumping well, recharge data, river stages, and water levels in observation wells were typically used to build a transient simulation. Transient data are entered in the conceptual model using data/time values. When the model is converted from the conceptual model to the grid model, the time values in the conceptual model are mapped to the appropriate time values corresponding to the MODFLOW stress periods.

The transient model was constructed using the calculated heads from the steady-state model as initial conditions (starting head). GMS begins with the first time step and repeatedly interpolates from the scatter point set to the target object, one time step at a time, for all of the time steps. As a result, a dataset is created on the target object with a set of time steps matching the time steps on the scatter point set.

Similar in the steady-state, input parameters were calibrated until the outputs match an observed data. Both point observation and flow observations were assigned for observation well and river where the gain or loss between the aquifer and observation has been estimated. GMS outputs the computed values at the observation points and outputs the computed flow for the flow observations. The magnitude of the residual error is displayed as a calibration target. A computed vs. observed plot displays how well the entire set of observed values match a model solution. GMS automatically draws a 45° line on the plot which represents a perfect correspondence between observed data and solution values (Usgs (2013))
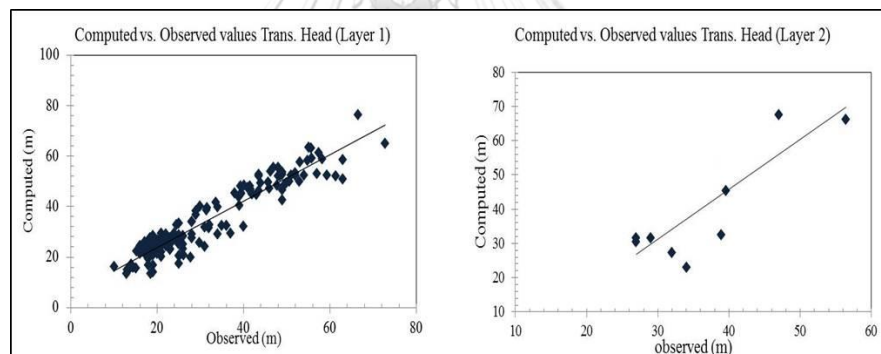
Figure 5.7 Comparison of computed and observed (calibration) piezometric heads
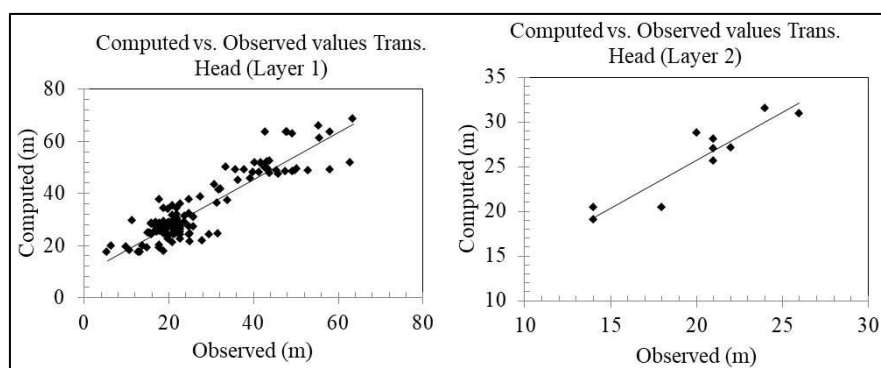
Figure 5.8 Comparison of computed and observed (verification) piezometric heads

As shown in Figure 5.7 (calibration) and Figure 5.8, the computed (verification) piezometric head values are closely related with observed data and give good

performance when compared with the observed data in both later 1 and 2. In order to evaluate the model calibration and verification results, the mean absolute error (MAE), the root mean square error (RMSE) and the Nash error (NSE) was calculated from the equations (17, 18, and 19). The error from this study is better than the previous study (Suthidhummajit and Koontanakulvong (2017)). The error summary in both states and the previous study are shown in Table 5.2.

Table 5.2 Error summaries of calibration results in both states with previous study

Error (m)	Steady-state		Transient state			
	Calibration		Calibration (1993-1999)		Verification (2000-2005)	
	Previous study	This study	Previous study	This study	Previous study	This study
Minimum	-6.98	-2.99	-14.51	-7.99	-14.17	-6.39
Maximum	9.74	3.13	7.28	8.14	8.62	8.75
Mean error (ME)	0.43	0.62	4.51	-2.75	3.84	1.72
Mean absolute error (MAE)	2.80	1.94	7.59	3.93	6.36	4.10
Root mean squared error (RMSE)	3.42	2.09	8.40	4.53	5.95	4.61
Nash-Sutcliffe coefficient (NSE)	0.92	0.98	0.67	0.94	0.497	0.93

The introduction of smaller grid size in regional groundwater model with more hydraulic conductivities data from more pumping well data and hydraulic conductivity distribution via Kriging methods redeveloped the regional groundwater model simulation in the study area. Hence, the proposed parameter estimation and its distribution were proved to workable under limited available well pump test data and can improve the piezometric head simulation when applied to the regional groundwater model in the study area.

5.2.2 Interaction mechanism from redeveloped regional groundwater model

From the previous study, the average water inflow-outflow for the year 2003 showed that the total inflow amount is 0.4MCM/day and outflow is 0.3MCM/day. The aquifer contributed an average 12% of the annual aquifer-recharge into the river (river gain) in the wet season, but is recharged from the rivers (river loss) in the dry season with 42% of the total recharge. The total groundwater used is 2.4MCM/day which is not enough for the local farmers.

Therefore, this study tried to find the interaction mechanism in more detail. For this purpose, the previous regional model was redeveloped as discussed in section 5.2. The total water flow budget boundary inflow is 0.3MCM/day (42%) and boundary outflow is 0.05MCM/day (8%) in the dry year. The net values of boundary inflow-outflow are 0.2, 0.19, 0.16 and 0.16 MCM/day in dry, drought, normal and wet year. The river loss is 0.4MCM/day in a drought year. The groundwater use is 0.6, 0.55, 0.44 and 0.43MCM/day in dry, drought, normal and wet years. The total flow budget by water year is shown in Table 5.3. Then the calibrated piezometric head will be used as a boundary for local groundwater model development as the next step.

Table 5.3 The average of total flow budget comparison with previous study and improvement

MCM/day (%)	Boundary in	River loss	Land recharge	Storage in	Total in
1993(Dry)	303,871 (42%)	36,420 (54%)	15,502 (2%)	12,615 (1.7%)	714,880
1994(Drought)	260,095 (35%)	432,467 (58%)	28,972 (4%)	7,583 (1.02%)	740,832
1997 (Normal)	230,439 (37%)	339,712 (55%)	28843 (5%)	10,333 (1.7%)	618,798
2003 (wet)	228023 (36%)	336,268 (53%)	55,994(9%)	14,191 (2.3%)	634,476
MCM/day (%)	Boundary out	River gain	Well	Storage out	Total out
1993(Dry)	57,970 (8%)	80,475 (11%)	576,204 (80%)	230 (0.03%)	714,881
1994(Drought)	65,885 (9%)	83,700 (11%)	573,417 (77%)	17,828 (2.4%)	740,833
1997 (Normal)	64,491 (10%)	81,611 (13%)	470,261 (76%)	2,433 (0.4%)	618,799
2003 (Wet)	66,162 (11%)	59,787 (10%)	495,165 (79%)	3,893 (0.6%)	625,008

NET Water Year	BC in-out	River change	Land recharge-Well	Storage change
1993(Dry)	245,901	-44,055	-646,232	12,385
1994(Drought)	194,210	348,767	-557,915	-10,245
1997 (Normal)	165,948	258,101	-441,418	7,900
2003 (Wet)	161,861	276,481	-439,171	10,298

From the Table 5.3, in the serious year (drought year), water shortage change is -0.01MCM/day which also represented by the drawdown map in the local area (to be discussed in section 5.8, Figure 5.26) showing hotspot for pumping drawdown map in the drought year.

5.3 Local groundwater model application

The main task of this section is to analyse the interaction functions and patterns of interaction mechanism in local area. Therefore, local groundwater model was developed using the required groundwater surface elevations, well locations, groundwater level, and surface water elevation. The piezometric heads from the redeveloped regional model (Aye and Koontanakulvong (2018)) were used as boundary conditions for the local groundwater model as shown in Figure 5.9. The recharge parameters: land and river and pumping were calibrated and adjusted during model calibration. The proper recharge parameters; land and river recharge were measured in the field and the values of these parameters were used to check with the calibrated interaction parameter between groundwater and surface water from the developed local groundwater model.

5.3.1 Local groundwater model development

The 3D block-centered grid model representing the groundwater basin has a grid size 400sq.m resulting in 890 elements in column and 390 elements in a row as shown in Figure 5.10. The thickness of the aquifer system for this study defined unconfined layer between 40-100m. Hydrological features are adjacent to and within the model domain represented in the model by mathematical boundary conditions. It was determined based on the geology, hydrogeology and piezometric head of the regional groundwater model (Aye and Koontanakulvong (2018)).
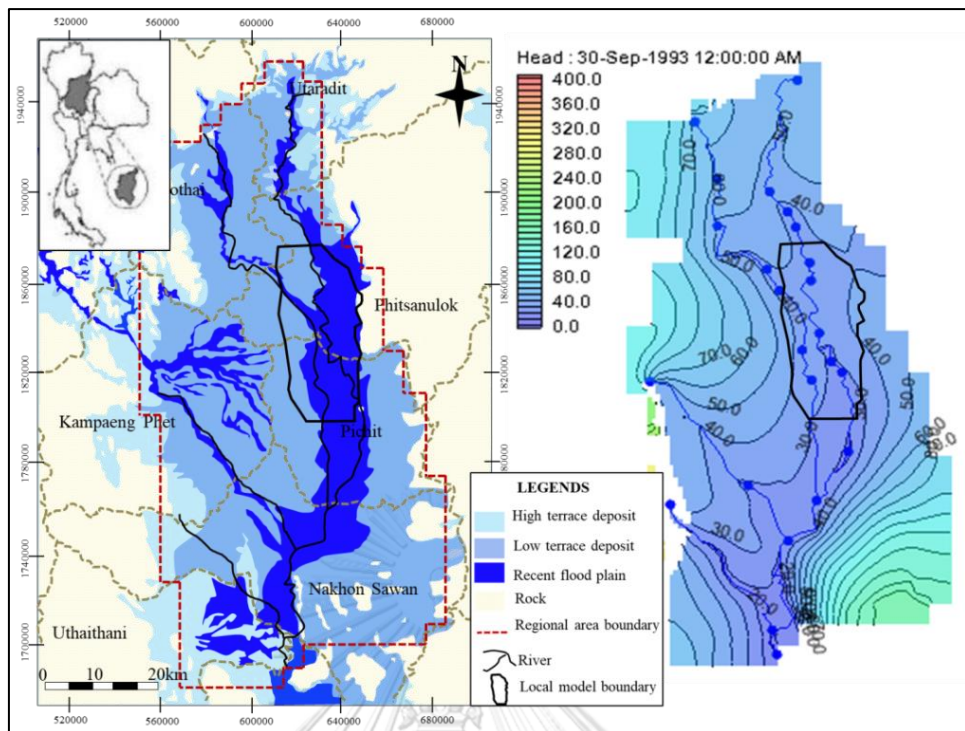
Figure 5.9 Boundary conditions for local groundwater model
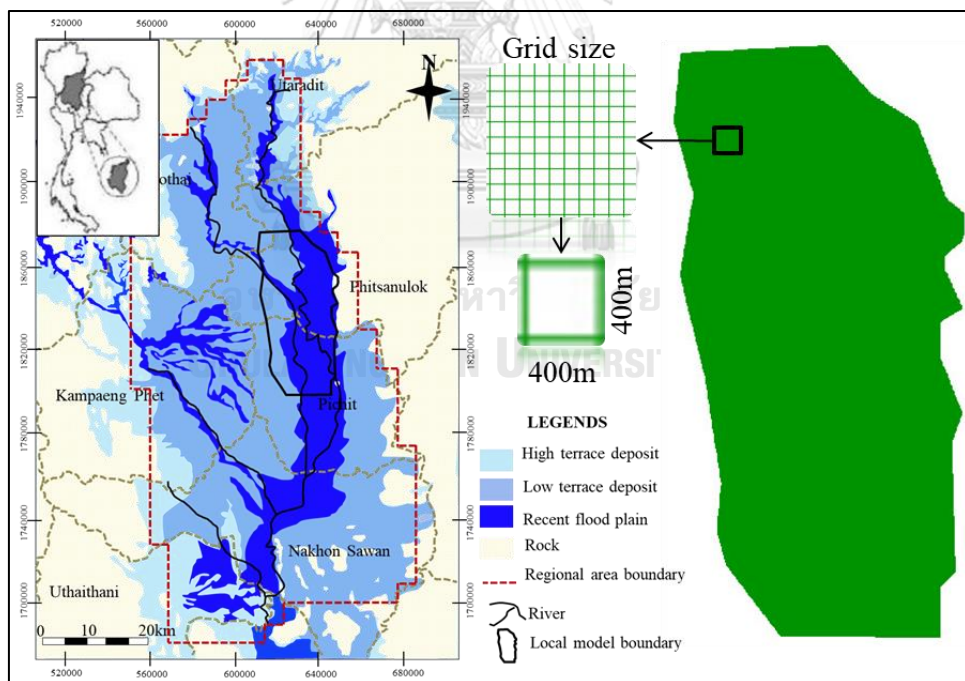
Figure 5.10 Local groundwater model grid design

5.3.2. Input parameter

Model input parameters are divided into three groups: (1) time, (2) space, as defined with layer top and bottom, and (3) hydrogeological characteristics such as

hydraulic conductivity, transmissivity, and storage parameters. Time parameters are specified when modelling transient (time-dependent) conditions, including time unit, the length, and number of time periods, and the number of time steps within each time period. The length of stress periods is not relevant for steady-state simulations. The elevation of layer top and bottom is required to calculate aquifer transmissivity, vertical leakage, or confined storage coefficient.

Recharge parameters: land and river recharge values are calibrated with the recharge coefficient (K in equation 11 and C_{riv} in equation 13) and defined to provide the best match between measured and simulated values of hydraulic heads. And pumping rates are also redistributed by seasonal and zoning with the same total annual pumping rate from the previous regional model study.

5.3.3 Interaction parameter calibrations
5.3.3.1 Land recharge

Land recharge is defined as the drawdown flow of water reaching the water table. In this study area, groundwater is mainly recharged by vertically infiltration of precipitation where it falls on the ground surface.

Land recharge parameter was calibrated by zoning based on the soil materials. Calibration used 13 wells far from the river out of total 34 wells. With this approach, input values are divided into zones where all of the cells in each zone share a single parameter value. Recharge rates were defined by percent of rainfall in each soil group zone. In this study, local area, recharge zones were defined by soil type such as zone 1 is sand; zone 3 is sandy clay; zone 4 is sandy clay loam, and zone 5 is clay as shown in Figure 5.11. The recharge coefficient (k) in equation 12 used to calibrate the recharge rate. From the previous study (Suthidhummajit and Koontanakulvong (2017)) regional groundwater model ranges from 0.003 to 0.009. The calibrated recharge coefficient is 0.004 in this study as shown in Figure 5.12 which ranges within the result of the previous study (Suthidhummajit and Koontanakulvong (2017)). The calibrated land recharge coefficient shows similar with the recharge coefficient from the field measurement (0.001-0.003) in Section 5.4.1.4 .The recharge rate is defined for each soil types. The initial recharge rate (previous study) is 6.2 cm/day for sandy clay loam. The calibrated recharge values are 3.5 cm/day for sandy

clay loam and sandy clay is 4.6 cm/day as shown in Table 5.4. The calibrated recharge rate is similar with the field measurement which is 4.43cm/day for sandy clay loam (in Section 5.4.1.4) and other studies (Lu et al. (2010), Long and Koontanakulvong (2019)) as well.
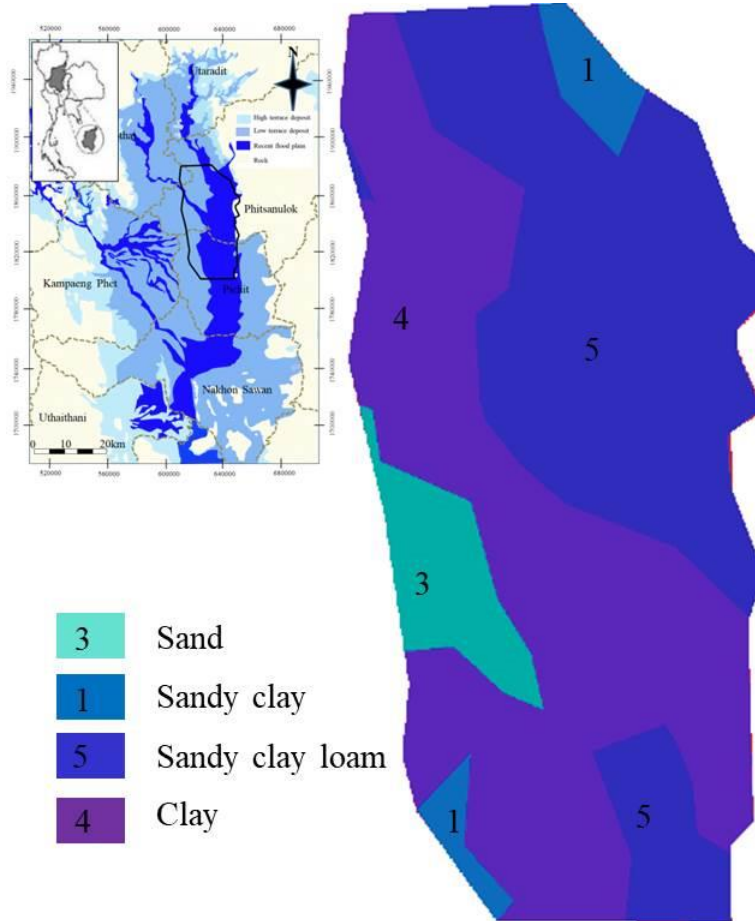
Figure 5.11 Recharge rate calibrations zoning by each soil zone (color)
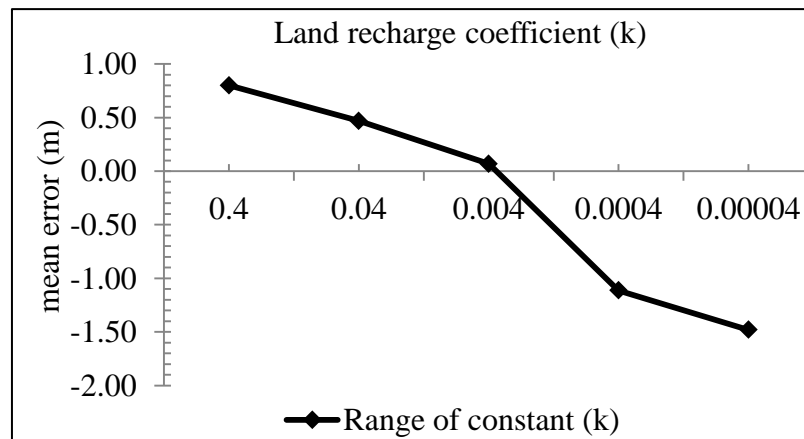
Figure 5.12 Recharge rate coefficient calibrations zoning by each soil

Table 5.4 Comparison of recharge rates by each soil types

Soil zone	Soil type	Initial recharge rate (past GW model)	Calibrated recharge rate (cm/d)
3	Sand	12.0	5.7
1	Sandy clay	9.8	4.6
5	Sandy clay loam	6.2	3.5
4	Clay	7.3	2.9

5.3.3.2 River conductance

The river is defined using a point and the river parameters include elevation, stage, and conductance. The elevation is constant. The river stage and conductance was constant in steady state and vary with time in transient state. When the river characteristic is assigned to an arc in the model, the conductance is applied over the arc (distance between two river stations), but separate elevation and stage values are applied to each of the node (river station) and the elevation and stage are assumed to vary linearly between the nodes.

The river conductance values are different from upstream to downstream base on river bed materials in this study. The bed materials of upstream, mid-stream and downstream are sand, sandy clay and clay (Chulalongkorn (2010)). The river recharge, hydraulic conductance, was calibrated with the recharge coefficient C_{riv} with equation 14 and calibrated the values 5well for upstream, 8wells for midstream, and 3wells for downstream in Nan River and 3 wells for midstream and 2wells for downstream in Yom River. Since the upstream is sand, there was a good interaction to the aquifer from upstream to downstream, the conductance values along the river is shown in Figure 5.13.

From the previous model calibration with monitored well records near rivers, the hydraulic conductance value range is from 2.2 to 2.0m/day in Nan River and 1.2 to 1.9 m/day in Yom River. The calibrated value ranges from 5.5 to 1.0m/day in Nan River and 1.5 to 1.0m/day in Yom River as shown in Table 5.5. The hydraulic conductance ranges between -0.04 to 1.63m/day for the Lower Nan and -0.02 to

1.98cm/day for the Lower Yom. (Soonthornnonda et al. (2019)). From the field measurement, seepage flux varies from 7.8 to 4.8 m/day (in Section 5.4.2.1). The field measured conductance values shows higher values than those previous model values which are caused by measured locations. The study found that the higher seepage fluxes were observed while the seepage meters were placed closer to the river bank. However, these calibrated values are closed to the other study (0.1 to 4.9 m/d) in Saigon River (Tuan and Koontanakulvong (2018)) and used in local groundwater model development.
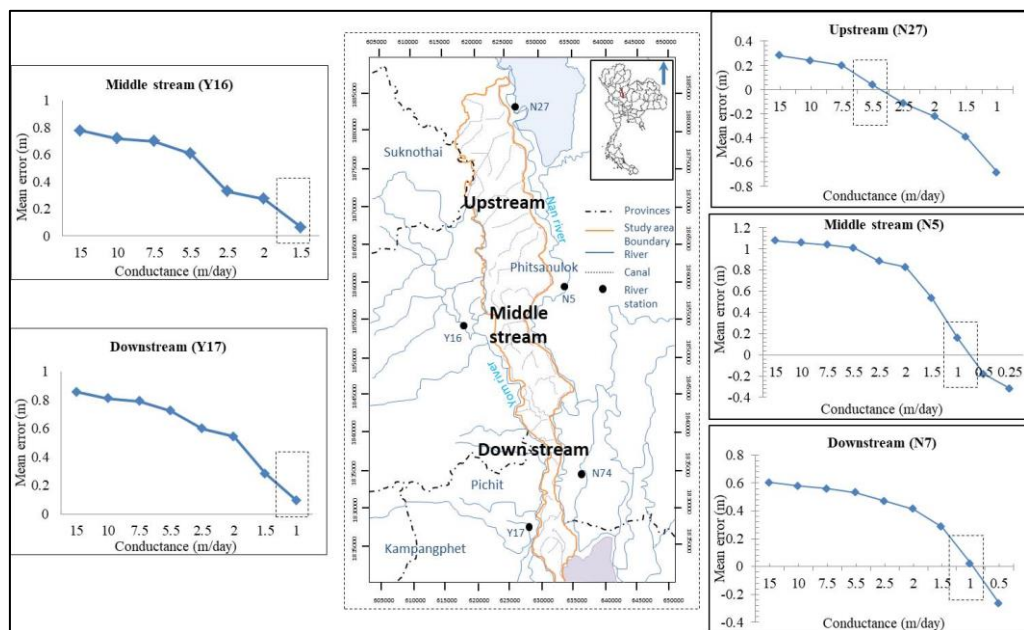
Figure 5.13 Recharge rate coefficient calibrations zoning by each soil

Table 5.5 Error estimation of river conductance value for each bed material

Stream	Bed material	Previous study		Calibrated value	
		Nan	Yom	Nan	Yom
Upstream	Sand	2.2	-	5.5	-
Midstream	Sandy clay	2.1	1.2	1.0	1.5
Downstream	Clay	2.0	1.9	1.0	1.0

5.3.3.3 *Pumping rate redistribution*

Pumping wells are specified by assigning a pumping rate to a cell at the location of each well. In Plaichumphol Irrigation Project area, the farmer used groundwater annually 143.6MCM/day with 69 MCM/day in the wet season and 74 MCM/day in the dry season (Bejranonda et al. (2008)). The average groundwater use in a normal water year is 134.4 MCM/day with 40% and 60% in the wet and the dry season (Koontanakulvong and Panot (2003)). The groundwater used from the previous model results (Suthidhummajit and Koontanakulvong (2017)) in the wet season is 109.2 MCM/day and in the dry season is 43.3 MCM/day. Annually groundwater use is 146.2 MCM/year. In this study, pumping rates were redistributed by seasonal and zoning of total 525 wells including 34 observed well separated by the river slope (up, mid, downstream) and side of the river (left and right in Figure 5.14) with same total annual pumping rate from the previous model study.
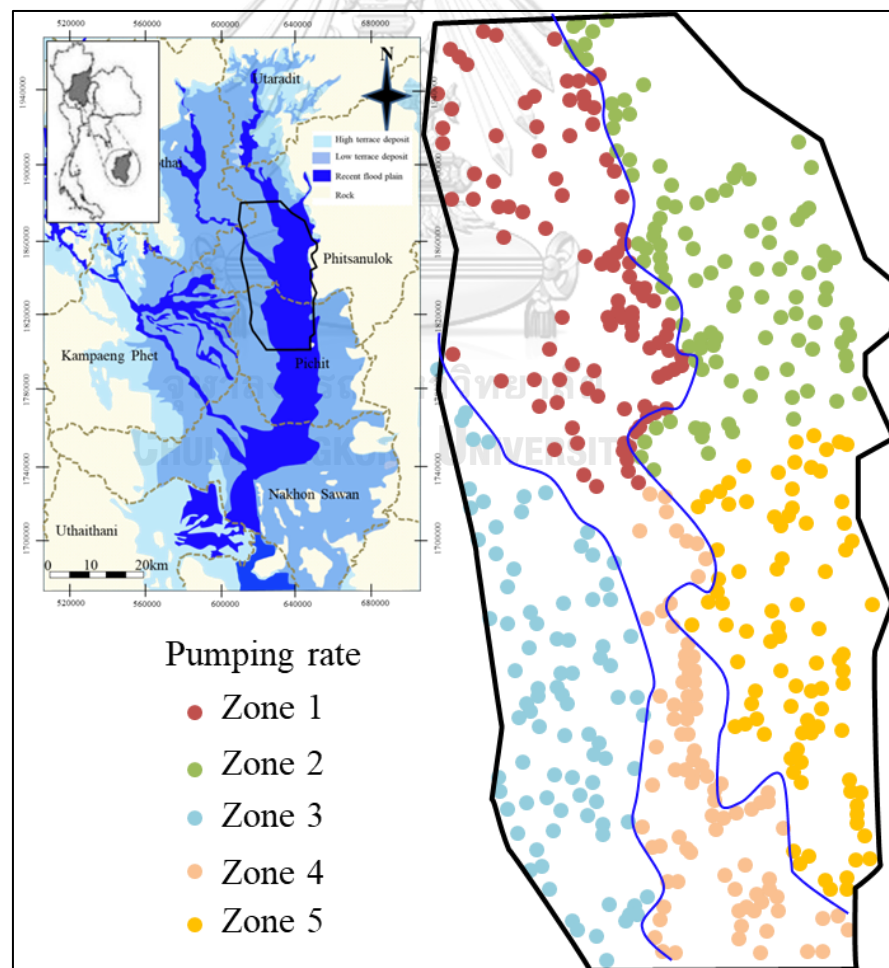
Figure 5.14 Pumping rate zone

Figure 5.15 and Table 5.6 show the error adjustment of the pumping rate for each pumping range. The pumping rate was adjusted in 0.5 times in the wet season and decrease 2.0 times in the dry season according to the error estimation. After adjustment, the groundwater pumping rate in wet season is 67.3 MCM/day in 75.7 MCM/day in the dry season. Annual groundwater use is 143.1 MCM/year.
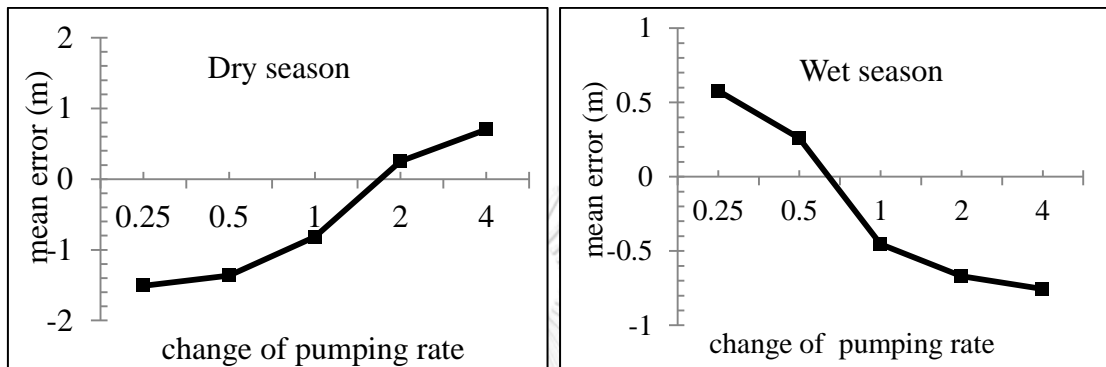
Figure 5.15 Pumping rate by error

Table 5.6 The pumping range by error (m)

Pumping range	Dry season (Error)	Wet season (Error)
0.25	-1.51	0.57
0.5	-1.36	0.25
1.0	-0.81	-0.45
2.0	0.25	-0.66
4.0	0.70	-0.75

5.3.4 Piezometric distribution comparison

First, the boundary conditions for the local model are defined from piezometric heads of the regional model and the groundwater conditions of the local model were checked. Then, piezometric heads at boundaries are repeatedly run and check until the local groundwater model gave close to the water level as shown in Figure 5.16.

Second, local groundwater model was calibrated with 34 observed wells whereby model parameter structure and parameter values are defined to provide the best match between measured and simulated values of hydraulic heads and flows. Finally, recharge parameters; land and river were calibrated with recharge coefficients and then, 525 pumping wells are redistributed from seasonal and zoning. When they are fixed, interaction parameters are calibrated one by one in the affected areas and checked with the field measurement data and other studies.
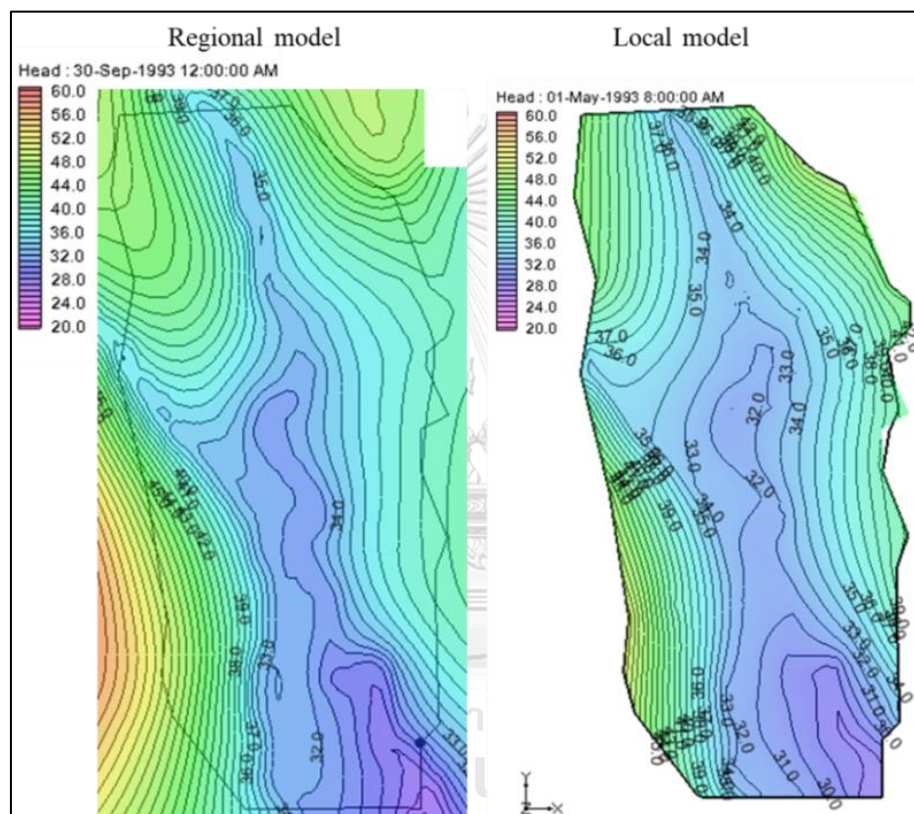
Figure 5.16 Groundwater level condition of the model: Right (regional); Left (local)

5.3.5 Model calibration

5.3.5.1 Steady-state model calibration

A steady-state model was then calibrated with data from development time. The purpose is to establish an initial/starting water level for transient calibration. The stress period for simulation is 1993. The results of the calibration model show that simulation values were closed with observation data Figure 5.17.
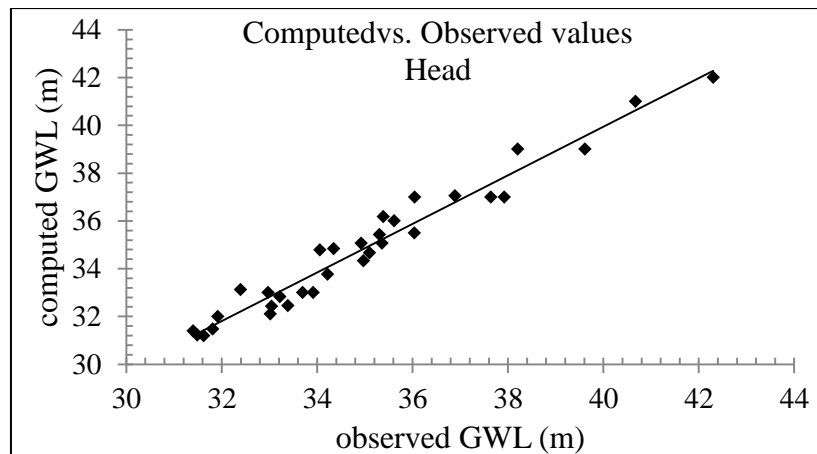
Figure 5.17 The steady-state model calibration

5.3.5.2 Transient model calibration

The transient model was constructed using the calculated heads from a steady-state model as initial head conditions. The transient period is from 1993 to 2003, divided into monthly stress period for which pumping rates were defined. Monthly stress periods were used to capture the changes in abstraction and recharge rates. Scaling factors for recharge and stream flows from the steady-state calibration were adopted in the transient calibration. Calibration was done by comparing simulated hydrographs with measured hydrograph. Similar to the result of the steady-state, the computed piezometric head values in the transient state gave good performance when compared with observed data (Figure 5.18). The total error summary in both states is shown in Table 5.7.
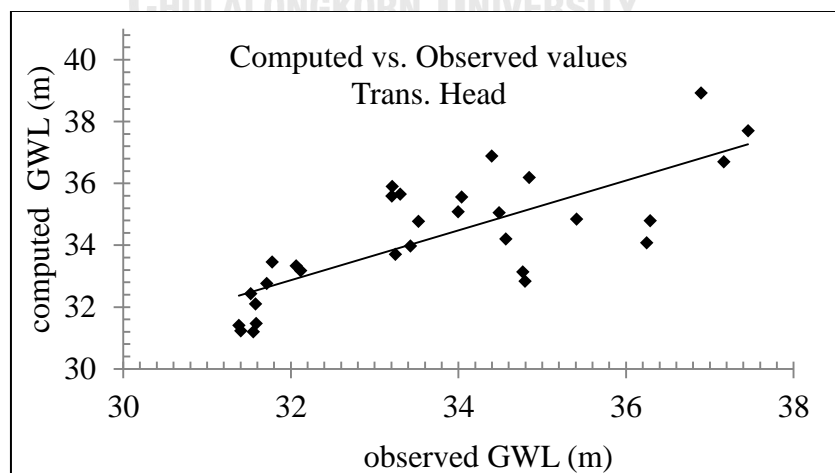
Figure 5.18 The transient state model calibration

Table 5.7 Error summaries of calibration results in both states

Error (m)	*Steady-state*	*Transient*
Minimum	-0.92	-2.18
Maximum	0.96	2.68
Mean error (ME)	-0.14	0.53
Mean absolute error (MAE)	0.50	1.16
Root mean squared error (RMSE)	0.58	1.39
Nash-Sutcliffe coefficient (NSE)	0.92	0.69

The local groundwater model was developed and calibrated in both steady and transient states. A steady-state model was calibrated with data from development time and the transient model was constructed using the calculated heads from a steady state mode as initial head conditions. The computed piezometric head values of a steady state and transient state gave a fairly good performance when compared with the observed data.

5.4 Parameter estimation via field measurement data

The goal of this study is to measure the proper recharge parameter: land and river in the field site. To investigate land recharge and river conductance, the values of the interaction parameters were used to check with the calibrated interaction parameters between groundwater and surface water from the developed local groundwater model. Figure 3.11 showed the site location where the measurement was conducted to estimate land and river recharge. A field investigation was done in Plaichumphol Irrigation Project (PIP), Phitsanulok Province to set up the soil moisture sensor for land recharge analysis and seepage meter installation for river conductance analysis (Aye et al. (2019)). Soil moisture sensor was installed to analyse land recharge for groundwater model development. Seepage measurement was done to measure the flow of water between groundwater and surface water along the rivers (Nan River and Yom River). The detailed soil moisture construction design, model setup and soil moisture data analysis in HYDRUS-1D are attached in Appendix IV. The data analysis for deep percolation and results are discussed as follows.

5.4.1 Deep percolation via soil moisture sensor

Deep percolation was calculated using equation 11(Šimůnek (2005)). For this calculation, soil moisture sensor system designed with Arduino was developed to understand deep percolation (land recharge) characteristic in the unsaturated zone for developing groundwater modelling and installed (1-4m) depth in the soil at an agricultural field (spacing 1m) for land recharge analysis.

5.4.1.1 Percolation characteristics

The percolation characteristics are described with percolation rate and soil moisture content and have different characteristics at the depths of 1 and 2 meter. The percolation rate at 0-1m depth has two different curves during wetting and drying stages of soil due to the evaporation and transpiration from soil storage. The daily percolation rate is 5.07 cm/day when the soil moisture reached to 41% (saturated) and decreases to 0.02 cm/day when the soil moisture is 17% (wilting point) (Figure 5.19). However, the daily deep percolation from 1m depth to 2m depth is almost in one curve both in the wetting and drying stages due to the effect of no evaporation to water storage in the soil and its daily maximum rate is 4.43 cm/day (Figure 5.20) when the soil moisture is saturated (39%). It can be seen that the effect of evaporation makes the different percolation characteristics of shallower (1m) and deeper (2 m) percolations. The recharge coefficient (k) is calculated using equation 12 to check the calibrated results from the model. The coefficient of recharge rate ranges from 0.001 to 0.003. Which is similar to the calibrated recharge coefficient from the model result (0.004) in Section 5.3.3.1.
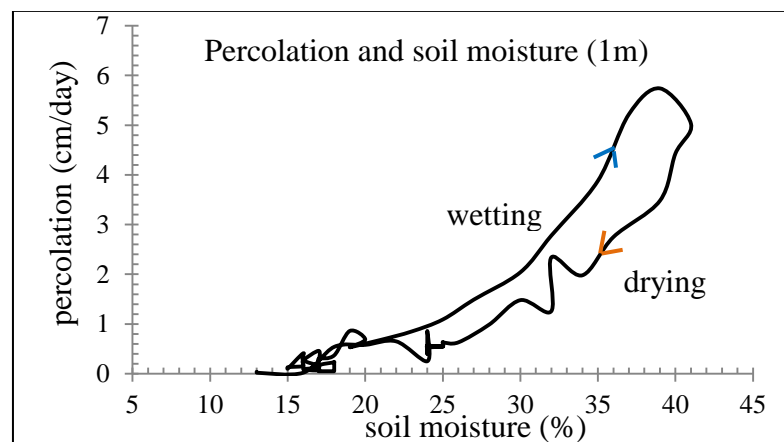
Figure 5.19 Percolation rate and soil moisture at 1m depth (wetting and drying)
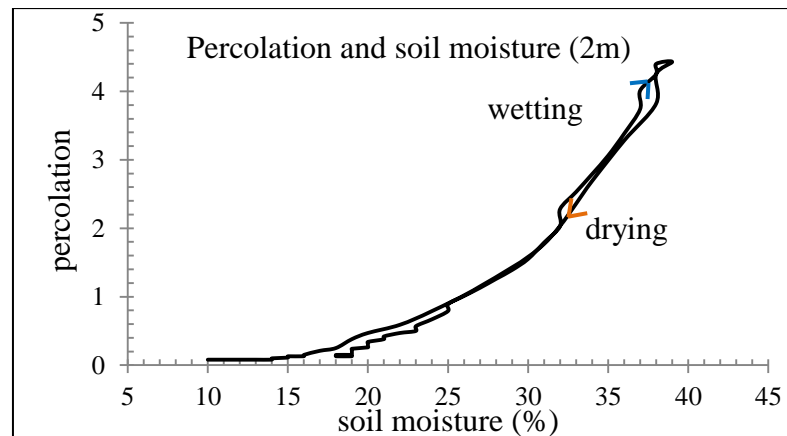
Figure 5.20 Percolation rate and soil moisture at 2 m depth (wetting and drying)

5.4.1.2 Percolation rate

From the field data and simulated percolations, the function of deep percolation can be established. The daily functions of effective infiltration and deep percolation at 1m and 2m depth can be derived for five stages namely wilting point (stage 1), field capacity (stage 2), saturation (stage 3), drying 1 (stage 4), and drying 2 (stage 5) as shown in Figure 5.21 and Figure 5.22. The functions of deep percolation (at 1 m and 2 m depths) and accumulated effective infiltration at each stage of soil moisture are shown in Table 5.8 and Table 5.9 (Cooper et al. (1990)). It can be seen that the percolation rate increased in soil with higher effective infiltration rate, deeper water table, soil moisture value in the subsoil (between saturation and field capacity). The average percolation at 2m depth during the study period is 0.52 cm/day in the rainy season which is in the range with the past study (Lu et al. (2010), Schincariol and Mcneil (2002)).
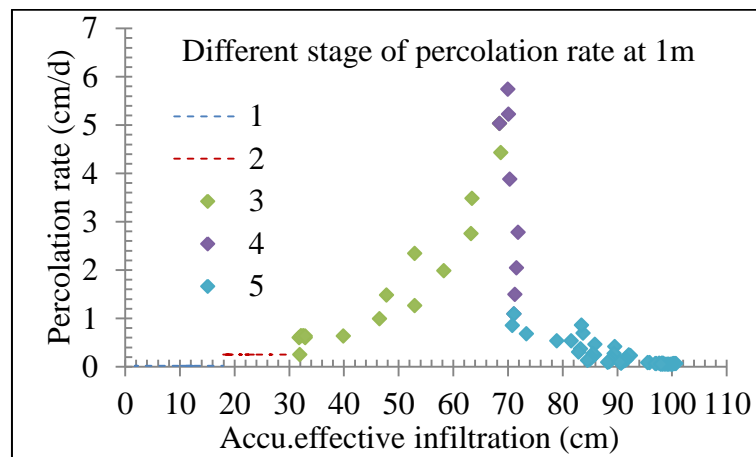
Figure 5.21 Percolation rate with different stages (1m)
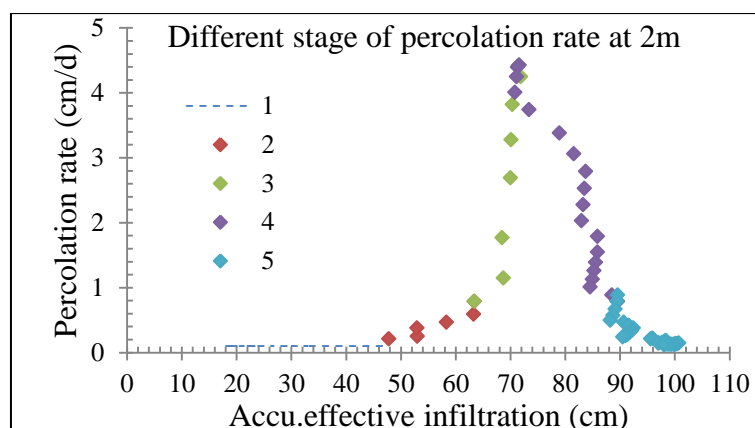
Figure 5.22 The deep percolation rate with different stages (2m)

Table 5.8 Functions of deep percolation at different stages (at 1 m depth)

Remarks: y=deep percolation rate (cm/day), x=accumulative effective infiltration

Stage	Phase (No. of Day)	Soil moisture (%)	Accumulative effective infiltration			Percolation rate			Percolation function	R^2
			max	min	avg	max	min	avg		
1	Wilting point (10)	<17	17.9	1.7	10.7	1.1	0.02	0.3	constant	—
2	Field capacity (8)	17-25	31.9	17.8	22.5	0.8	0.3	0.5	constant	—
3	Saturation (35)	25-41	68.6	31.8	47.3	5.0	0.5	1.8	y=0.09x-2.74	0.84
4	Drying 1 (7)	25	71.8	68.4	70.6	5.7	1.1	3.4	y=-1.2433x+91.14	0.57
5	Drying 2 (45)	<17	100.7	70.8	90.4	1.1	0.1	0.2	y=-0.0268x+2.65	0.70
	Avg	21.12	100.7	1.7	55.6	5.7	0.02	0.7		

Table 5.9 Functions of deep percolation at different stages (at 2 m depth)

Remarks: y=deep percolation rate (cm/day), x=accumulative effective infiltration

Stage	Phase (No. of Day)	Soil moisture (%)	Accumulative effective infiltration			Percolation rate (land recharge rate)			Land recharge function	R^2
			max	min	avg	max	min	avg		
1	Wilting point (49)	<17	47.7	17.8	26.6	0.2	0.1	0.1	constant	—
2	Field capacity (13)	17-25	63.4	47.7	56.4	0.8	0.2	0.5	y=0.03x-1.39	0.86
3	Saturation (7)	25-41	71.8	63.4	69.3	4.4	0.8	2.8	y=0.45x-28.64	0.74
4	Drying 1 (15)	25	89.5	70.8	81.2	4.4	0.8	0.5	y=-0.19x+17.98	0.89
5	Drying 2 (31)	<17	00.7	8.2	5.0	0.8	1	0.3	y=-0.04x+4.09	0.67
	Avg	20.92	100.7	17.8	55.6	4.4	0.1	0.5		

5.4.2 River conductance via seepage meter

    Cylindrical seepage meter was constructed inexpensively in the Plaichumphol Irrigation Project area to investigate the river conductance value. The seepage meter used in this study was modified to measure the flow of surface water and groundwater along the river (Nan and Yom Rivers) from those described by (Lee et al. (1978)) and consists of a pan and a collection bag. The detail seepage meter installation and design are attached in Appendix VI.

5.4.2.1 Data analysis

    The purpose of seepage measurement is to know discharge and recharge from river seepage to analysis interaction mechanism and to compare and check the local groundwater model (flux) is correct. Table 5.10 shows the results of the seepage meter measurement. Based on the soil type, seepage flux range varies from 4.8 is clay, 5.5 to 5.7 is silt and 6.3 to 7.8 is sand. The results show that the seepage rate in the Yom River is higher than the rate in the Nan River due to the groundwater flow situation and river bed materials. These would indicate that the fluxes were observed while the seepage meters were places near the river bank. The results from seepage measurement were used to check with the calibrated recharge parameter from a developed local groundwater model.

Table 5.10 Seepage meter measured data

River	bed material		hydraulic conductivity (m/d)	Conductance (m^2/d)	Seepage (m/d)	Hydraulic conductivity (Todd et al. (1976))
Yom River	mid	sand	0.27	7.18	0.40	0.2
	down	sand	0.18	6.30	0.33	0.2
Nan River	up	silt	0.14	5.70	0.17	0.08
	mid	silt	0.13	5.50	0.10	0.08
	down	clay	0.04	4.80	0.08	0.002

5.5 Comparison of model and field parameter data

The goal of this section is to compare and check the interaction parameter with the developed local model results to determine the interaction mechanism in the next study. The recharge parameters; land recharge and river conductance, from model results were checked with the field measurement data and other studies.

Land recharge rates were defined by each soil types as shown in Table 5.4. The initial recharge rate form previous model is 6.2cm/day for sandy clay loam which is higher than the field measurement data (4.43cm/day) for the same soil type due to the recharge coefficient. The calibrated land recharge rate from the model result for sandy clay is 4.6cm/day and sandy clay loam is 3.5cm/day is sandy clay loam which is closed to the field measured data and is also in the range with the other studies (Lu et al. (2010), Schincariol and Mcneil (2002)). Table 5.11 shows the seepage values which are different from upstream to mid-stream and downstream on river bed materials.

Table 5. 11 The comparison of the calibrated river conductance

Stream	Bed material	Previous study (m/d)		Present study (m/d)		Field measurement (m/d)	
		Nan River	Yom River	Nan River	Yom River	Nan River	Yom River
Upstream	sand	2.2	-	5.5	-	7.8	-
Mid-stream	sandy clay	2.1	1.2	1.0	1.5	5.7	5.5
Downstream	clay	2.0	1.9	1.0	1.0	4.8	4.4

The riverbed materials are sand, sandy clay and clay (Chulalongkorn (2010)). From the previous model calibration with monitored well records near rivers, the hydraulic conductance value range from 2.2 to 2.0m/day in Nan River and 1.2 to 1.9m/day in Yom River. From the field measurement, seepage flux varies from 7.8 to 6.3m/day in Yom River and 5.7 to 4.8m/d in Nan River. The field measured conductance values shows higher values than those previous model values which are

caused by the near bank measured locations (Soonthornnonda et al. (2019)). Since the upstream is sand, there was a good interaction to the aquifer from upstream to downstream. The calibrated values range from 5.5 to1.0m/day in Nan River and 1.5 to 1.0m/day in Yom River which values are smaller than field measurement data. However, these calibrated values are closed to the other study (0.1 to 4.9 m/day) in the Saigon River (Tuan and Koontanakulvong (2018)).

5.6 Groundwater flow budget from local groundwater model

This section aims to investigate the groundwater flow budget change patter mainly focused on analysing the groundwater and river interaction pattern and volume by seasonal and water year in term of groundwater recharge, river recharge, groundwater storage, and groundwater pumping. Flow budget of local groundwater model was analysed using equation (15) to present the exchange of flow volume of all components of groundwater budget including surface water and groundwater interactions. The data output from the groundwater model attached in Appendix III.

The groundwater flow budget is analysed in seasonal: rainy (April to September) and dry (October to March) and water year patterns (very dry, dry, normal, wet based on dam storage volume) (Suthidhummajit and Koontanakulvong (2017)) from well-calibrated groundwater model results. The annual average rainfall is about 1243mm/year (Chulalongkorn (2010)). From the analysis, the groundwater flow budget can be described as shown in Figure 5.23 (wet season, dry season). It is clear that groundwater flow from the boundary area into the aquifer is the main input to the aquifer system with 8.95MCM/day (wet season) and 4.22MCM/day (dry season) and the boundary outflow is less about 2.14MCM/day (wet season) and 2.04MCM/day (dry season). Annually groundwater flow budget is shown in Table 5.12.
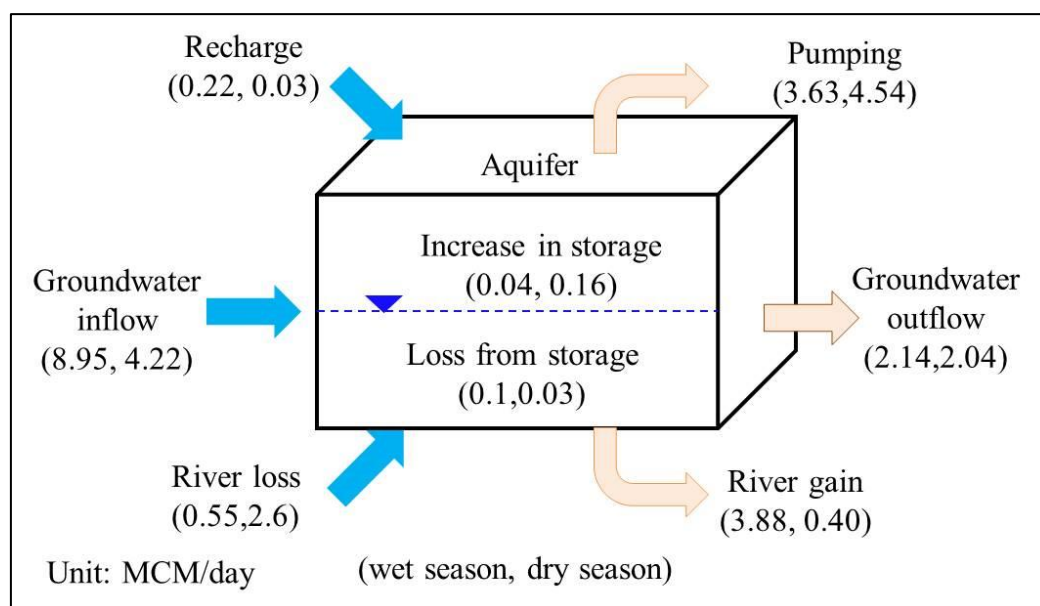
Figure 5.23 The conditions of groundwater flow budget

Table 5.12 Annual groundwater flow budget; unit: MCM/day

Annual	Boundary Inflow	River loss	Land recharge	Storage in	Total in
Average of total	13.17	3.15	0.25	0.19	16.76

Annual	Boundary outflow	River gain	Pumping	Storage out	Total out
Average of total	4.18	4.28	8.1	0.13	16.69
Annual Net	+8.99	-1.13	-7.93	+0.06	-0.01

5.7 Interaction parameter estimation

The purpose of this section is to understand surface water and groundwater interaction mechanism (volume and patterns) via the development of groundwater model. For this purpose, the interaction parameters were estimated in Section 5.4. In this section, the estimated interaction parameters were used in a developed local groundwater model and the interaction mechanism was analysed from the flow budget of local groundwater model and river loss and gain regime. The schematic illustration

for evaluating stream-aquifer interaction is shown in Figure 5.24. Rainfall as land recharge, groundwater inflow, river recharge to groundwater are recharge parameters to the aquifer and groundwater outflow, river discharge and well abstraction are output from the aquifer.

5.7.1 Interaction volume by water year

The groundwater interaction volume is determined by water year which is defined by the reservoir storage of Bhumipol and Sirikit Dam as shown in Table 4.1. According to flow budget analysis from local groundwater model as shown in Table 5.13, well abstraction is 8.9MCM/day in a drought year and 6.4MCM/day in a wet years. River discharge is 4.3MCM/day in a drought and 0.3MCM/day in a wet year. In average, the land recharge is 0.24MCM/day, river change is 2.02MCM/day and groundwater use is 7.38CMCM/day. Land recharge seems not to affect to the flow interaction. River recharge plays a major role to balance the groundwater accumulation in this area.
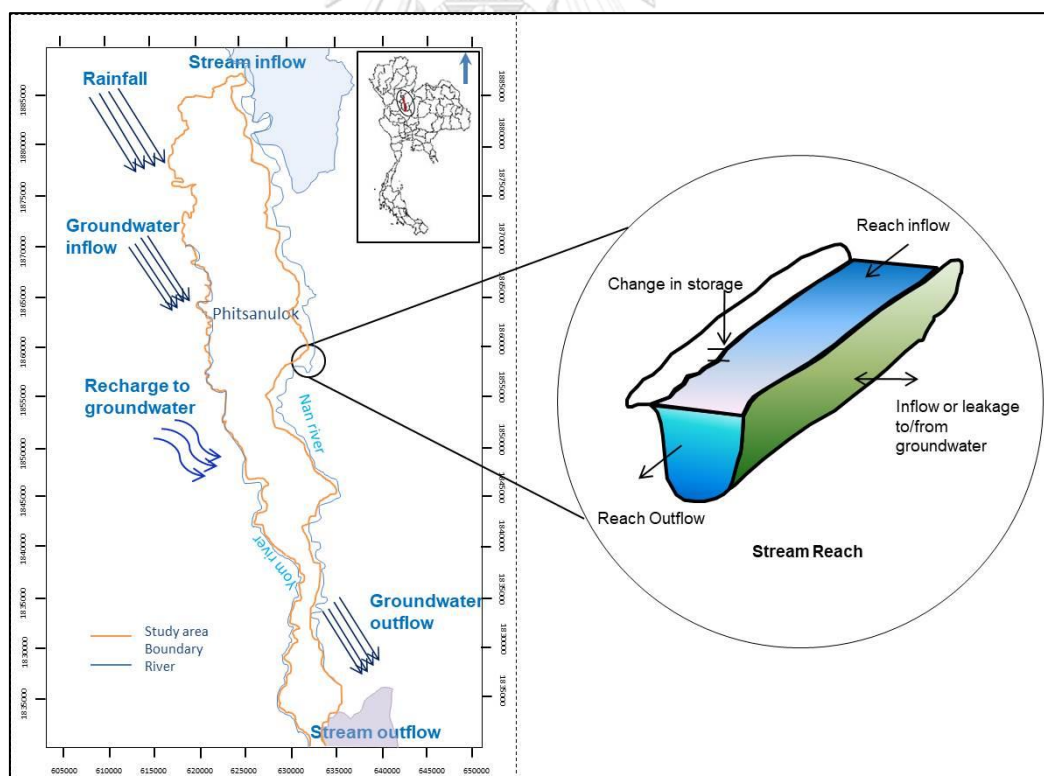
Figure 5.24 Schematic illustrations for evaluating stream-aquifer interaction

Table 5.13 Water budget by water year in each parameter; unit: MCM/day

Water year	Drought	Dry	Normal	Wet	Avg
Land recharge	0.20	0.22	0.22	0.30	0.24
River loss	4.37	4.62	4.83	5.35	4.79
River gain	3.01	2.46	2.66	2.95	2.77
Well	8.92	7.03	7.10	6.48	7.38

5.7.2 River loss and gain

There are two main aspects of the interaction between surface water and groundwater (Darul et al. (2015)). Firstly, the flow of groundwater support rivers flow and secondly the flow from rivers to groundwater. In this study, the river flow is derived essentially from precipitation. The interaction of surface water and groundwater is primarily determined by the relation between surface water and groundwater levels. The rate of flow between the stream and the aquifer is calculated from the different in hydraulic heads in the river and the adjacent aquifer using the equation (15) (Mcdonald et al. (1988)). There are totally three river stations along Nan River and two stations at Yom River. During the dry season (October to March) the observed groundwater level increased than river water level. In the rainy season (April to September) the annual average rainfall is about 1243mm/year and the river water level rises (Chulalongkorn (2010)). The condition of river loss and gain during the period study period (1993-2003) is shown in Table 5.14 and Figure 5.25. Nan River gain from the aquifer in upstream is 2,385m^3/day and water store in the mid-stream 903m^3/day and aquifer gain the water 1,491m^3/day in downstream. Aquifer loss to Yom River is 897-708m^3/day from mid-stream to downstream. It means that the river store water in the upstream and release flow to the downstream.

Table 5.14 The conditions of river loss and gain during the study period (1993-2003)

Nan River	Upstream	Mid-stream	Downstream
Aquifer gain	+1.234.20	+1,276.29	+2,200.53
Aquifer loss	-3,628.59	-373.07	-708.62
NET	-2,385.39	+903.22	+1,491.91
Yom River	Upstream	Mid-stream	Downstream
Aquifer gain	-	+1,058.06	+785.24
Aquifer loss	-	+160.20	-76.45
NET	-	+897.86	+708.9
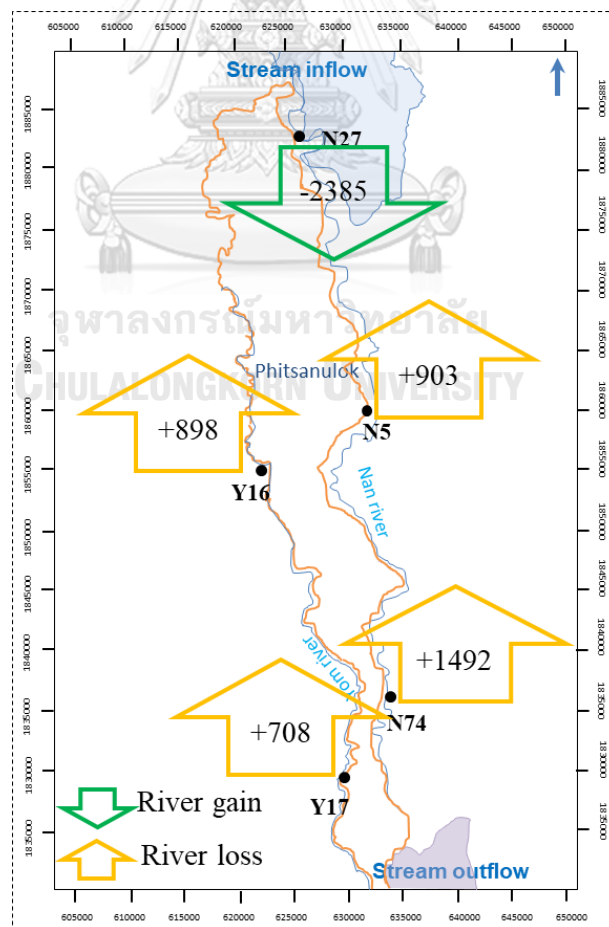
Figure 5.25 River stations and the conditions of river gain and loss

5.8 Applications to groundwater management

From this study, the groundwater management was assessed from the flow budget for a dry year (1993), a drought year (1994), a normal year (1997) and a wet year (2001). As shown in Figure 5.26, the main component of the inflow to the aquifer in this area is the boundary from the outside area. The net of the boundary inflow/outflow is 70.7, 70.3, 67.5 and 68.4MCM/day (dry, drought, normal and wet year) in the wet season and 27.9, 36.1, 24.2 and 28.0MCM/day (dry, drought, normal and wet year) in the dry season. The net of the water storage change is 0.1MCM/day in the dry season and -0.1MCM/day in the wet season (a drought year). Groundwater mainly received the water inflow from the boundary of the outside area.

Wet season	Boundary in	River loss	Recharge	Storage in
Dry	95.9	1.6	2.1	0
Drought	95.6	2.3	2.0	0.01
Normal	92.4	4.8	2.1	0.07
Wet	88.6	9.1	2.5	0.02
Wet season	Boundary out	River gain	Well	Storage out
Dry	25.1	48.0	25.5	0
Drought	25.3	43.5	31.3	0.13
Normal	24.9	40.9	34.1	0.01
Wet	20.2	34.7	44.2	0.08
NET	Boundary in-out	River change	Recharge-Well	Storage change
Dry	70.7	-46.4	-23.0	0.0
Drought	70.3	-41.2	-29.2	-0.1
Normal	67.5	-36.1	-32.1	0.1
Wet	68.4	-25.6	-42.1	-0.1

Dry season	Boundary in	River loss	Recharge	Storage in
Dry	58.7	38.8	0.4	0.18
Drought	66.5	30.7	0.3	0.15
Normal	55.2	42.5	0.4	0.13
Wet	61.1	36.8	0.5	0.09
Dry Season	Boundary out	River gain	Well	Storage out
Dry	30.8	3.3	65.1	0.00
Drought	30.4	12.0	57.6	0.06
Normal	31.0	4.2	64.7	0.01
Wet	33.0	4.1	62.0	0.05
NET	Boundary in-out	River change	Recharge-Well	Storage change
Dry	27.9	35.6	-64.7	0.2
Drought	36.1	18.7	-57.3	0.1
Normal	24.2	38.3	-64.3	0.1
Wet	28.0	32.7	-61.5	0.0

Figure 5.26 Flow interaction parameters by water year/season (MCM/day)

In a drought year, groundwater received 2.1MCM/ay (2.1%) in the wet season and 0.3MCM/day (0.34%) in the dry season from land recharge. In a wet year, groundwater received from the land recharge is 2.5%) in the wet season and 0.51% in of total inflow in the dry season. Additionally, the river discharge (river loss) to the

aquifer is 9.08% in the wet season and 37% in the dry season. It means that the groundwater received mainly from the river as an inflow in this area.

Wells abstraction from the aquifer is 31% in the wet season and 57% in the dry season during the drought year of the total outflow. The river gain from the aquifer is 43% in the wet season and 12% in the dry season (a drought year). The output (well + river gain) from the aquifer is 143% (both dry and wet season) which is higher than the input (land recharge + river loss is 49.09% to the aquifer in a drought year. However, the boundary is filled back to the aquifer to complete the requirements. It means that the groundwater needs more input from the upstream and upper boundary, thus, the groundwater stores the water in a wet year and supports in a drought year.

From the above flow budget study, the drought year is the serious year in this area for the interaction. Then Figure 5.27 discussed the groundwater use using a pumping hotspot approach by water year to respond to the future water risks. From groundwater model analysis, the water level in the central part of the study area is lower than 32m. The groundwater level in this area (local) is 40m above mean sea level (MSL). The location of each point represented by water year is shown in Appendix III, Section III.2.5.
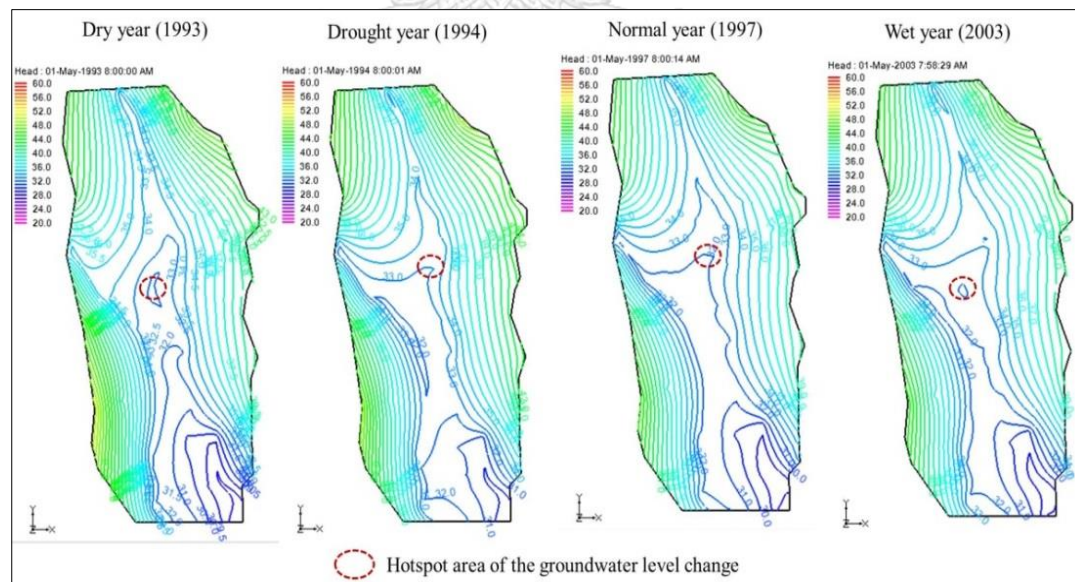
Figure 5.27 Changes in groundwater level by water year

As shown in Figure 5.28 and Figure 5.29, changes in water drawdown were calculated for drought, dry, normal and wet year by the water season from the relationship of pumping and groundwater storage. In drought year (wet season), the

groundwater storage is -279MCM/day while the groundwater pump out 37m^3/day and observed water level is 29m above MSL. In a drought year(the dry season), the groundwater storage is (-9965)MCM/day when groundwater pump out 52m^3/day and the observed water level is drawdown 21m in advance. When groundwater abstractions increase 89m^3/day, the groundwater retained (-10244) MCM/day in a drought year, meanwhile, the observed water level drawdown 25.78m. From this study, the limited observed water level is 25m in drought year and pumping rate is 89m^3/day to control the water storage and water management in this area.

Wet season	Storage (MCM/day)	Pumping (m³/day)
1994 (Drought)	-279.30	-37.75
1993 (Dry)	1384.92	-34.35
1997 (Normal)	4195.89	-24.71
2003 (Wet)	5012.46	-22.63

Dry season	Storage (MCM/day)	Pumping (m³/day)
1994 (Drought)	-9965.38	-52.05
1993 (Dry)	0.00	-48.35
1997 (Normal)	2887.74	-39.10
2003 (Wet)	4102.15	-34.14

Annual	Storage (MCM/day)	Pumping (m³/day)
1994 (Drought)	-10244.68	-89.80
1993 (Dry)	1384.92	-82.69
1997 (Normal)	7083.63	-63.81
2003 (Wet)	9114.61	-56.77

Figure 5.28 Estimated changes in groundwater storage and pumping rate

Wet season	Storage (MCM/day)	Observed Water level (m)
1994 (Drought)	-279.30	29.63
1993 (Dry)	1384.92	31.21
1997 (Normal)	4195.89	36.18
2003 (Wet)	5012.46	36.59

Dry season	Storage (MCM/day)	Observed Water level (m)
1994 (Drought)	-9965.38	21.93
1993 (Dry)	0.00	23.42
1997 (Normal)	2887.74	25.38
2003 (Wet)	4102.15	25.46

Annual	Storage (MCM/day)	Observed Water level (m)
1994 (Drought)	-10244.68	25.78
1993 (Dry)	1384.92	27.32
1997 (Normal)	7083.63	30.78
2003 (Wet)	9114.61	31.02

Figure 5.29 Estimated changes in groundwater storage and observed water level

CHAPTER VI: CONCLUSIONS AND RECOMMENDATIONS

In this chapter, the conclusions derived from the findings of this study. The conclusions were based on the purpose and results of the study. The aim of this study was to analyse the mechanism of surface water and groundwater interaction. The recommendations were based on the conclusions and purpose of the study.

6.1 Conclusions

To understand the interactions of land and river recharge, the regional groundwater model was redeveloped from the previous study with smaller grid size, adding more wells data, parameter estimation, and distribution by interpolating with Kriging method. From the flow budget analysis, the total inflow of the groundwater from the previous study is 0.4MCM/day and outflow 0.3 is MCM/year. However, the total used of groundwater is 2.4MCM/day which is not enough for the local farmers. Therefore, this study tried to find the interaction mechanism in more detail. The total average water flow budget of inflow from the redeveloped regional model is 0.3MCM/day and outflow is0.05MCM/day. The net of the river change is 0.3MCM/day in a drought year. Land recharge is 0.03MCM/day in a drought year and 0.05MCM/day in a wet year. The groundwater use 0.5MCM/day (80%) in a drought year. From this study, the interaction is mainly imported from the boundary inflow and river recharge in drought year.

To analyse the surface water and groundwater interaction parameter, local groundwater model was developed with 2sq.km gird size using piezometric heads as boundary conditions from the regional model. The parameters (land recharge, river conductance, pumping) were calibrated during the model calibration. The calibrated land recharge coefficient shows similar to the recharge coefficient from the field measurement (0.001-0.003). The recharge rate is defined for each soil types. The calibrated recharge values are 3.5 cm/day for sandy clay loam and sandy clay is 4.6 cm/day which are closed with the field measurement; 4.43cm/day for sandy clay loam. The calibrated values of river conductance are in the ranges from 5.5 to 1.0m/day in Nan River and 1.5 to 1.0m/day in Yom River. From the field measurement, the calibrated values are closed to the other studies (0.1 to 4.9m/d) in the Saigon River and the calibrated parameters are a better match with the observed

value of 1.63m/day for the Lower Nan and 1.98cm/day for the Lower Yom of the other study.

Finally, the interaction mechanism was estimated via the water budget of developed local groundwater model by time (water year/season) and by space (river upstream, mid-stream, and downstream). The groundwater flow budget is analysed in seasonal: rainy (April to September) and dry (October to March) and water year patterns (very dry, dry, normal, wet based on dam storage volume) from well-calibrated groundwater model results. From the analysis, the average of groundwater flow from the boundary area into the aquifer is the main input to the aquifer system with 13.17MCM/day. The boundary outflow is less about 4.18MCM/day. Well abstraction is 8.13MCM/day. River discharge is 3.15MCM/day and river gain is 4.28MCM/day. Land recharge seems not to affect the flow interaction about 0.25MCM/day. It means that river recharge plays a major role to balance the groundwater accumulation in this area. The average of annual river loss is 1.6% in a drought year and 9.1% in a wet year of the total inflow. The river (Nan) recharged to the aquifer in the upstream ($1,243m^3/d$) and released back to the river again in the mid ($1,276m^3/d$) and down streams ($2,200m^3/d$) reaches. This study found that the main factors for groundwater flow inputs are from the upstream boundary area and river recharge. According to the groundwater use is raising in the central part, it means that the drawdown is about 31-32m along the river as the main hotspot area.

6.2 Recommendations

To counter with the water shortage in the area, more intensive groundwater management is necessary to keep groundwater level at the appropriate level before the dry season. From the study, inflow from boundary solve to more inflow water as a major input to the groundwater system and more river recharge follows as second important in the area especially in the wet year to be used in the drought year. The river recharges in the upstream in a wet year through the aquifer and filled back to river gain in the mid and downstream reaches. Thus, to manage more sustainable groundwater resources in the area, it is recommended to improve upstream watershed management to increase inflow from upstream boundaries and to investigate the possibility of weir construction in the upstream of the rivers to increase river recharge.

From this study, the groundwater should be used 89m^3/day in a drought year (37m^3/day in the wet season and 52m^3/day in the dry season) with groundwater level not less than 25m MSL as warning level in a drought year.

REFERENCES

Aggarwal, P. K., et al. (2005). Isotopes in the water cycle, Springer.

Allison, G., et al. (1994). "Vadose-zone techniques for estimating groundwater recharge in arid and semiarid regions." *Soil science society of America journal* **58**(1): 6-14.

Arnold, J. G., et al. (2000). "Regional estimation of base flow and groundwater recharge in the Upper Mississippi river basin." *Journal of Hydrology* **227**(1-4): 21-40.

Aye, P. P. and Koontanakulvong, S. (2017). Estimation of Hydrological Parameter Distribution by Geostatistical methods in the Upper Central Plain, Thailand. THA 2017 "Water Management and Climate Change Towards Asia's Water-Energy-Food Nexus" Bangkok, Thailand, Bangkok, Thailand.

Aye, P. P. and Koontanakulvong, S. (2018). "Hydrogeological Parameter Distribution Estimation By Geostatistical Methods in Regional Groundwater Modeling in the Upper Central Plain, Thailand." *International Journal of Civil Engineering and Technology (IJCIET)* **9**(3): 313–322.

Aye, P. P., et al. (2017). Estimation of Transmissivities from Well Test Data in the Upper Central Plain, Thailand for Regional Groundwater Modeling. International Symposium of the 11th SSMS and the 5th RCND 20th September 2017, Bangkok, Thailand**:** 9.

Aye, P. P., et al. (2019). "Deep percolation characteristics via field soil moisture sensors-case study in Phitsanulok, Thailand-." *Taiwan Water Conservance* **67**(1): 1-10.

Baier, W. (1972). Soil moisture estimator program system, Agrometeorology Section, Plant Research Institute.

Baier, W. and Robertson, G. W. (1966). "A new versatile soil moisture budget." *Canadian Journal of Plant Science* **46**(3): 299-315.

Bartier, P. M. and Keller, C. P. (1996). "Multivariate interpolation to incorporate thematic surface data using inverse distance weighting (IDW)." *Computers & Geosciences* **22**(7): 795-799.

Baskaran, S., et al. (2009). "Investigating groundwater–river interactions using environmental tracers." *Australian Journal of Earth Sciences* **56**(1): 13-19.

Bejranonda, et al. (2013). "Surface water and groundwater dynamic interaction models as guiding tools for optimal conjunctive water use policies in the central plain of Thailand." *Environmental earth sciences* **70**(5): 2079-2086.

Bejranonda, et al. (2006). Groundwater modelling for conjunctive use patterns investigation in the upper Central Plain of Thailand. International smposium-Aquifers Systems Management-30th May-1st June 206. Dijon, France**:** 161--174.

Bejranonda, et al. (2007). "Groundwater modelling for conjunctive use patterns investigation in the upper Central Plain of Thailand." *Aquifer Systems Management: Darcy's Legacy in a World of Impending Water Shortage*: 161-174.

Bejranonda, et al. (2008). Study of the Interaction between Streamflow and Groundwater toward the Conjunctive use Management: a Case Study in an Irrigation Project. 1st NPRU Academic Conference, Oct. Annals. p, Citeseer.

Belanger, T. and Montgomery, M. (1992). "Seepage meter errors." *Limnology and Oceanography* **37**(8): 1787-1795.

Brevik, E. C., et al. (2015). "The interdisciplinary nature of soil" **1**(1): 117-129.

Brunner, P., et al. (2010). "Modeling surface water-groundwater interaction with MODFLOW: some considerations." *Groundwater* **48**(2): 174-180.

Cable, J. E., et al. (1997). "Magnitude and variations of groundwater seepage along a Florida marine shoreline." *Biogeochemistry* **38**(2): 189-205.

Cao, G. (2011). Recharge estimation and sustainability assessment of groundwater resources in the North China Plain, University of Alabama Libraries.

Carsel, R. F. and Parrish, R. S. (1988). "Developing joint probability distributions of soil water retention characteristics." *Water Resources Research* **24**(5): 755-769.

Cerdà, A. (1999). "Seasonal and spatial variations in infiltration rates in badland surfaces under Mediterranean climatic conditions." *Water Resources Research* **35**(1): 319-328.

Chulalongkorn (2010). The impact of Climate Change on Irrigation Systems and Adaptation Measuers (Case Study: Plaichumphol Irrigation Project, Thailand), presented at JIID Seminar on Impact of Climate Change on Irrigaiotn Systems, Bangkok, Jan 26**:** 301.

Cooper, et al. (1990). "Soil controls on recharge to aquifers." *Journal of Soil Science* **41**(4): 613-630.

Cousquer, Y., et al. (2017). "Estimating River Conductance from Prior Information to Improve Surface-Subsurface Model Calibration." *Groundwater* **55**(3): 408-418.

Darul, A., et al. (2015). Groundwater and river water interaction on Cikapundung River: Revisited. AIP Conference Proceedings, AIP Publishing.

Dincer, T., et al. (1970). "Snowmelt runoff from measurements of tritium and oxygen-18." *Water Resources Research* **6**(1): 110-124.

Driscoll, F. G. (1986). "Ground Water and Wells: Published by Johnson Division, St." *Paul Minnesota* **551**(12): 769-777.

Drost, W. (1989). Single-well and multi-well nuclear tracer techniques: A critical review. International Hydrological Programme, Unesco. **3**.

El-Naqa, A. (1994). "Estimation of transmissivity from specific capacity data in fractured carbonate rock aquifer, central Jordan." *Environmental Geology* **23**(1): 73-80.

Fayer, M. J. and Jones, T. (1990). UNSAT-H Version 2. 0: Unsaturated soil water and heat flow model, Pacific Northwest Lab., Richland, WA (USA).

Feddes, R. A., et al. (1974). "Field test of a modified numerical model for water uptake by root systems." *Water Resources Research* **10**(6): 1199-1206.

Fellows, C. R. and Brezonik, P. L. (1980). "Seepage flow into florida lakes 1." *JAWRA Journal of the American Water Resources Association* **16**(4): 635-641.

Freeze, R. A. (1971). "Three-dimensional, transient, saturated-unsaturated flow in a groundwater basin." *Water Resources Research* **7**(2): 347-366.

Genuchten, M. T. v. (1980). "A Closed-form Equation for Predicting the Hydraulic Conductivity of Sunaturated Soils." *Soil science society of America journal* **44**(5): 892-898.

Guizerix, J. (1983). Use of tracers for studying leaks in reservoirs.

Hamm, S. Y., et al. (2005). "Relationship between transmissivity and specific capacity in the volcanic aquifers of Jeju Island, Korea." *Journal of Hydrology* **310**(1-4): 111-121.

Hatch, C. E., et al. (2006). "Quantifying surface water–groundwater interactions using time series analysis of streambed thermal records: Method development." *Water Resources Research* **42**(10).

Hoeksema, R. J. and Kitanidis, P. K. (1984). "An application of the geostatistical approach to the inverse problem in two-dimensional groundwater modeling." *Water Resources Research* **20**(7): 1003-1020.

Johansson, P.-O. (1988). Methods for estimation of natural groundwater recharge directly from precipitation—comparative studies in sandy till. Estimation of natural groundwater recharge, Springer**:** 239-270.

Kalbus, E., et al. (2006). "Measuring methods for groundwater? surface water interactions: a review." *Hydrology and Earth System Sciences Discussions* **10**(6): 873-887.

Kaveh, et al. (2015). "Presenting a Mathematical Model for Estimating the Deep Percolation Due to Irrigation." *International Journal of Hydraulic Engineering* **4**(1): 17-21.

Khalil, M., et al. (2003). "Current and prospective applications of zero flux plane (ZFP) method." *J. Jpn. Soc. Soil Phys* **95**: 75-90.

Khalil, M., et al. (2006). "Analysis of zero flux plane behavior under periodical water supply." *Transactions of the Japanese Society of Irrigation, Drainage and Reclamation Engineering (Japan).*

Kitanidis, P. K. and Vomvoris, E. G. (1983). "A geostatistical approach to the inverse problem in groundwater modeling (steady state) and one-dimensional simulations." *Water Resources Research* **19**(3): 677-690.

Kojima, et al. (2016). "Low-Cost Soil Moisture Profile Probe Using Thin-Film Capacitors and a Capacitive Touch Sensor." *Sensor* **16**(8): 1-14.

Koontanakulvong, S. (2002). "Groundwater Potential and Demand Study for Groundwater Management in the Northern Part of Lower Central Plain." *Chulalongkorn University.*

Koontanakulvong, S., et al. (2014). "Climate change's impact on irrigation system and farmers' response: a case study of the Plaichumpol Irrigation Project, Phitsanulok Province, Thailand." *Paddy and water environment* **12**(2): 241-254.

Koontanakulvong, S. and Panot, S. (2003). Groundwater Modelling in The North Part of Lower Central Plain, Thailand. Proceedings of the International Conference on water and Environment, December 15-18, Bhopal, India.

Koontanakulvong, S. and Suthidhummajit, C. (2015). "The Role of Groundwater to Mitigate the Drought and as an Adaptation to Climate Change in the Phitsanulok Irrigation Projrct, in the Nan Basin,Thailnd." *jurnalteknologi,utm.my* **76**(15): 89-95.

Kumar, C. (1997). "Estimation of natural ground water recharge." *ISH Journal of Hydraulic Engineering* **3**(1): 61-74.

Lee, et al. (1978). "A Field Exercise on Groundwater Flow Using Seepage Meters and Mini-piezometers." *Journal of Geological Education* **27**(1): 6-10.

Lee and Robert, D. (1947). "A device for measuring seepage flux in lakes and estuaries." *Limnology and Oceanography* **22**(1): 140-147.

Li, Y., et al. (2017). "Modeling of soil water regime and water balance in a transplanted rice field experiment with reduced irrigation." *Water* **9**(4): 248.

Libelo, E. L. and Macintyre, W. G. (1994). "Effects of surface-water movement on seepage-meter measurements of flow through the sediment-water interface." *Applied Hydrogeology* **2**(4): 49-54.

Liu, J., et al. (2011). Sustainability of groundwater resources in the North China Plain. Sustaining groundwater resources, Springer**:** 69-87.

Logan, J. (1964). "Estimating transmissibility from routine production tests of water wells." *Groundwater* **2**(1): 35-37.

Long, T. T. and Koontanakulvong, S. (2017). "Groundwater balance and river interaction analysis in Pleistocene aquifer of the Saigon River basin, South of Vietnam by stable isotope analysis and groundwater modeling." *THA2017: Water Management and Climate Change Towards Asia's Water-Energy-Food Nexus, Bangkok, Thailand*.

Long, T. T. and Koontanakulvong, S. (2019). "Deep Percolation Characteristics via soil moisture sensor approach in Saigon River Basin, Vietnam." *International Journal of Civil Engineering and Technology (IJCIET)* **10**(03): 403-412.

Lu, et al. (2011). "Groundwater recharge at five representative sites in the Hebei Plain, China." *Groundwater* **49**(2): 286-294.

Lu, et al. (2010). "Groundwater Recharge at FIve Representative Sites in the Hebei Plain, China." *National Ground Water Association* **49**(2): 286-294.

Mace, R. E. (2001). Estimating transmissivity using specific-capacity data, Bureau of Economic Geology, University of Texas at Austin.

Mcdonald, et al. (1988). A modular three-dimensional finite difference ground-water flow model. US Geological Survey**:** 83-875.

Moriasi, D. N., et al. (2007). "Model evaluation guidelines for systematic quantification of accuracy in watershed simulations." *Transactions of the ASABE* **50**(3): 885-900.

Moser, H. and Rauert, W. (2005). Isotopic tracers for obtaining hydrologic parameters. Isotopes in the Water Cycle, Springer**:** 11-24.

Mualem, Y. (1976). "A new model for predicting the hydraulic conductivity of unsaturated porous media." *Water Resources Research* **12**(3): 513-522.

Murdoch, L. C. and Kelly, S. E. (2003). "Factors affecting the performance of conventional seepage meters." *Water Resources Research* **39**(6).

Nash, J. E. and Sutcliffe, J. V. (1970). "River flow forecasting through conceptual models part I - A discussion of principles." *Journal of Hydrology* **10**(3): 282-290.

Phillips, R. W. (2007). "Measuring deep percolation for an irrigated alfalfa crop in south central Colorado."

Raju, B. V. (2017). "An Automatic Form Monitoring System Using Arduino and Wireless Sensor Networks." *Internaltional Journal of Innovative Research in Science, Engineering and Technology* **6**(7): 14777-14785.

Rawls, W. J., et al. (1982). "Estimation of soil water properties." *Transactions of the ASAE* **25**(5): 1316-1320.

Reddy, S. J. (1983). "A simple method of estimating the soil water balance." *Agricultural Meteorology* **28**(1): 1-17.

Richard, S. K., et al. (2016). "Estimating the reliability of aquifer transmissivity values obtained from specific capacity tests: examples from the Saguenay-Lac-Saint-Jean aquifers, Canada." *Hydrological sciences journal* **61**(1): 173-185.

Rosenberry, D. O. and Labaugh, J. W. (2008). Field techniques for estimating water fluxes between surface water and ground water, Geological Survey (US).

Rotzoll, K., et al. (2007). "Estimating Hydraulic Properties of Volcanic Aquifers Using Constant-Rate and Variable-Rate Aquifer Tests 1." *JAWRA Journal of the American Water Resources Association* **43**(2): 334-345.

Roy, P. K., et al. (2015). "Study of impact on surface water and groundwater around flow fields due to changes in river stage using groundwater modeling system." *Clean Technologies and Environmental Policy* **17**(1): 145-154.

Sandvig, R. M. and Phillips, F. M. (2006). "Ecohydrological controls on soil moisture fluxes in arid to semiarid vadose zones." *Water Resources Research* **42**(8).

Scanlon, B. R., et al. (2002). "Choosing appropriate techniques for quantifying groundwater recharge." *Hydrogeology Journal* **10**(1): 18-39.

Schaap, M. G., et al. (2001). "Rosetta: A computer program for estimating soil hydraulic parameters with hierarchical pedotransfer functions." *Journal of Hydrology* **251**(3-4): 163-176.

Schincariol, R. A. and Mcneil, J. D. (2002). "Errors with small volume elastic seepage meter bags." *Ground Water* **40**(6): 649-651.

Seiler, K. (1998). Isotope studies of the hydrological impact of large scale agriculture. Isotope techniques in the study of environmental change.

Sharma, P. and Gupta, S. (1985). Soil water movement in semi-arid climate. An isotopic investigation.

Shaw, R. and Prepas, E. (1989). "Anomalous, short-term influx of water into seepage meters." *Limnology and Oceanography* **34**(7): 1343-1351.

Shaw, R. and Prepas, E. (1990a). "Groundwater-lake interactions: I. Accuracy of seepage meter estimates of lake seepage." *Journal of Hydrology* **119**(1-4): 105-120.

Shaw, R. and Prepas, E. (1990b). "Groundwater-lake interactions: II. Nearshore seepage patterns and the contribution of ground water to lakes in central Alberta." *Journal of Hydrology* **119**(1-4): 121-136.

Shepard, D. (1968). A two-dimensional interpolation function for irregularly-spaced data. Proceedings of the 1968 23rd ACM national conference, ACM.

Shepherd, R. G. (1989). "Correlations of permeability and grain size." *Groundwater* **27**(5): 633-638.

Sibson, R. (1981). "A brief description of natural neighbour interpolation." *Interpreting multivariate data*.

Simmers, I. (2013). Estimation of natural groundwater recharge, Springer Science & Business Media.

Šimůnek, J., M. Th. van Genuchten and M. Šejna (2005). The HYDRUS-1D software package for simulating the one-dimensional movement of water, heat, and multiple solutes in variably-saturated media. HYDRUS Software Series 1. Riverside, California, USA, University of California RIverside, **:** 270.

Simunek, J., et al. (2005). "The HYDRUS-1D software package for simulating the one-dimensional movement of water, heat, and multiple solutes in variably-saturated media." *University of California-Riverside Research Reports* **3**: 1-240.

Slavich, et al. (1995). "The effect of gypsum on deep drainage from clay soil used for rice." *Australian sodic soils: distribution, properties and management. CSIRO, Melbourne*: 205-210.

Slavich, et al. (1990). "Estimation of field scale leaching rates from chloride mass balance and electromagnetic induction measurements." *Irrigation Science* **11**(1): 7-14.

Song, J., et al. (2009). "Feasibility of grain-size analysis methods for determination of vertical hydraulic conductivity of streambeds." *Journal of Hydrology* **375**(3-4): 428-437.

Soonthornnonda, P., et al. (2019). Assessments of Groundwater–Surface Water Connectivity for the Lower Yom and Nan Rivers THA2019 International Conference on Water Management and Climate Change towards Asia's Water -Energy-Food Nexus and SDGs. Swissotel Bangkok Ratchada, Thailand.

Sophocleous and Marios (1991). "Combining the soilwater balance and water-level fluctuation methods to estimate natural groundwater recharge: practical aspects." *Journal of Hydrology* **124**(3-4): 229-241.

Sophocleous and Marios (2002). "Interactions between groundwater and surface water: the state of the science." *Hydrogeology Journal* **10**(1): 52-67.

Suthidhummajit, C. and Koontanakulvong, S. (2017). Flow budget and conjunctive use pattern of groundwater system under climate change in Upper Central Plain, Thailand. THA 2017 International Conference on ―Water Management and Climate Change Towards Asia's Water-Energy-Food Nexus. Bangkok, Thailand**:** 186-191.

Taher, L. S. B. (2018). "Estimating Ground Water Aquifer Transmissivity Using well Specific Capacity Data For Tazerbo Wellfield, SE-Libya." *Gharyan Journal of Technology, High Institute of Science & Technoogy Gharian*(4): 16.

Taniguchi, M., et al. (2002). "Investigation of submarine groundwater discharge." *Hydrological Processes* **16**(11): 2115-2129.

Thompson, S., et al. (2010). "Vegetation-infiltration relationships across climatic and soil type gradients." *Journal of Geophysical Research: Biogeosciences* **115**(G2).

Todd, et al. (1976). Groundwater Hydrology, John Wiley & Sons, Inc.

Toth, J. (1963). "A theoretical analysis of groundwater flow in small drainage basins." *Journal of geophysical research* **68**(16): 4795-4812.

Tsujimura, M., et al. (2001). "Behavior of subsurface water revealed by stable isotope and tensiometric observation in the Tibetan Plateau." *Journal of the Meteorological Society of Japan. Ser. II* **79**(1B): 599-605.

Tuan, P. V. and Koontanakulvong, S. (2018). "Groundwater and River Interaction Parameter Estimation in Saigon River, Vietnam." *Engineering Journal* **22**(1): 257-267.

USGS (2013). The Groundwater Modeling System User Manual.

Vogel, J., et al. (1970). "Isotopic fractionation between gaseous and dissolved carbon dioxide." *Zeitschrift für Physik A Hadrons and nuclei* **230**(3): 225-238.

Wellings, S. (1984). "Recharge of the Upper Chalk aquifer at a site in Hampshire, England: 2. Solute movement." *Journal of Hydrology* **69**(1-4): 275-285.

Willis, T. M., et al. (1997). "Estimates of deep percolation beneath cotton in the Macquarie Valley." *Irrigation Science* **17**(4): 141-150.

Winter, T. C. (1998). Ground water and surface water: a single resource, DIANE Publishing Inc.

Winter, T. C. (1999). "Relation of streams, lakes, and wetlands to groundwater flow systems." *Hydrogeology Journal* **7**(1): 28-45.

Winter, T. C. and Rosenberry, D. O. (1995). "The interaction of ground water with prairie pothole wetlands in the Cottonwood Lake area, east-central North Dakota, 1979–1990." *Wetlands* **15**(3): 193-211.

Yeh, H.-F., et al. (2007). "Estimation of groundwater recharge using water balance model." *Water Resources* **34**(2): 153-162.

APPENDIX

IV   SOIL MOISTURE MEASUREMENT VIA SENSOR

        IV.1 Work Content of Soil Moisture Sensor Installation

        IV.2 Soil physical parameters

        IV.3 Hardware design

        IV.4 Soil moisture sensor module

        IV.5 Soil moisture sensor design and monitoring

        IV.6 Soil moisture construction and design

        IV.7 Soil moisture sensor setup

        IV.8 Soil moisture data convert from electrical resistance

        IV.9 Soil moisture data analysis

V   DEEP PERCOLATION ESTIMATION VIA HYDRUS SOFTWATER
        APPLICATION

        V.1 Sensitivity curve analysis

        V.2 Calibration and verification data

        V.3 Soil moisture patterns in each phase

        V.4 Water balance of percolation system

VI   SEEPAGE METER INSTALLATION FOR RIVER CONDUCTANCE

        VI.1 Seepage meter instrumentation and design

        VI.2 Seepage meter installation and measurement

        VI. 3 Seepage flux field data

APPENDIX I

GEOSTATISTIC METHODS APPLICATION AND VARIOGRAM MODEL GENERATION IN GMS

Groundwater modeling system (GMS) includes an interpolation option associated with the 2D scatter point to generate a set of datasets which exhibit heterogeneity and are conditioned to values at scatter points. This section explained the application of geostatic methods for interpolation and the processes to generate the variogram in GMS to find the best fit of the each point with Gaussian simulation as input for parameter (hydraulic conductivity).

I.1 Geostatistic method application

In groundwater model (GMS), the various geostatistic methods such as Inverse Distance Weight (IDW), Natural Neighbor (NN) and Kriging can be used to interpolate the observed water level.

Inverse distance weight techniques was used for interpolation of point data which are based on the assumption that interpolating surface should be influenced most by the nearby points and less by the more distant points. The interpolated surface is a weighted average of the point data; the weight assigned to each point diminishes as the distance to the interpolation location increases.

As with IDW interpolation, the nodal function can be selected using Natural neighbour interpolation. The difference between IDW and NN is the method used to compute the weights and to select the subset of point data used for interpolation. Natural neighbour interpolation is based on the Thiessen polygon network of the point data and constructed from the triangulation of a set of points. The polygon encloses the area that is closer to the enclosed point than any other point.

Kriging method is based on the assumption that the parameter being interpolated can be treated as a regionalized variable. It is a set of linear regression routines which minimized estimation variance from a predefined covariance model. It varies in a continuous manner from one location to the next and therefore points that are near each other correlation but points are widely separated statistically. Before interpolating a scatter point set using the Kriging option, a model variogram is defined as follow.

I.2 Variogram data analysis

A variogram consists of two parts: an experimental variogram and a model variogram. The experimental variogram is computed by calculating the variance of each point in the set with respect to each of the other points and plotting the variances versus distance between the points. When computing an experimental variogram, distances are subdivided into a number of intervals called lags as illustrated in Figure I.1. The distance between each pair of scatter points is checked to see which lag interval it lies within. The variances for all pairs of points whose separation distance falls within the same lag interval are average. The resulting average is plotted in the experimental variogram vs. the distance corresponding to the lag interval. Once a set of experimental variogram are computed, a model variogram is constructed to fit the matches the experimental variogram as the next step.
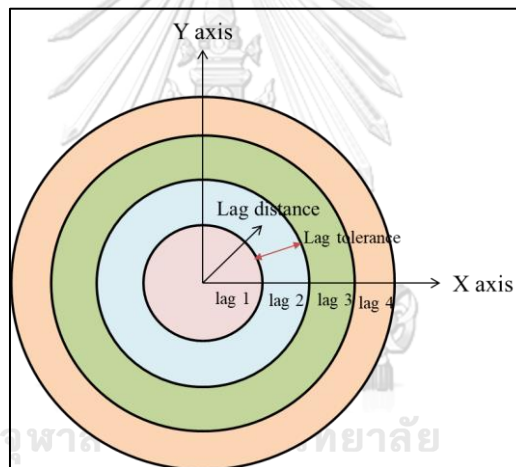
Figure I.1 The diagram of the lag distance between each pair of scatter point

A model variogram is a simple mathematical function that models trend in the experimental variogram. Four types of model functions are supported for building model variogram;

1. Spherical model which is defined by a range "a" and a contribution "c" as,

$$\gamma(h) = \begin{cases} c\left[1.5\dfrac{h}{a} - 0.5\left(\dfrac{h}{a}\right)^3\right], & if\ \dfrac{h}{a} \leq a \\ c & if\ \dfrac{h}{a} > a \end{cases} \tag{1}$$

2. Exponential model which is defined by a parameter "a" and a contribution "c" as,

$$\gamma(h) = c\left[1 - \exp\left(-\frac{3h}{a}\right)\right] \tag{2}$$

3. Gaussian mode which is defined by a parameter "a" and contribution "c" as,

$$\gamma(h) = c\left[1 - \exp\left(-\frac{3h^2}{a}\right)\right] \tag{3}$$

4. Power model which is defined by a power "$0 < a < 2$" and a slope "c" as

$$\gamma(h) = ch^a \tag{4}$$

Each of the functions is characterized by a nugget, contribution, and range as illustrated in Figure I.2. The nugget represents a minimum variance. The contribution is sometimes called the "sill" and represents the average variance of points at such a distance away from the point. The range represents the distance at which there is no longer a correlation between the points.
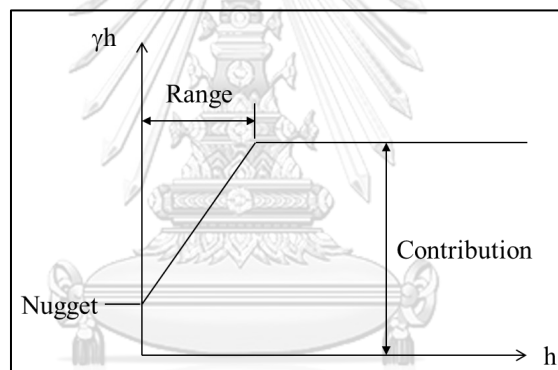
Figure I.2 Parameters used to define a model variogram

I.3 Construction of the empirical variogram

To construct the empirical variogram, a new experimental variogram is computed. In this study, the parameters for the Gaussian model are using $h = 5,000$ to represent lag distance, $a = 46,846$ to represent range, and $c = 30.268$ to represent contribution. The estimated hydraulic conductivity between points is divided into lags of 2km which are used to find the distribution of hydraulic conductivity field and conformed to hydrogeological map for the next step. The step to construct the variogram shows as follows.

1. Select the data for each scatter point with respect to each of the other scatter points

2. Choose the geometric variables of the variogram: lag width (Figure I.3) and number of intervals into which the range of distance to be analysed is divided.
3. Analyse the possible anisotropy.
4. Visually analyse the variogram graphics in function of the chosen parameters in order to approximately identify the structural parameters of the variogram: nugget, range and sill (Figure I.4).
5. Analyse the statistical results of the variogram
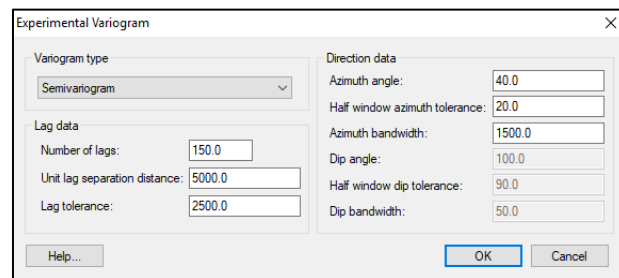
Figure I.3 Graphic of the empirical variogram
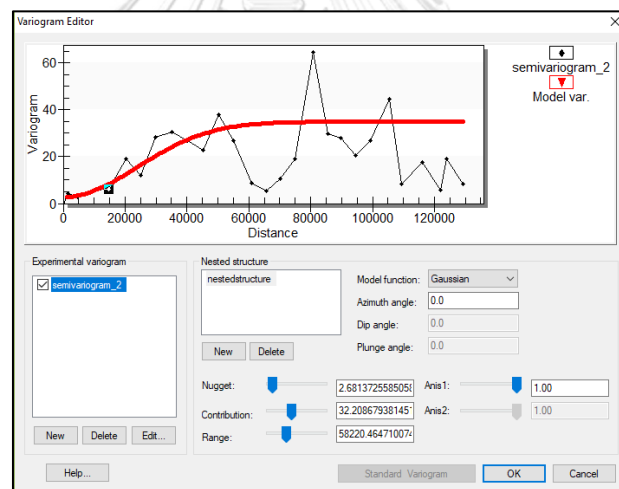
Figure I.4 The structural parameters to be identified of a variogram

I.4 Generation of the variogram model

Finally, variogram model was generated to find the function that best fits the points of the empirical variogram. The generated variogrm with Kriging method (Gaussian simulation) was used to estimate the hydraulic conductivity distribution in section 5.1.3. The process of variogram generation described as follow.

1. Choose the function that visually best fits the empirical variogram

2. Determine the approximate parameters of the chosen function, which identify the aimed, for structure: nugget effect, range and sill (contribution) for the rest as showed in Figure I.4.

3. Visually compare the variogram model to the empirical variogram

4. Repeat step 3 until an appropriate solution is found.

5. Choose a different function and repeat step 3 and 4.

From the above study i.e. the interpolation of the scatter point set via geostatistic methods (IDW, NN, Kriging), the generated new data set were compared with the original dataset and find the error using equations (17, 18, 19). The good method was selected to estimate the hydraulic conductivity distributions which are discussed in section 5.1.3, Table 5.1.

จุฬาลงกรณ์มหาวิทยาลัย

CHULALONGKORN UNIVERSITY

APPENDIX II

DATA AND INPUT PARAMETERS FOR GROUNDWATER MODEL

The model grid design and the required parameters: aquifer layer, surface elevation, hydraulic parameters (transmissivity, hydraulic conductivity), river water level and recharger rates, raw data (rainfall, evaporation), boundary condition, pumping rates, observed well, defining proper zones and grid settings were explained as follows.

II.1. Aquifer layer, boundary and river

The aquifer system in this study was defined as two layers aquifer, where the thickness of the upper layer (semi-confined) is 40-100m (layer 1) and the lower layer (confined) is 100-200m (layer 2) with the grid size of 2sq.km (Figure II.1).

The western, eastern and northern part of the study area is impermeable consolidated rock and mountainous area which defined as specific inflow boundaries derived from the head distribution along these boundaries. The southern part forms narrow trough between the mountains in the east and west, was outflow boundary. There are two mains rivers, namely Nan River in the eastern part and Yom River in the western part which parallel flow upstream to north stream in the area. The width of the river is 100m from east to west.
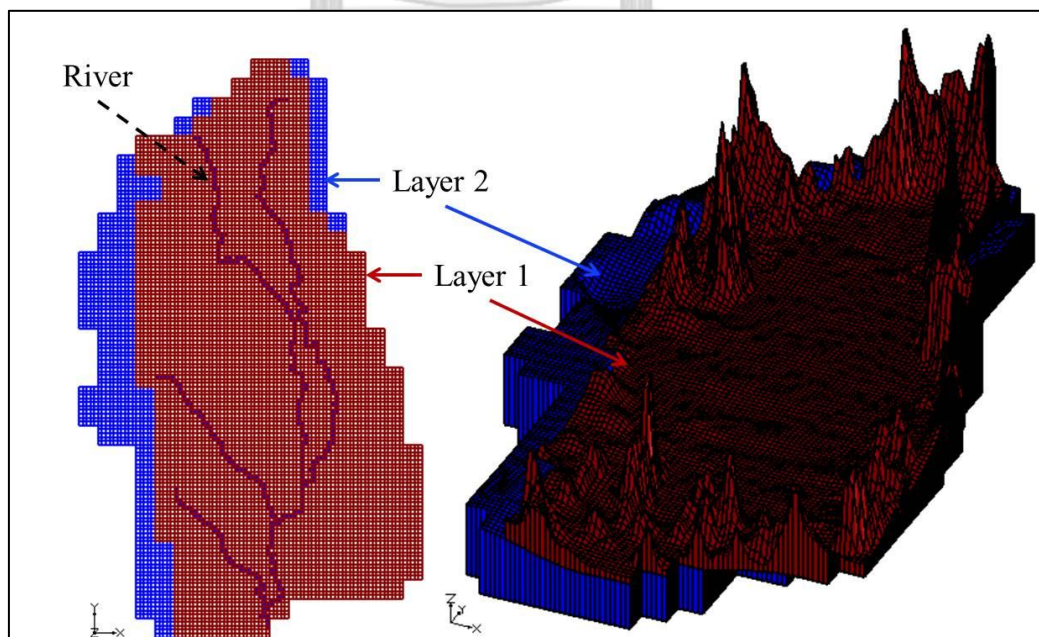
Figure II.1 Groundwater model grid and layer design

II.2. Surface elevation of top and bottom of aquifer

This area is raising and falling terrain area and the heights varies between 40-60m above mean sea level. The bottom of the layer 2 was assumed 200m. The sample of surface elevation interpolated in regional groundwater model is shown in Table II.1.

Table II.1 The sample of surface elevation interpolated in groundwater model

X	Y	Top	Bot 1	Bot 2
613291	1889057	14	-40	-200
623094	1889057	13	-40	-200
632896	1889057	13	12	-200
613291	1879157	13	-35	-200
623094	1879157	53	-30	-200
632896	1879157	56	-40	-200
642699	1879157	28	-15	-200
613291	1869257	11	-19	-200
623094	1869257	13	-20	-200
632896	1869257	16	-40	-200
642699	1869257	12	-20	-200
613291	1859356	13	-26	-200
623094	1859356	13	-25	-200
632896	1859356	29	-40	-200
642699	1859356	21	-38	-200
623094	1849456	18	-52	-200
632896	1849456	17	-60	-200
642699	1849456	19	-58	-200

II.3. Transmissivity

The hydraulic parameter, transmissivity and specific capacity (yield divided by drawdown) were calculated from the recorded well data (259 wells) to estimate the hydraulic conductivity using equation 2. This method was suggested by Logan (1964). Koontanakulvong (2003) used the same method to define the hydraulic parameter with constants a=2.5 and b=1.01 which are used in this study to estimate the hydraulic conductivity distribution for the future study. Figure II.2 shows the sample of transmissivity value used in the regional groundwater model improvement.
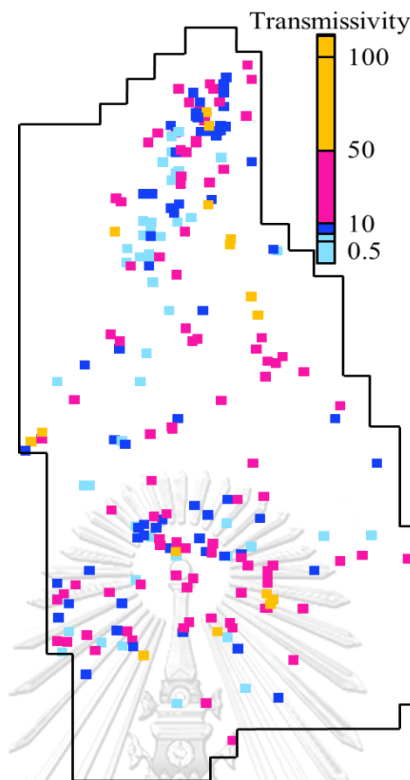
Figure II.2 Locations of transmissivity values

II.4. Hydraulic conductivity

The hydraulic conductivity was estimated the parameter estimation from the previous section to be used in groundwater model. It was calculated by transmissivity divided by aquifer thickness using equation 3. The thickness of the aquifer varies from 15-60m. The calculated hydraulic conductivity values were checked with the hydrogeology map. The value range from 20m/d to 30m/d along the river and the mountainous area ranges from 10m/d to 20m/d. value along the river (flood plain deposit) is higher than the value far from the river (low terrace deposit). It means that the pattern follow the hydrogeological map.

II.5. River water level

The observed river water levels were derived from the river bed materials and the river stages. There are main four river stations along the Nan River and two stations in Yom River. The previous data was used in this study. Table II.2 shows the observed river water level used in the regional model improvement to estimate the river-aquifer interaction.

Table II.2 The observed river water level (unit: m)

Year	Y16	Y17	N27	N68	N5A	N74	N7A
30-09-93	31.79	30.56	34.42	35.87	35.21	30.10	26.87
01-04-94	35.77	32.452	34.61	39.06	37.9	33.29	30.94
30-09-94	31.97	30.64	35.65	37.10	36	31.33	28.87
01-04-95	42.16	35.48	37.62	43.07	41.3	37.30	36.02
30-09-95	32.6	30.94	36.26	37.71	36.43	31.94	29.8
01-04-96	42.25	35.53	38.25	45.71	44.76	39.94	37.21
30-09-96	32.24	30.77	34.96	36.41	35.67	30.65	27.56
01-04-97	38.67	33.82	37.57	43.02	41.83	37.25	34.95
30-09-97	31.87	30.59	34.77	36.22	35.56	30.45	27.22
01-04-98	37.7	33.36	38.21	39.66	38.53	33.89	31.49
30-09-98	31.73	30.53	34.65	36.10	35.16	30.33	27.59
01-04-99	37	33.03	36.42	37.87	36.78	32.10	29.62
30-09-99	32.18	30.74	34.53	35.98	35.07	30.21	27.42
01-04-00	38.1	33.55	38.2	41.65	40.32	35.88	33.82
30-09-00	32.43	30.86	36.04	37.50	36.63	31.73	28.86
01-04-01	38.91	33.94	37.94	41.39	39.59	35.63	34.4
30-09-01	32.09	30.70	35.38	36.83	36.32	31.06	27.56
01-04-02	41.1	34.98	37.61	43.06	41.89	37.29	34.95
30-09-02	32.3	30.80	35.02	36.475	35.76	30.70	27.56
01-04-03	41.64	35.24	37.36	42.82	41.51	37.05	34.95
30-09-03	31.91	30.61	35.32	36.78	36.24	31.01	27.56
01-04-04	38.32	33.66	37.76	41.21	38.99	35.44	34.95

II.6. Recharge rate

The recharge rates used in this study were computed by Koontanakulvong and Suthidhummajit (2015) from the simple water budget analysis i.e. precipitation minus evaporation for each soil layer (Table II.3). There were six soil types in the regional (Upper Central Plain) area. This recharge rates are used to estimate the interaction parameters in the groundwater model.

Table II.3 The recharge rate for each soil zone

Time	zone 1	zone 2	zone 3	zone 4	zone 5	zone 6
01-04-93	8.22E-05	7.2E-05	0.000103	0.000206	6.17E-05	0.000123
30-09-93	1.07E-05	9.35E-06	1.34E-05	2.67E-05	8.01E-06	0.000016
01-04-94	9.64E-05	8.45E-05	0.00012	0.000241	7.23E-05	0.000145
30-09-94	1.25E-05	1.1E-05	1.57E-05	3.13E-05	9.39E-06	1.88E-05
01-04-95	0.000115	0.000101	0.000144	0.000288	8.63E-05	0.000173
30-09-95	0.000015	1.31E-05	1.87E-05	3.74E-05	1.12E-05	2.24E-05

01-04-96	0.00011	9.66E-05	0.000138	0.000276	8.28E-05	0.000166
30-09-96	1.43E-05	1.26E-05	1.79E-05	3.59E-05	1.08E-05	2.15E-05
01-04-97	7.57E-05	6.63E-05	9.47E-05	0.000189	5.68E-05	0.000114
30-09-97	9.84E-06	8.60E-06	1.23E-05	2.46E-05	7.38E-06	1.48E-05
01-04-98	8.52E-05	7.45E-05	0.000106	0.000213	6.39E-05	0.000128
30-09-98	1.11E-05	9.70E-06	1.38E-05	2.77E-05	8.30E-06	1.66E-05
01-04-99	0.000112	9.81E-05	0.00014	0.00028	8.41E-05	0.000168
30-09-99	1.46E-05	1.28E-05	1.82E-05	3.64E-05	1.09E-05	2.18E-05
01-04-00	0.000101	8.88E-05	0.000127	0.000254	7.61E-05	0.000152
30-09-00	1.32E-05	1.16E-05	1.65E-05	0.000033	9.89E-06	1.98E-05
01-04-01	9.2E-05	8.05E-05	0.000115	0.00023	6.9E-05	0.000138
30-09-01	0.000012	1.05E-05	1.49E-05	2.99E-05	8.97E-06	1.79E-05
01-04-02	0.000111	9.7E-05	0.000139	0.000277	8.31E-05	0.000166
30-09-02	1.44E-05	1.26E-05	0.000018	0.000036	1.08E-05	2.16E-05
01-04-03	7.89E-05	0.000069	9.86E-05	0.000197	5.92E-05	0.000118
30-09-03	1.03E-05	8.95E-06	1.28E-05	2.56E-05	7.69E-06	1.54E-05

II.7. Raw data

To calculate the recharge rate, the raw data such as the monthly rainfall (precipitation) (Table II.4) and evapotranspiration Table II.5 were collected from Royal Irrigation Department (RID).

Table II.4 Monthly rainfall data during the study period (1993-2003)

Monthly	1993	1994	1995	1996	1997	1998	1999	2000	2001	2002	2003
Jan	0	16	0	0	0	9.9	0.2	3.6	1.6	9.1	4
Feb	1.8	0	95.8	0	23.2	0	14.1	1.5	0.7	15.2	30.1
Mar	191.8	18	24	0	10.2	10	0	62.2	7.3	62.8	20.3
Apr	38.5	40.2	5.9	230.7	74.6	65	155.2	55.2	0	10.6	0
May	113.3	369.3	244.2	178.7	50.9	151.7	198.6	124.3	312	96.3	109.4
Jun	144.2	233.1	198.7	253.4	94.9	67.6	128.8	257	116.3	120.4	147.4
Jul	176.3	125.6	253.3	108.4	263.8	470.7	234.7	176.5	158.9	82.4	156.9
Aug	227.8	274.8	491.3	170.3	94.9	221	232.1	169.5	271.9	357.8	183.7
Sept	192.2	162.3	286.2	240.8	249.6	201.7	327.3	274.4	175.3	405.7	231.8
Oct	43.7	106.8	187.9	76	201.9	131.2	339.9	266.1	158.8	86.8	27.9
Nov	0	2.9	49.9	168.2	0.5	88.4	41.7	0.3	9.8	63.9	0
Dec	0	68.4	0	0	0	7.5	0.6	0	0	63.9	0

Table II.5 Monthly evapotranspiration data during the study period (1993-2003)

Month	1993	1994	1995	1996	1997	1998	1999	2000	2001	2002	2003
Jan	3.5	3.9	3.7	3.6	3.7	3.4	3.1	3.6	3.3	3.1	3.0
Feb	4.1	4.8	4.6	4.4	4.4	4.4	3.8	3.6	3.7	3.7	3.8
Mar	5.4	4.8	5.7	5.2	4.8	5.5	5.3	4.7	3.8	4.5	4.4
Apr	6.4	6.3	7.0	5.9	6.2	6.2	4.7	4.9	5.7	6.3	5.6
May	6.5	5.6	5.5	5.2	6.4	6.3	4.2	4.6	4.5	5.9	5.7
Jun	6.1	4.4	5.0	4.9	6.4	5.8	4.0	3.9	4.4	5.0	4.2
Jul	5.0	4.2	4.1	4.3	5.2	4.5	4.2	3.8	4.2	3.6	4.3
Aug	4.6	3.9	4.1	4.0	3.7	4.1	3.7	3.5	3.8	3.9	3.8
Sep	4.1	4.0	3.7	3.9	3.8	3.8	3.8	3.4	3.8	3.3	3.1
Oct	4.4	4.4	3.7	3.7	4.1	3.7	3.0	3.4	3.7	3.3	3.5
Nov	4.2	4.1	3.6	3.6	3.4	3.4	3.2	3.7	3.5	3.2	4.0
Dec	4.1	4.0	3.6	3.8	3.6	3.2	3.0	3.4	3.4	3.0	3.3

II.8. Boundary condition

The boundary condition for the Regional model was defined at the western, eastern and northern borders of the model where assumes as an impermeable body of consolidated rock were defined as specific inflow boundaries divided from the available head distribution along these boundary. The southern boundary is partially blocked by impermeable rocks and forms a narrow through between the mountains in the east and west, was set as outflow boundary. The calibrated piezometric head from the Regional model in the local area was selected as boundary for local model (Figure II.3).

II.9. Pumping well (flow rate (m³/d))

The groundwater used in this area is mainly by agriculture. The pumping wells are assigned to each point. More than 3000 wells are used in regional model and 525 wells from the regional were selected for local model as shown in Figure II.4 and Table II.6.

II.10. Observed well data

The groundwater level data from 185 observed wells for regional model and 34 wells for local model (Figure II.5) were recorded by using a water level using these data, hydraulic gradient and direction of the flow are also determined.
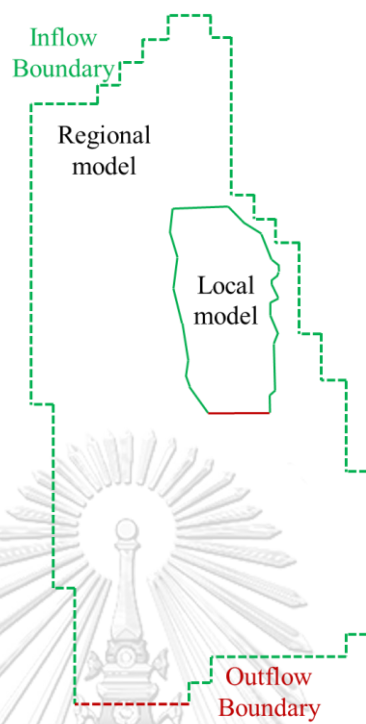
Figure II.3 Boundary conditions for groundwater model development
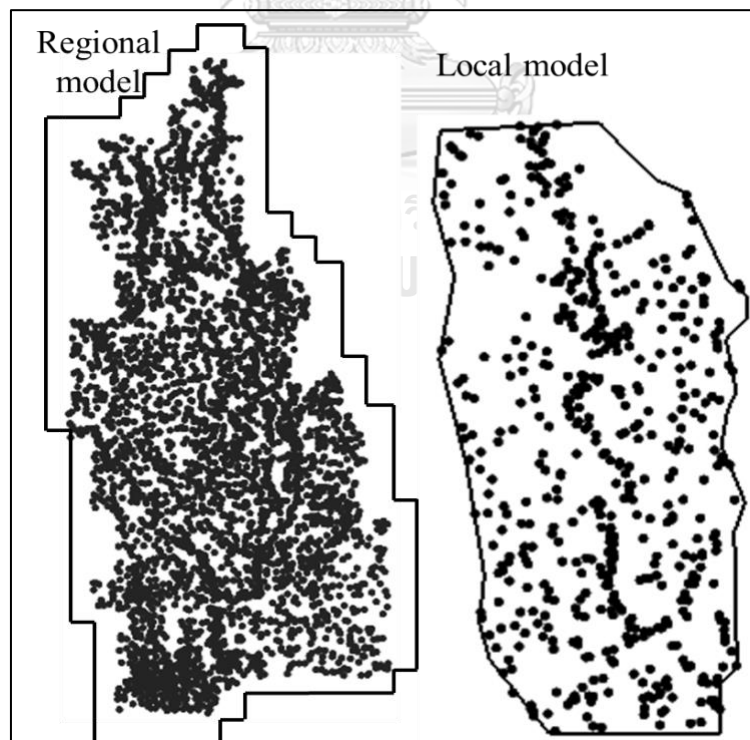
Figure II.4 Location of pumping wells

Table II.6 Sample of pumping well used in regional model

Time	Well 1	Well 2	Well 3	Well 4	Well 5
01-04-93	-39.8449	-237.18	-345.647	-157.166	-23.9228
30-09-93	-152.355	-906.905	-1321.65	-600.954	-91.4735
01-04-94	-17.8018	-105.967	-154.427	-70.2182	-10.6882
30-09-94	-186.525	-1110.31	-1618.07	-735.736	-111.989
01-04-95	-33.0104	-196.497	-286.359	-130.208	-19.8194
30-09-95	-65.1545	-387.838	-565.202	-256.998	-39.1187
31-03-96	-35.243	-209.787	-305.726	-139.014	-21.1598
29-09-96	-73.4551	-437.248	-637.209	-289.739	-44.1023
31-03-97	-43.7125	-260.203	-379.197	-172.421	-26.2449
29-09-97	-154.076	-917.15	-1336.58	-607.743	-92.5069
31-03-98	-43.7125	-260.203	-379.197	-172.421	-26.2449
29-09-98	-154.076	-917.15	-1336.58	-607.743	-92.5069
31-03-99	-44.3893	-264.231	-385.069	-175.091	-26.6513
29-09-99	-223.642	-1331.25	-1940.05	-882.144	-134.275
30-03-00	-46.0331	-274.016	-399.328	-181.575	-27.6382
28-09-00	-167.764	-998.632	-1455.32	-661.737	-100.725
30-03-01	-38.6824	-230.26	-335.562	-152.58	-23.2249
28-09-01	-86.2425	-513.366	-748.137	-340.179	-51.7799
30-03-02	-39.6479	-236.007	-343.937	-156.389	-23.8045
28-09-02	-89.832	-534.733	-779.275	-354.337	-53.935
30-03-03	-39.6479	-236.007	-343.937	-156.389	-23.8045
28-09-03	-89.832	-534.733	-779.275	-354.337	-53.935
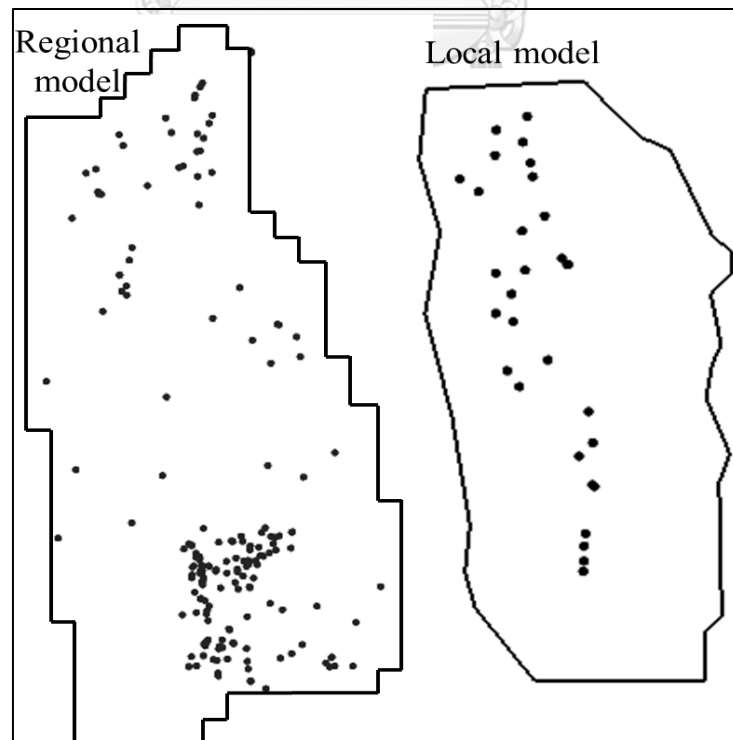
Figure II.5 Locations of observed wells

II.11. Defining property zone

Zonation for the input parameters was carried out based on geological information, point hydraulic conductivity and transmissivity data of the pumping tests. Initially the hydraulic parameters estimated from pumping test results of the previous studies were applied; later the parameters were adjusted during the calibration process. The specific storage is calculated by dividing storage coefficient by the thickness of aquifer layer and average value of specific storage in all wells and it is found out to be 0.00002 (1/m).

II.12. Grid settings
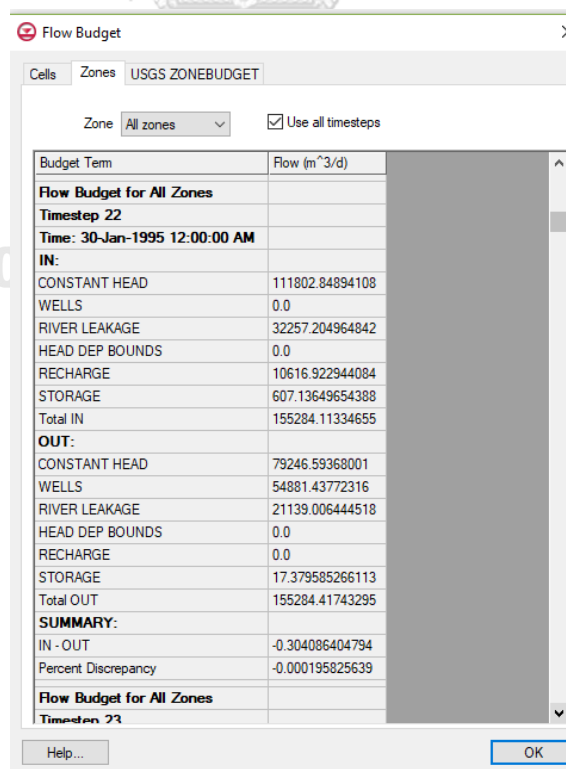
Finite difference grid of 152 ×93 numbers of rows and columns are taken into consideration for Regional model which have 2km width and height and respectively. The grids are aligned N-S and E-W. The boundary condition is defined as the western, eastern and northern borders of the model where it assumed as an impermeable body of the consolidated rock.

The above input parameters and model grid design were used to develop groundwater mode both regional and local in sections 5.2 and 5.3. Then model calibration results were discussed in next appendix.

APPENDIX III

GROUNDWTAER FLOW MODEL

The most widely used numerical groundwater flow model (GMS), MODFLOW, which is three-dimensional model, originally developed by the U.S. Geological Survey (Mcdonald et al. (1988)) was used in this study. It provides tools for every phase of a groundwater simulation including site characterization, model development, and calibration. Model design includes all parameters such as grid size and spacing, layer elevations, hydraulic parameters, recharge rates, observed water level which are used to develop a calibration model. In this study, two models; regional and local was developed for the study goal. Regional model was redeveloped from the previous study for the boundary to be used in local model. Local model was developed using the calibrated piezometric heads from the redeveloped regional model to analyse the interaction mechanism. The flow budget tools in groundwater model provide the inflow (boundary in, land recharge, river loss and storage in) and outflow (boundary out, river gain, well abstraction, and storage out) volume at each cell as shown in Figure III.1.

Figure III.1 Sample of input, output parameter in flow budget

III.1 Regional groundwater model redevelopment

The Upper Central Plain (Regional area) was selected as study area because the farmers in that area tend to grow rice more often now and resulting in a high demand for irrigation water (Bejranonda et al. (2006)). Groundwater model for this area (Regional) was developed by Suthidhummajit and Koontanakulvong (2017) to study the flow budget of groundwater system for conjunctive use pattern under climate change. It was redeveloped with smaller grid size, more well data, parameter used with geostatistics method interpolation in this study.

III.1.1 Calibration and verification results

The model was simulated during 1993-2003 stress periods which are divided by seasonal as April to October is wet season and September to March is dry season. The model was calibrated both steady state and transient state to modify the input parameters to match with an observed data set. It calibrated piezometric head will used as boundary condition in local groundwater model development.

III.1.1.1 Steady-state model calibration results

Steady-state performed using only the selected time step (1993). Steady state model was used to evaluate the initial model construction which provide consistent starting conditions for the transient calibration; adjust model parameters including horizontal and vertical hydraulic conductivity, recharge, parameters for the stream-flow and general head boundary to assess the sensitivity of simulation results to model properties. The steady state model was incorporated into the transient model as the first stress period.

During the steady state calibration, model parameters were adjusted to improve the matches between simulated and observed water levels. Resulting simulated water levels for the steady state condition are shown in section 5.2.1.1. Over the entire model does a good matching water level. The sample of calibration results are shown in Table III.1.

Table III.1 Sample of steady state model calibration

ID	observed	computed	ID	observed	computed	ID	observed	computed
MQ0232	65	63.252	MQ0235	51	46.049	MR0197	53.99	61.625
MB0221	61.85	66.343	DC0044	55	60.112	MM0057	49	53.447
MB0409	55.5	46.773	DC0052	32.9	36.917	MB0300	47.38	49.897
MB0124	58.04	62.741	MM0056	52.87	61.046	MM0008	44.88	47.233
MB0217	55.1	62.478	DI0034	49.5	47.28	MM0194	48.5	53.611
MB0335	50.72	42.312	MM0173	51.34	56.26	MM0049	49.3	59.104
MM0107	54.3	56.425	MQ0348	49	45.88	DI0102	43.55	44.476
MM0059	55.06	59.562	MB0653	38.5	37.397	DI0104	43.29	43.891
MB0506	51.1	54.63	DI0031	53.5	47.647	MB0295	49.22	57.022
TZ0069	28	30.171	MQ0236	31.7	30.772	MM0013	40.24	39.345
MM0266	43	43.883	MB0740	35.67	35.171	MM0009	41.05	43.58
MB0674	42.62	45.559	DC0330	31.5	33.815	MB0546	35.67	34.223
MB0832	42.58	45.499	MB0741	30.5	32.828	N0126	35.56	35.991
DC0047	32.5	35.278	MB0501	30.07	31.668	DC0324	38	39.557
MM0016	42	44.778	TY0239	26	30.012	MB0597	33.08	32.744
DI0025	43.6	48.27	MA0003	25.5	34.594	MB0191	39.88	38.682

III.1.1.2 Transient state model calibration results

Model was calibrated from 1993-1999 and verified from 2000 -2003. The model was run for six month period i.e. April-September for transient calibration during 1993-1998 and 1998-2003 for verification. The calibration results indicated a reasonable agreement between the calculated and observed heads discussed in section 5.2.1. Table III.2 shows the sample of calibration and verification results.

Table III.2 Sample of transient model calibration and verification results

Calibration results								
ID	Observed	Computed	ID	Observed	Computed	ID	Observed	Computed
MR0202	53	48.982	DC0228	41.5	48.099	MC1167	29.8	24.404
DI0102	43.55	49.426	DC0165	31.9	41.46	DC0190	36.6	44.975
DI0104	43.29	52.216	DC0231	44	47.659	MC1168	25.1	24.497
DI0109	44.04	52.598	DC0232	46	47.556	MC1177	17.14	28.916
DI0112	55.65	65.95	DC0233	40.08	48.059	MC1179	22.05	30.714
DI0115	48.15	63.482	DC0171	39.4	45.866	MC1182	22.1	34.35
DI0117	49.4	63.034	DI0187	63.6	68.748	MC1191	25.05	27.404
DI0121	58.2	63.626	DC0238	58.3	49.022	MC1198	21.06	31.743
MB0881	38	49.185	MC1153	16.43	24.948	MC1203	17.1	25.536
MB0883	42	51.532	MC1154	15.19	24.992	MB0960	43.54	48.995

Verification results								
ID	Observed	Computed	ID	Observed	Computed	ID	Observed	Computed
MB0882	42	51.882	DC0242	50.34	49.517	MC1210	18.14	26.565
MB0884	40.5	51.914	MC1155	15.68	24.903	DF0240	15.1	19.056
DI0136	55.8	61.43	MC1156	18.9	26.526	MC1221	11.02	18.107
DI0140	63	51.697	MC1157	19.88	26.576	MC1222	10.08	19.528
DI0142	43	63.545	MC1158	18.66	26.59	MC1223	13.44	17.623
DI0143	47.8	63.656	MC1159	19.14	26.585	MC1224	14.08	19.929
MP0298	20.13	28.859	MC1161	17.92	25.611	MC1225	31.77	24.709
DI0170	33.63	50.121	MC1162	17.28	25.108	MC1226	5.49	17.625
DC0220	32.5	41.736	DC0187	27.6	38.602	MC1240	11.44	29.589
DC0224	49.4	48.451	MC1164	17.18	27.328	MC1241	18.51	27.371

The calibration and verification results were discussed in section 5.2.1 and the error summaries of calibration results were compared with the previous study which showed in Table 5.2.

III.1.2 Groundwater flow budget

The interaction parameters from the groundwater flow budget analysis from the redeveloped regional model results are shown in Table III.3.

Table III.3 Flow budget from redeveloped Regional model

Time	Boundary in	River loss	Land recharge	Storage in	Total in
01-04-93	37.31	0.00	59.84	0.00	97.15
30-09-93	18.30	5.30	7.76	2.31	33.67
01-04-94	35.04	0.00	70.04	0.03	105.11
30-09-94	12.56	7.45	9.10	1.36	30.46
01-04-95	35.83	0.00	83.62	0.76	120.22
30-09-95	16.50	2.84	10.87	2.69	32.89
31-03-96	37.03	0.00	80.22	1.32	118.57
29-09-96	17.43	1.84	10.42	3.05	32.75
31-03-97	31.12	0.00	55.02	0.81	86.95
29-09-97	11.06	7.01	7.15	1.08	26.29
31-03-98	29.26	0.00	61.88	0.15	91.28
29-09-98	10.93	5.14	8.04	1.47	25.58
31-03-99	33.42	0.00	81.45	0.01	114.87
29-09-99	11.99	7.27	10.58	2.70	32.54
30-03-00	32.69	0.00	73.73	0.27	106.68

28-09-00	11.78	5.44	9.58	2.07	28.87
30-03-01	31.80	0.00	66.85	0.36	99.01
28-09-01	10.88	4.22	8.69	1.04	24.83
30-03-02	35.43	0.00	80.52	0.81	116.75
28-09-02	13.44	3.57	10.46	1.89	29.37
30-03-03	30.89	0.05	57.32	1.52	89.79
28-09-03	10.84	5.23	7.45	1.08	24.59
SUM	515	55	871	27	1468
Time	Boundary out	River gain	Wells	Storage out	Total out
01-04-93	6.60	86.42	4.13	0.00	97.15
30-09-93	4.01	19.03	10.59	0.04	33.67
01-04-94	7.47	93.06	2.73	1.86	105.11
30-09-94	4.59	11.87	12.59	1.41	30.46
01-04-95	8.06	105.17	3.62	3.37	120.22
30-09-95	5.40	20.87	5.49	1.13	32.89
31-03-96	7.54	105.08	3.75	2.21	118.57
29-09-96	5.02	21.47	5.98	0.28	32.75
31-03-97	5.68	76.74	4.24	0.28	86.95
29-09-97	6.12	9.32	10.69	0.16	26.29
31-03-98	6.46	79.34	4.24	1.25	91.28
29-09-98	5.19	9.65	10.69	0.04	25.58
31-03-99	8.01	99.28	4.28	3.30	114.87
29-09-99	5.86	11.67	14.76	0.25	32.54
30-03-00	7.96	92.21	4.38	2.13	106.68
28-09-00	5.18	11.92	11.49	0.27	28.87
30-03-01	6.98	86.83	3.95	1.25	99.01
28-09-01	5.69	11.40	6.73	1.01	24.83
30-03-02	7.82	102.57	4.00	2.35	116.75
28-09-02	5.74	15.58	6.94	1.11	29.37
30-03-03	6.05	79.33	4.00	0.40	89.79
28-09-03	6.06	11.29	6.94	0.31	24.59
SUM	138	1160	146	24	1468

To summarize the flow budget from the redeveloped regional model, the groundwater received 48MCM/year (35%) from the boundary, 8MCM/year (5.5%) from the river, 79MCM/year (58%) from the land recharge of the total inflow in drought year (1994). River received from the aquifer is 105MCM/year (77%), wells

abstraction is 15MCM/year (11%) and the boundary out is 12MCM/year (9%) of the total outflow.

In a wet year, the boundary inflow is 52MCM/year (34%), river loss is 3MCM/year (2%) and land recharge is 94MCM/year (61%) of the total inflow. Boundary out is 13MCM/year (9%), river gain is 126MCM/year (82%) and wells abstraction is 9MCM/year (6%) of the total inflow.

It means that, the boundary inflow is the main factor to recharge the aquifer in a drought year and land recharge is the main factor to fill the water into the aquifer in a wet year.

III.2 Local groundwater model development

The local groundwater model was developed with small gird size 2sq.km by using the boundary, and hydraulic parameters from the redeveloped regional model. The model was calibrated both a steady state and a transient state. The calibration process and results were explained and discussed in section 5.3.5.

III.2.1 Steady-state calibration results

ID	Observed	Computed	ID	Observed	Computed	ID	Observed	Computed
PCP-01	42	42.302	PCP-13	32	31.917	PCP-26	34.67	35.097
PCP-02	39	40.673	PCP-15	35.5	36.038	PCP-27	33.76	34.22
PCP-03	39	39.615	PCP-16	37	36.042	PCP-28	32.46	33.384
PCP-04	39	38.2	PCP-17	34.79	34.055	PCP-29	32.1	33.019
PCP-05	35.07	35.356	PCP-18	33	32.968	PCP-30	32.42	33.047
PCP-06	37	37.923	PCP-19	32.83	33.219	PCP-31	31.47	31.81
PCP-08	37.05	36.89	PCP-20	36.18	35.388	PCP-32	31.19	31.622
PCP-09	37	37.638	PCP-22	35	33.914	PCP-33	31.22	31.488
PCP-10	35.07	34.923	PCP-23	33	33.693	PCP-34	31.4	31.401
PCP-11	33.13	32.394	PCP-24	35.43	35.307			
PCP-12	34.84	34.347	PCP-25	34.33	34.972			

III.2.2 Transient state calibration results

ID	Observed	Computed	ID	Observed	Computed	ID	Observed	Computed
PCP-01	43.968	42.3017	PCP-13	38.187	31.91664	PCP-27	32.761	34.21995
PCP-02	38.92	40.673	PCP-15	38.89	36.03806	PCP-28	33.455	33.38411
PCP-03	39.201	39.61501	PCP-16	39.587	36.04189	PCP-29	32.098	33.01874
PCP-04	37.7	38.19959	PCP-17	34.791	34.05544	PCP-30	32.421	33.04683
PCP-05	34.071	35.35586	PCP-18	36.55	32.96815	PCP-31	31.466	31.81049

PCP-06	37.879	37.92302	PCP-19	32.828	33.21879	PCP-32	31.194	31.62209
PCP-08	38.05	36.88952	PCP-20	36.175	35.38776	PCP-33	31.222	31.48812
PCP-09	33.692	37.63759	PCP-22	35.77	33.91354	PCP 34	31.396	31.40135
PCP-10	35.074	34.9228	PCP-23	33.694	33.69334	PCP-33	31.22	31.488
PCP-11	33.133	32.39366	PCP-25	34.329	34.97246	PCP-34	31.4	31.401
PCP-12	34.836	34.34749						

III.2.3 Groundwater flow budget

BC in (wet season)	April	May	June	July	August	September
1993	5984717	5984717	5984717	5984717	5984717	5984717
1994	6370254	5836799	5787985	5778882	5776790	5776263
1995	7337199	6457733	6373084	6356827	6352982	6351989
1996	7152399	6549629	6503124	6495948	6494515	6494187
1997	5457776	5426091	5427398	5428126	5428349	5428414
1998	5750055	5443628	5418368	5413692	5412608	5412338
1999	7728405	6963950	6895804	6882850	6879787	6878994
2000	7307004	6722602	6672065	6662755	6660629	6660099
2001	6661539	6304194	6276118	6271201	6270102	6269828
2002	7536722	6916237	6868041	6860117	6858429	6858020
2003	6101566	6055073	6057067	6058225	6058572	6058667
BC in (dry season)	October	November	December	January	February	March
1993	2676474	3146910	3190191	3199099	3201241	3201791
1994	2432352	2857535	2867840	2870244	2870932	2871143
1995	2384265	3203486	3217903	3220458	3221190	3221422
1996	2199870	2990737	3024297	3031642	3033523	3034038
1997	2088280	2337032	2357592	2361600	2362554	2362802
1998	2566764	2931189	2953715	2958105	2959128	2959388
1999	2564515	3247135	3278296	3284424	3285875	3286245
2000	2614314	3197556	3221339	3226109	3227269	3227574
2001	2096363	2381457	2386092	2386719	2386873	2386923
2002	2304532	2859669	2870758	2873111	2873750	2873939
2003	2174317	2442415	2460166			
River loss (wet season)	April	May	June	July	August	September
1993	36534.02	36534.01	36534	36533.99	36533.98	36533.96
1994	184.5627	108.4314	99.33448	97.84038	97.41338	97.2503

1995	1175.804	995.4806	963.712	957.9908	956.7459	956.4013
1996	39975.2	37440.97	37017.43	36955.52	36943.94	36940.91
1997	95832.92	99406.47	99459.22	99484.66	99497.6	99504.3
1998	104902.9	104508.5	104477.7	104473.3	104472.3	104472
1999	376746.4	370955.4	370328.3	370215.1	370181.2	370167
2000	672869	666442.7	665135.5	664854.2	664773.9	664747.1
2001	424341.8	423743.6	423355.2	423268.1	423239.8	423228
2002	338031.2	336288.7	335475.7	335337.1	335297.6	335282.7
2003	564236.8	574767.8	574760.1	574759.2	574758.3	574757.7
River loss (dry season)	October	November	December	January	February	March
1993	2001130	2027464	2033379	2035121	2035614	2035766
1994	2624471	2559926	2554533	2555422	2555986	2556205
1995	1371252	1367938	1361686	1361849	1362198	1362360
1996	1009598	1072912	1079373	1081552	1082227	1082439
1997	2652201	2666978	2675913	2678755	2679569	2679811
1998	3179085	3233851	3247268	3250805	3251737	3252003
1999	3790069	3875182	3891781	3896409	3897649	3897993
2000	3391464	3439198	3449968	3453496	3454507	3454800
2001	1993255	1908071	1899832	1899221	1899258	1899304
2002	1835789	1777369	1771839	1772231	1772589	1772733
2003	2054701	2048327	2051535			
Recharge (wet season)	April	May	June	July	August	September
1993	2091543	2091543	2091543	2091543	2091543	2091543
1994	2451714	2451714	2451714	2451714	2451714	2451714
1995	2927079	2927079	2927079	2927079	2927079	2927079
1996	2794560	2794560	2794560	2794560	2794560	2794560
1997	1916633	1916633	1916633	1916633	1916633	1916633
1998	2155619	2155619	2155619	2155619	2155619	2155619
1999	2837349	2837349	2837349	2837349	2837349	2837349
2000	2555996	2555996	2555996	2555996	2555996	2555996
2001	2317715	2317715	2317715	2317715	2317715	2317715
2002	2791406	2791406	2791406	2791406	2791406	2791406
2003	1986834	1986834	1986834	1986834	1986834	1986834
Recharge (dry season)	October	November	December	January	February	March

1993	271649.5	271649.5	271649.5	271649.5	271649.5	271649.5
1994	318389.6	318389.6	318389.6	318389.6	318389.6	318389.6
1995	393369.3	393369.3	393369.3	393369.3	393369.3	393369.3
1996	374187.7	374187.7	374187.7	374187.7	374187.7	374187.7
1997	260726.4	260726.4	260726.4	260726.4	260726.4	260726.4
1998	295685.2	295685.2	295685.2	295685.2	295685.2	295685.2
1999	394030.6	394030.6	394030.6	394030.6	394030.6	394030.6
2000	357442.2	357442.2	357442.2	357442.2	357442.2	357442.2
2001	331708.2	331708.2	331708.2	331708.2	331708.2	331708.2
2002	384152.3	384152.3	384152.3	384152.3	384152.3	384152.3
2003	260692.7	260692.7	260692.7			
Storage in (wet season)	April	May	June	July	August	September
1993	0.0	0.0	0.0	0.0	0.0	0.0
1994	7974.12	0	0.0011	0.0014	0.0027	0.0080
1995	166135.71	5728.86	103.97	0.0019	0.0022	0.0046
1996	339011.97	14051.56	605.85	13.152	0.0036	0.0088
1997	171172.71	11984.22	2165.78	524.21	131.58	33.749
1998	40162.53	130.43	0.0014	0.0040	0.022	0.038
1999	7356.60	0	0.0010	0.0015	0.0028	0.0073
2000	38480.42	0.2935	0.0010	0.0013	0.0027	0.008
2001	73032.41	460.20	0.0010	0.00157	0.0057	0.0135
2002	194093.46	2270.28	3.0722	0.00157	0.00240	0.00864
2003	309196.59	20185.37	3920.09	954.819	240.208	61.205
Storage in (dry season)	October	November	December	January	February	March
1993	710611.3	89237.67	20392.81	5021.714	1265.861	321.658
1994	654166.6	26975.06	6149.842	1699.021	498.086	147.6079
1995	1154996	33816.32	6870.054	1937.763	593.2468	187.7449
1996	1103599	70520.02	17527.14	4703.55	1282.255	351.1466
1997	361025.1	40820.6	9212.195	2226.459	543.3404	133.1104
1998	503887	46618.16	10029.43	2286.37	526.0212	121.5216
1999	935744.1	63236.07	14192.31	3433.499	842.8975	207.8604
2000	784529.7	47785.93	11050.61	2771.377	702.5268	178.675
2001	415639	13603.86	1733.676	340.264	87.61163	24.98652
2002	788446.8	26612.23	5892.666	1610.196	469.5085	138.6545
2003	379067	34726.68	7833.636			

Total in (wet season)	April	May	June	July	August	September
1993	8112793	8112793	8112793	8112793	8112793	8112793
1994	8830127	8288621	8239799	8230694	8228602	8228074
1995	10431589	9391535	9301230	9284864	9281017	9280024
1996	10325946	9395681	9335307	9327476	9326018	9325687
1997	7641414	7454114	7445656	7444768	7444611	7444585
1998	8050740	7703886	7678465	7673784	7672700	7672429
1999	10949856	10172254	10103480	10090414	10087317	10086509
2000	10574349	9945040	9893196	9883605	9881399	9880842
2001	9476628	9046112	9017188	9012184	9011057	9010771
2002	10860253	10046201	9994926	9986860	9985132	9984708
2003	8961833	8636859	8622581	8620773	8620404	8620320
Total in (dry season)	October	November	December	January	February	March
1993	5659865	5535261	5515612	5510891	5509771	5509529
1994	6029380	5762826	5746913	5745755	5745806	5745885
1995	5303882	4998609	4979828	4977614	4977350	4977339
1996	4687255	4508357	4495386	4492086	4491220	4491016
1997	5362232	5305557	5303444	5303308	5303393	5303472
1998	6545421	6507343	6506698	6506882	6507077	6507198
1999	7684358	7579583	7578299	7578297	7578398	7578476
2000	7147749	7041982	7039800	7039818	7039921	7039995
2001	4836966	4634840	4619366	4617989	4617926	4617961
2002	5312920	5047802	5032642	5031104	5030960	5030963
2003	4868778	4786161	4780227			
Boundary out (wet season)	April	May	June	July	August	September
1993	304685.8	304685.8	304685.8	304685.8	304685.8	304685.8
1994	341254	349687.7	350520.3	350700	350745.2	350757.2
1995	369661.9	380133.4	381300.8	381572.5	381639	381656.9
1996	365906.7	373092.3	373618.5	373694.1	373709.6	373713.5
1997	292527.6	292592.1	292495.4	292471.7	292466	292464.5
1998	299248.1	303036.5	303489.4	303602.2	303630.6	303637.6
1999	340060.2	348146.2	349260.1	349545.7	349628.6	349650.3
2000	328953.3	335524.4	336152.1	336303.4	336344.8	336356.4
2001	315383.5	319758.8	320083.5	320162.8	320182.7	320188.1

2002	358137.2	365226.1	365744.5	365838.7	365861	365867.2
2003	295062.4	295239.4	295081.2	295043.7	295035.5	295033.5
Boundary out (dry season)	October	November	December	January	February	March
1993	271364.1	230568.5	229708.7	229538.2	229494.7	229481.3
1994	334642.1	281905.7	281770.3	281716.7	281694.5	281685.5
1995	224836.7	158578.5	158975.6	158993.1	158980.6	158973.9
1996	248803.2	171915	171176.4	171011.4	170962.4	170946.9
1997	272159	256003.3	255015.5	254802.1	254743.5	254725.3
1998	181922.1	159233.9	158062.6	157824.7	157769.1	157753.9
1999	304364.4	246388.1	245406.2	245214.4	245162.8	245147.7
2000	209644.6	167192.2	166358.6	166175.3	166126.5	166112.1
2001	200654.6	183952.8	184329.4	184368.8	184367.6	184364.5
2002	222892.3	169246.7	169388.5	169368	169352.3	169345.6
2003	283858.2	269435.4	268796.2			
River gain (wet season)	April	May	June	July	August	September
1993	4441032	4441032	4441032	4441032	4441032	4441032
1994	4898606	4974202	4994852	5000282	5001757	5002162
1995	5423802	5443979	5472016	5480871	5483416	5484146
1996	5606650	5462023	5465625	5468027	5468757	5468967
1997	3827540	3735383	3730245	3729332	3729113	3729051
1998	3834151	3847443	3857593	3860507	3861293	3861499
1999	3959259	4066071	4096056	4104173	4106382	4106998
2000	3656038	3703647	3722817	3728010	3729406	3729785
2001	3702962	3696547	3705771	3708467	3709203	3709407
2002	4781704	4719900	4732071	4735758	4736786	4737077
2003	3682927	3516325	3508125	3506687	3506366	3506287
River gain (dry season)	October	November	December	January	February	March
1993	803121.1	729917.4	711073.5	706297.7	705058.1	704733.9
1994	227431.9	230226.8	230578.5	230592.9	230586.5	230582.7
1995	547163	575241.6	579547	579540.9	579374	579301.3
1996	672074.2	656909.9	647159.1	643840.7	642874.8	642599.4
1997	260974.5	259031	257773.1	257475	257405	257386.8
1998	232901.2	231271.1	231028.8	230966.9	230947.2	230939.9
1999	276090.4	271183.3	270774.6	270665	270633	270622.9

2000	215052	215145	214910.2	214838.4	214815	214807.3
2001	221832.4	232687	234861.8	235042.4	235042.8	235036.5
2002	302112.6	300767.6	301796.1	301571.3	301446.9	301403
2003	320414.8	324300.6	321250			
Wells (wet season)	April	May	June	July	August	September
1993	2843879	2843879	2843879	2843879	2843879	2843879
1994	2321152	2321152	2321152	2321152	2321152	2321152
1995	2794897	2794897	2794897	2794897	2794897	2794897
1996	2883219	2883219	2883219	2883219	2883219	2883219
1997	2916990	2916990	2916990	2916990	2916990	2916990
1998	2959503	2959503	2959503	2959503	2959503	2959503
1999	5044730	5044730	5044730	5044730	5044730	5044730
2000	5222998	5222998	5222998	5222998	5222998	5222998
2001	4416374	4416374	4416374	4416374	4416374	4416374
2002	4274245	4274245	4274245	4274245	4274245	4274245
2003	4270751	4270751	4270751	4270751	4270751	4270751
Wells (dry season)	October	November	December	January	February	March
1993	4181808	4181808	4181808	4181808	4181808	4181808
1994	4751913	4751913	4751913	4751913	4751913	4751913
1995	3684332	3684332	3684332	3684332	3684332	3684332
1996	3163293	3163293	3163293	3163293	3163293	3163293
1997	4350962	4350962	4350962	4350962	4350962	4350962
1998	5718665	5718665	5718665	5718665	5718665	5718665
1999	6598581	6598581	6598581	6598581	6598581	6598581
2000	6186234	6186234	6186234	6186234	6186234	6186234
2001	3652420	3652420	3652420	3652420	3652420	3652420
2002	4003746	4003746	4003746	4003746	4003746	4003746
2003	3682723	3682723	3682723			
Storage out (wet season)	April	May	June	July	August	September
1993	0	0	0	0	0	0
1994	718905.4	90290.54	19532.41	4800.359	1237.547	327.3904
1995	1230473	154978.4	34486.86	8826.982	2372.644	653.0272
1996	872568.5	78224.23	13288.22	2912.29	717.3027	185.4245
1997	98664.03	3570.756	90.68267	4.90345	0.123081	0.015392

1998	412678	46874.15	10424.77	2610.349	674.8679	176.0648
1999	1026272	129416.1	28840.49	7295.656	1932.373	521.1517
2000	778336.5	91882.97	19790.77	4835.699	1234.665	321.2319
2001	478713.9	48888.16	10229.52	2473.661	626.7343	161.5207
2002	840899.7	79724.84	15454.86	3634.592	913.8092	234.979
2003	163029.3	6124.591	324.3726	30.33139	2.735224	0.219612
Storage out (dry season)	October	November	December	January	February	March
1993	8108.554	0	0.0002	0.0002	0.000229	0.000286
1994	234264	18326.87	1540.971	95.56523	1.338415	0.002117
1995	289796.6	26796.36	2740.524	239.54	10.12353	0.0632
1996	84895.93	2666.028	35.41855	0.000286	0.000286	0.000629
1997	39429.2	485.2624	5.590224	0.000172	0.0002	0.000429
1998	13491.25	0	0.000114	0.000114	0.000114	0.000372
1999	38528.79	214.2278	0.000172	0.000172	0.0002	0.000401
2000	62387.57	1521.216	17.99044	0.000172	0.000172	0.000601
2001	217291.6	20546.58	2013.583	191.4051	15.70365	0.572691
2002	226380.7	18238.5	1569.435	103.1007	2.185678	0.002489
2003	74402.86	2598.85	69.5234			
Total out (wet season)	April	May	June	July	August	September
1993	7589596	7589596	7589596	7589596	7589596	7589596
1994	8279917	7735332	7686056	7676934	7674891	7674399
1995	9818834	8773988	8682701	8666167	8662325	8661353
1996	9728345	8796559	8735751	8727852	8726404	8726085
1997	7135722	6948536	6939822	6938799	6938570	6938506
1998	7505579	7156856	7131010	7126222	7125101	7124815
1999	10370321	9588364	9518887	9505745	9502673	9501900
2000	9986326	9354052	9301758	9292147	9289984	9289461
2001	8913434	8481568	8452459	8447478	8446387	8446131
2002	10254986	9439097	9387516	9379476	9377806	9377424
2003	8411769	8088440	8074282	8072511	8072155	8072071
Total out (dry season)	October	November	December	January	February	March
1993	5264402	5142294	5122591	5117644	5116361	5116024
1994	5548251	5282372	5265802	5264318	5264195	5264181
1995	4746128	4444948	4425595	4423105	4422697	4422607

1996	4169066	3994783	3981663	3978145	3977130	3976839
1997	4923525	4866482	4863757	4863239	4863111	4863074
1998	6146979	6109170	6107756	6107456	6107381	6107358
1999	7217565	7116367	7114762	7114460	7114377	7114352
2000	6673318	6570092	6567520	6567247	6567175	6567153
2001	4292198	4089606	4073625	4072022	4071846	4071821
2002	4755131	4491999	4476500	4474788	4474547	4474494
2003	4361399	4279058	4272839			

III.2.4 River loss and gain

To understand the aquifer-river interaction, river loss and gain from upstream to downstream flow was studied along the Nan River (3 stations) and Yom River (2 stations). The river water level for the study period was collected from the Royal Irrigation Department (RID). The river hydraulic conductance is calculated using equation 13 with the width 100m. The calibrated values are shown in Table III. 4.

Table III. 4 River loss and gain by location

Nan river	Upstream	Midstream	Downstream
Loss	1243.2	1276.289	2200.532
Gain	-3628.59	-373.071	-708.617
Net	-2385.39	903.2187	1491.916
Yom River	Upstream	Midstream	Downstream
Loss	-	1058.063	785.2401
Gain	-	-160.2	-76.4511
Net	-	897.8625	708.7891

Table III.5 The location of the drawdown hotspot represent by water year from above

Location	North	East	X	Y
Dry year (1993)	16°46′46.85″	100°12′59.17″	629640	1855580
Drought year (1994)	16°48′0.64″	100°14′5.17″	631580	1857860
Normal year (1997)	16°48′0.57″	100°14′16.99″	631930	1857860
Wet year (2003)	16°45′17.54″	100°12′31.58″	628840	1852830

APPENDIX IV

SOIL MOISTURE MEASUREMENT VIA SENSOR

There are three main factors which impact groundwater system on the Phitsanulok Province, Thailand (local area): land recharge from precipitation, leakage from river and groundwater pumping (Koontanakulvong and Panot (2003)), i.e. water passed through soil performs under infiltration and percolation. In this study, the soil moisture sensor was adapted from low-cost soil moisture profile probe (Kojima et al. (2016)) to estimate the deep percolation characteristic in the unsaturated zone for developing local groundwater model.

IV.1 Work Content of Soil Moisture Sensor Installation

At the Rice Water Use Experimental Station 2 of Royal Irrigation Department at Amphoe Phrom Phiram in the North-western part of Phitsanulok Province, Upper Central Plain, Thailand, automated profile soil moisture measurements at an hourly time step are collected from the soil surface from 1m to 4m depth with a TDR system. Also, the circuit of resistance soil moisture sensors have been placed from 1m to 5 m depths to measure profile soil moisture. The soil moisture sensor for field percolation analysis can be used to detect moisture, when the soil is wet. The follows are the detail of field measurement of soil moisture sensor for percolation analysis.

IV.2 Soil physical parameters

Drilled bore holes from different soil group until the depth higher 1 m than the top of first aquifer (5m) and collected the soil sample (Figure IV.1). Soil cores samples were used for laboratory analysis of soil hydraulic characteristics. Soil texture, water retention and saturated soil hydraulic conductivity were measured. The laboratory analysis was further expanded to include near-saturated hydraulic properties estimated using both inverse approaches based on the collected data on water content. Then, PVC pipe was inserted into the bore hole to protect borehole collapsed.

Figure IV.1 Collected soil sample

IV.3 Hardware design

Arduino is a microcontroller for making computers that can sense and control different devices (Figure IV.2). It is an open source platform based on an ATmega328 microcontroller board, and a development environment for writing software for the board. Arduino projects are stand-alone, and they can be operated on displaying devices with software. The preassembled devices are available or they can be assembled as per our need. The Arduino programming language is working done on wires, a similar physical computing platform, which is based on the Processing multimedia programming environment. The hardware consists of a simple open hardware design for the Arduino board with an onboard input/output support. The software consists of a standard programming language compiler and the boot loader that runs on the Arduino board.
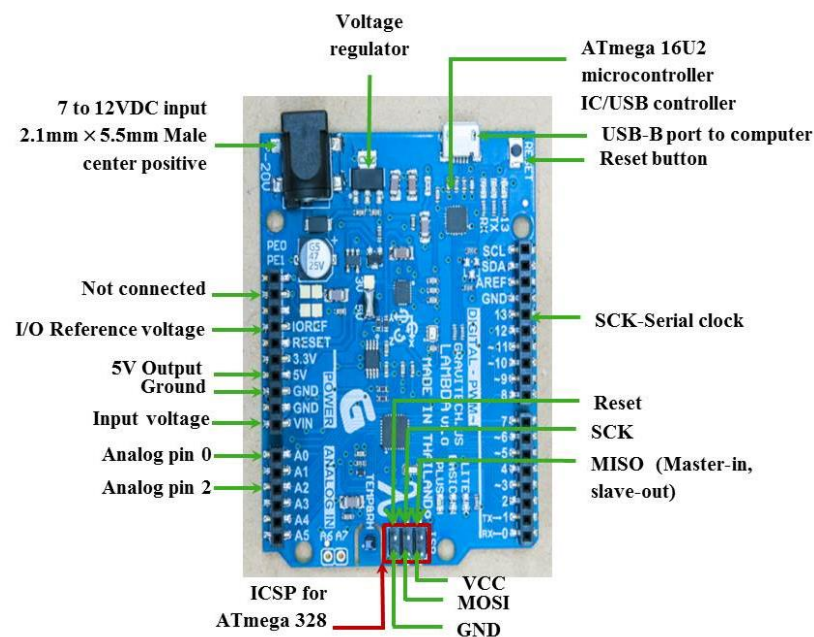
Figure IV.2 Arduino Board

IV.4 Soil moisture sensor module

The soil moisture sensor module can be used to detect the moisture of the soil if there is water around the sensor. Connected this module with sensor and insert module into the soil and then adjust the on-board potentiometer to adjust the sensitivity. The sensor would outputs resistance of soil which could convert to soil moisture. The soil moisture module is shown in Figure IV.3.
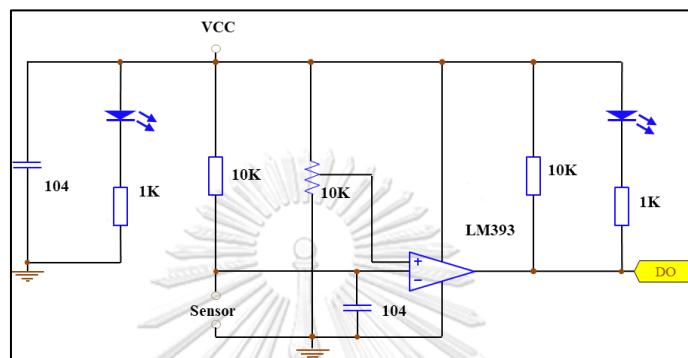
Figure IV.3 Schematic of soil moisture module

IV.5 Soil moisture sensor design and monitoring

There are two probes in the soil moisture sensor and there is circuitry inside the sensor for measuring the resistance and converting it into voltage as output. The circuit includes Arduino board, soil moisture module, and soil moisture sensor (made from copper plate) as shown in

Figure IV.4.
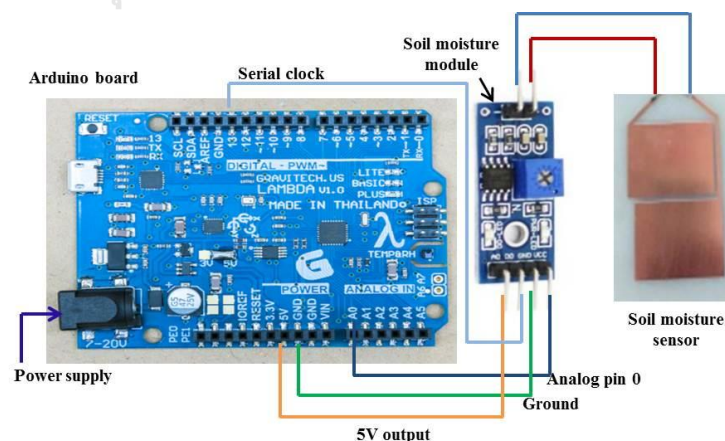
Figure IV.4 The schematic of digital measurement soil moisture by developed sensor

The soil moisture sensors (copper plate) with wire are attached in aluminium bar at 1m, 2m, 3m, and 4m. Then after insert the bar to the soil, put the soil back into the

bore hole to connect the soil with water, the wire will be connecting with soil moisture module and Arduino board as shown in Figure IV.5.

Figure IV.5 The process of soil moisture sensor installation

IV.6 Soil moisture construction and design

To set up the soil moisture sensors in the field, two boreholes with 4 inches diameter and 4 meters deep were drilled, i.e., one borehole is to monitor the groundwater level of shallow aquifer and another borehole is to put the sensor equipment. Open screened PVC pipe at each 1 m depth was inserted into the second borehole. Then soil moisture sensors were developed and attached at 1 m interval. The field investigation and monitoring method of soil moisture sensor for land recharge analysis is shown in Figure IV.6.
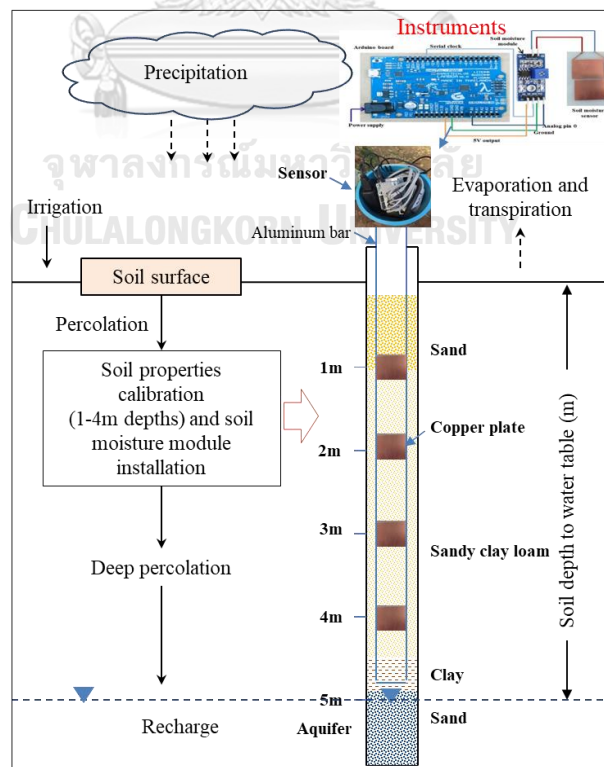
Figure IV.6 Field investigations and monitoring method for land recharge analysis

IV.7 Soil moisture sensor setup

The Hydrus-1D atmospheric boundary condition (Eq. (7)) used the required daily rainfall, irrigation water, evaporation, and shallow groundwater levels were all measured during the experiment. The daily potential transpiration used the estimate from field data of the Rice Water Use Experimental Station. Rainfall was measured at the location within 500 m of the experimental site. The Hydrus-1D atmospheric boundary condition at the soil surface is defined by effective infiltration value (equal to rainfall-evaporation +irrigation). A minimum allowed pressure head of 0 cm was specified. Measured soil moisture at day one at soil depths of 1.0, 2.0, 3.0, 4.0 m were used as initial conditions. Soil hydraulic properties were represented using the soil water retention and hydraulic conductivity functions of (Mualem (1976)) and (Genuchten (1980)). Soil moisture for observation nodes demonstrating soil depths were output at the end of each day to be compared with observed data. Furthermore, outflow at the bottom of the modelling domain was cumulated over the same time intervals as deep percolation data. Deep percolation is implemented as functional relation that relates bottom recharge to the position of the groundwater in the soil profile. The percolation rate assigned to bottom node (n) is determined by the program as equal to difference of soil moistures at each soil depth multiplied with unsaturated hydraulic conductivity at that time step.

IV.8 Soil moisture data convert from electrical resistance

From the measured data, the relationship of water content and the electrical resistance were converted to get the actual soil moisture data. In this study, the soil moisture is converted from electrical resistance which was measured by modifying soil moisture sensor. The calibrated curves of resistance and soil moisture via the gravimetric method were developed from each soil type and at each soil depth. Figure IV.7 shows the relationship between volumetric water content and electrical resistance for each soil depth. If resistance is less than 200, the soil almost wet (40%) in each depth.
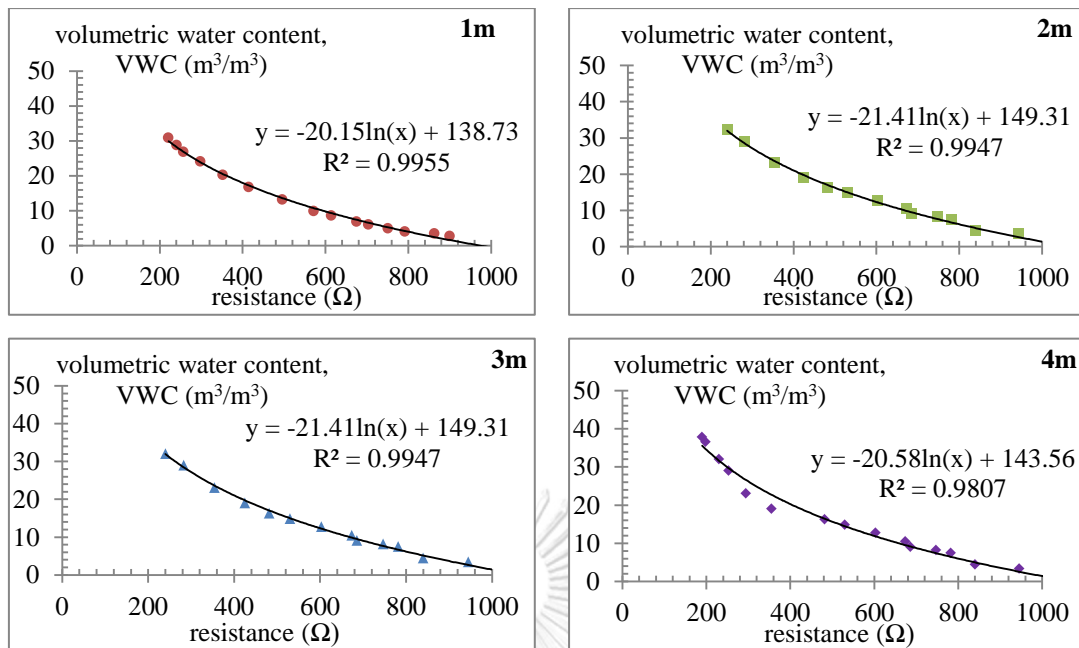
Figure IV.7 Relationship between volumetric water content and electrical resistance at 1-4 m depth

IV.9 Soil moisture data analysis

The daily measured soil moisture data in the field (at 1-4m depths) are shown in Figure IV.8. The soil sample in the field was taken and was classified as well-drained sandy clay loam. The shallow groundwater table was constant at 5 meter from the ground surface during the study period (rainy season). The calibrated soil moisture data analysis will be used in Hydrus simulation to estimate deep percolation in next appendix.
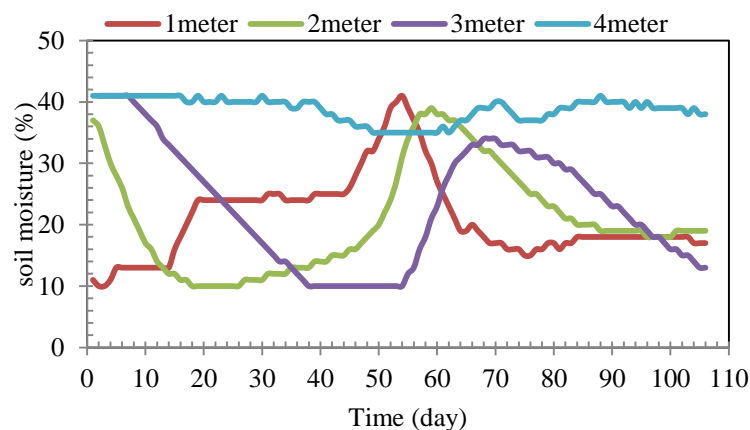
Figure IV.8 Observed soil moisture data at 1-4m depth

APPENDIX V

DEEP PERCOLATION ESTIMATION VIA HYDRUS SOFTWATER APPLICATION

Deep percolation from irrigation water is a key role in irrigation demand and groundwater supply by replenishing shallow aquifers at the local and regional scales. To estimate the deep percolation characteristics (land recharge rate), the HYDRUS-1D atmospheric boundary condition was constructed with the required daily (108days) rainfall, irrigation water, evaporation and shallow groundwater level (Figure V.1) that were all measured during the experiment.
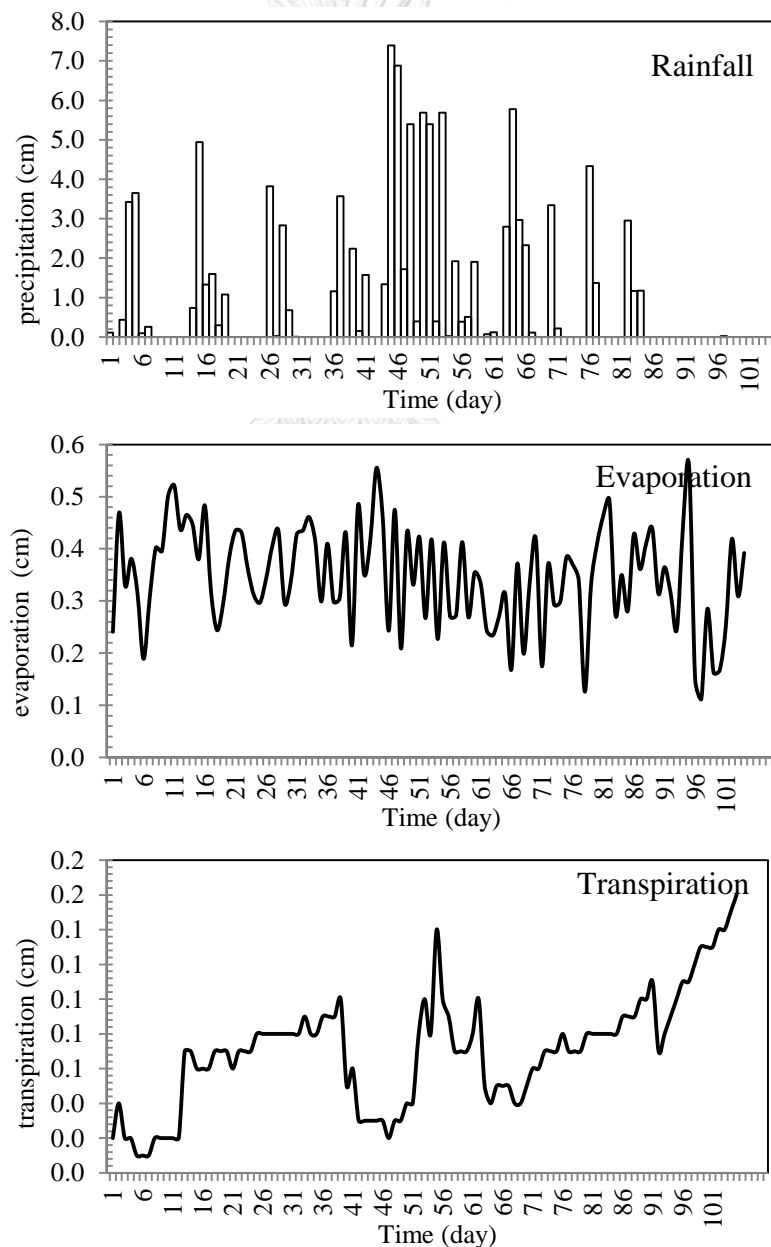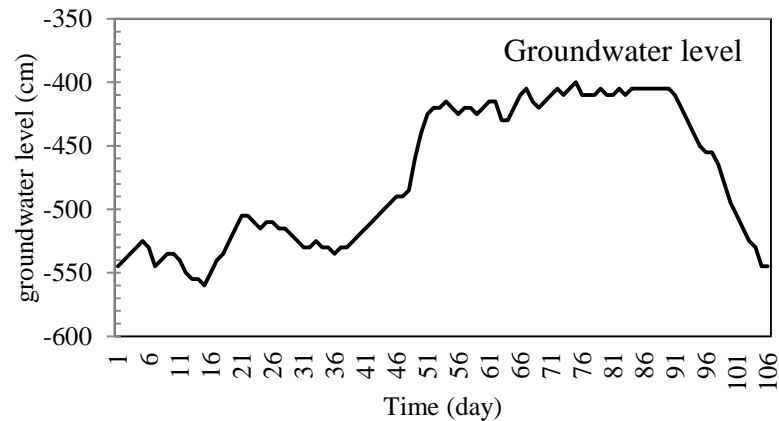
Figure V.1 Input data to estimate deep percolation rate during study period

V.1 Sensitivity curve analysis

The initial estimates of the optimized soil hydraulic parameters were specified to check appropriate checkboxes and provide parameter limitations for the optimization. Soil hydraulic parameters were optimized for the analytical functions of Genuchten (1980) for two materials (Sandy clay loam and Sandy clay) according to (Rawls et al. (1982), Carsel and Parrish (1988), Schaap et al. (2001)) and present study. Table V.1 shows parameter value used in each type. Figure V.2 and Table V.2 shows the error summary of the sensitivity of the soil parameter for each depth based on the less error.

Table V.1 Calibrated parameter value used in each type

Rawls et al 1982 (R)					
Materials	θ_r	θ_s	α	n	K_s
Sandy Clay Loam (0m)	0.07	0.33	0.04	1.25	10.3
Sandy Clay Loam (1m)	0.10	0.41	0.02	4.2	6
Sandy Clay Loam (2m)	0.10	0.41	0.12	3.9	7
Sandy Clay Loam (3m)	0.10	0.41	0.04	3.6	5
Sandy Clay (4m)	0.11	0.32	0.03	1.7	2.8
Sandy Clay (5m)	0.10	0.41	0.01	1.7	1.4
Carsel and Parrish 1988 (C)					
Materials	θ_r	θ_s	α	n	K_s
Sandy Clay Loam (0m)	0.10	0.40	0.06	1.60	4.00
Sandy Clay Loam (1m)	0.10	0.41	0.02	4.20	6.00

Sandy Clay Loam (2m)	0.10	0.41	0.12	3.90	7.00
Sandy Clay Loam (3m)	0.10	0.41	0.04	3.60	5.00
Sandy Clay (4m)	0.10	0.38	0.03	1.23	2.88
Sandy Clay (5m)	0.10	0.41	0.01	1.70	1.40
Schaap et al. 2001(S)					
Materials	θ_r	θ_s	α	n	K_s
Sandy Clay Loam (0m)	0.06	0.38	0.02	1.33	4.00
Sandy Clay Loam (1m)	0.08	0.41	0.02	4.20	6.00
Sandy Clay Loam (2m)	0.10	0.41	0.12	3.90	7.00
Sandy Clay Loam (3m)	0.10	0.41	0.04	3.60	5.00
Sandy Clay (4m)	0.12	0.39	0.03	1.21	11.40
Sandy Clay (5m)	0.10	0.41	0.01	1.70	1.40
Genuchten et al. 1980 (A) (Present study)					
Material	θ_r	θ_s	α	n	K_s
Sandy Clay Loam (0m)	0.1	0.4	0.18	1.6	4
Sandy Clay Loam (1m)	0.095	0.41	0.12	4.2	6
Sandy Clay Loam (2m)	0.095	0.41	0.12	3.9	7
Sandy Clay Loam (3m)	0.095	0.41	0.035	3.6	5
Sandy Clay (4m)	0.095	0.41	0.02	2.4	3
Sandy Clay (5m)	0.095	0.41	0.009	1.7	1.4
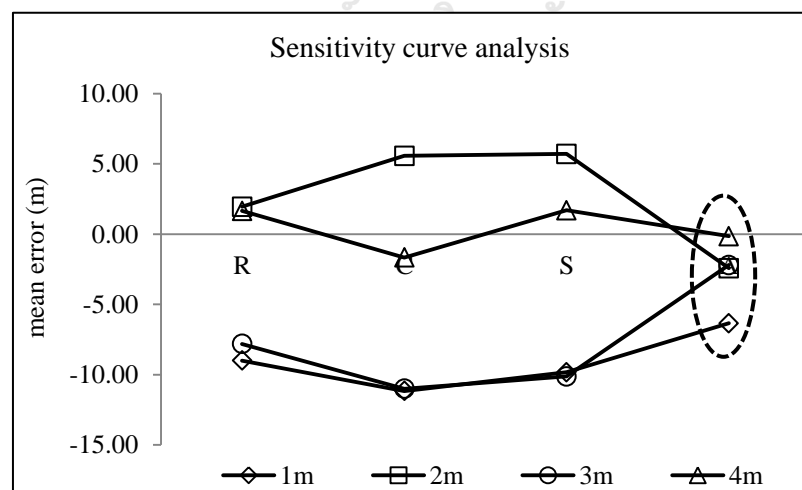
Figure V.2 Sensitivity curve analysis for each soil meter depth

(Remarks; R is (Rawls et al. (1982)), C is (Carsel and Parrish (1988)), S is (Schaap et al. (2001)) and A is present study (Genuchten (1980)))

Table V.2 Error summary of soil properties sensitivity for each depth

Soil parameter set with Mean error	1m	2m	3m	4m
R (Rawls et al., 1982)	-9.00	1.96	-7.82	1.66
C (Carsel et al. 1988)	-11.17	5.57	-11.00	-1.67
S (Schaap et al., 2001)	-9.83	5.71	-10.13	1.70
A (Genuchten et al., 1980)	-6.35	-2.43	-2.20	-0.15

V.2 Calibration and verification data

Soil water content and water fluxes were simulated for soil moisture scheme on a daily basis with Hydrus-1D for a period of 108 days. The soil receives the result of effective infiltration from their supply of water from precipitation plus irrigated water and minus evaporation. Hydrus-1D inverse module was used to improve estimate of the hydraulic parameters in terms of providing optimal descriptions of the field data. Because of the large number of parameters involved, many of them correlated, values of selected parameters were calibrated only when the differences between the calculated and field-measured water content. The simulated and observed soil moistures calibration was done for 106 days and verification was not done due to unavailability of observed data. The calibration result for 1m and 2m depths was shown in Figure V.3. The final identified parameters, which provided a close fit between simulated and measured water contents using data from four depths, are shown in Table V.3. The estimated errors of calibration at each soil depths was shown in Table V.4 with acceptable error ranges.
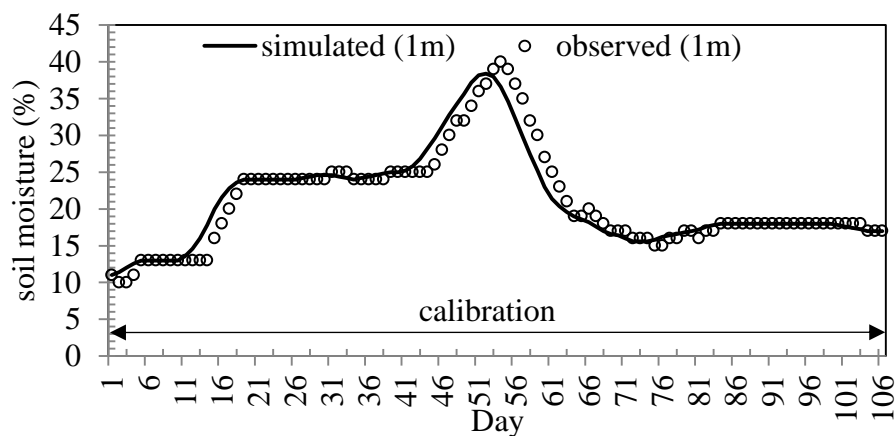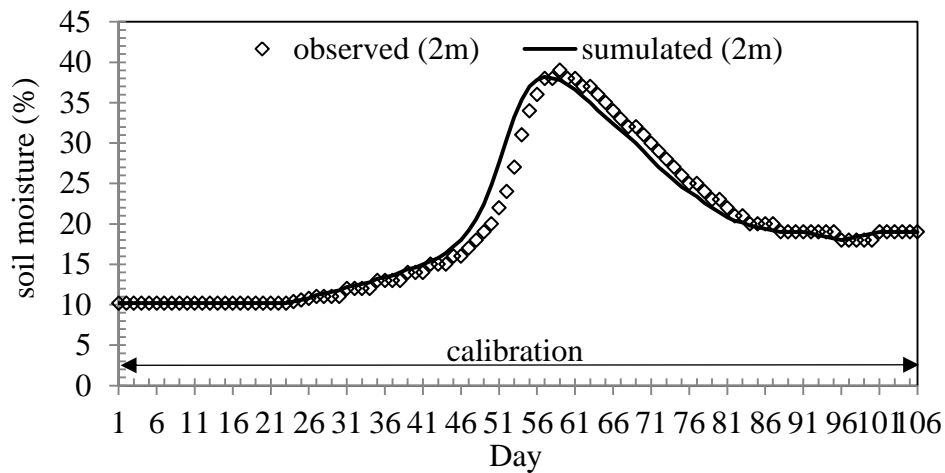
Figure V.3 Sample of simulated and observed soil moisture content calibration at 2m depth

Table V.3 Calibrated soil hydraulic parameters (Remarks: S_{cl} = sandy clay loam; S_c =sandy clay)

Materials	θ_r	θ_s	α	n	Ks	λ
S_{cl} (0m)	0.1	0.4	0.18	1.5	4	0.5
S_{cl} (1m)	0.095	0.41	0.11	4.2	8	0.5
S_{cl} (2m)	0.095	0.41	0.09	5.2	7.5	0.5
S_{cl} (3m)	0.095	0.41	0.08	5.1	5.5	0.5
S_c (4m)	0.095	0.41	0.11	3.4	3	0.5

Table V.4 Calibration error of soil water content

Error (%)	Calibration (106 days)	
	1m	2m
Maximum	14.5	9.74
Minimum	0	3.64
Mean	5.29	0
RMSE	0.85	0.82
Nash	0.59	0.62

V.3 Soil moisture patterns in each phase

The simulated soil moisture patterns at the depth of 1-4 meter are shown with accumulative effective infiltration in Figure V.4. It can be seen that soil moisture in

the deep level 3 and 4 meter were wet due to the previous rainfall (since the experiment started from the mid of rainy season) but the soil moistures at the depths of 1 and 2 meter responded well with the rainfall during the study period. Thus, in this study, the percolations at 1 and 2 meter are used to explore the soil moisture and deep percolation.
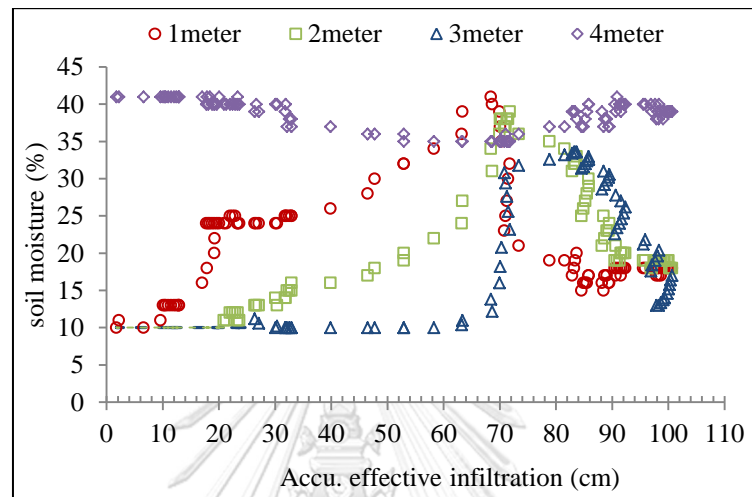
Figure V.4 Comparison of simulated soil moisture and accumulative effective infiltration at 1-4m depth

The deep percolation patterns excluded soil moisture data in the beginning stage due to the effect from the previous rainfall and the percolation rates were set to be constant as later stage as shown in dotted line in Figure V.5 and Figure V.6. The effective infiltration during the experimental period can be distributed into five stages based on soil characteristics and causes different soil moisture values. The first rainfall event causes soil moisture up to wilting point (17%) and the precipitation intensity of second event causes soil moisture up to field capacity (25%) and third event causes soil moisture to be saturated (42%). On the other hand, the moisture of soil begins to dry after less rain and the soil water content dropped to the value closed to the wiling point. Thus, wetting and drying processes of the soil moisture are controlled by infiltration, evaporation and soil characteristics which will link to the percolation characteristics in section 5.4.1.
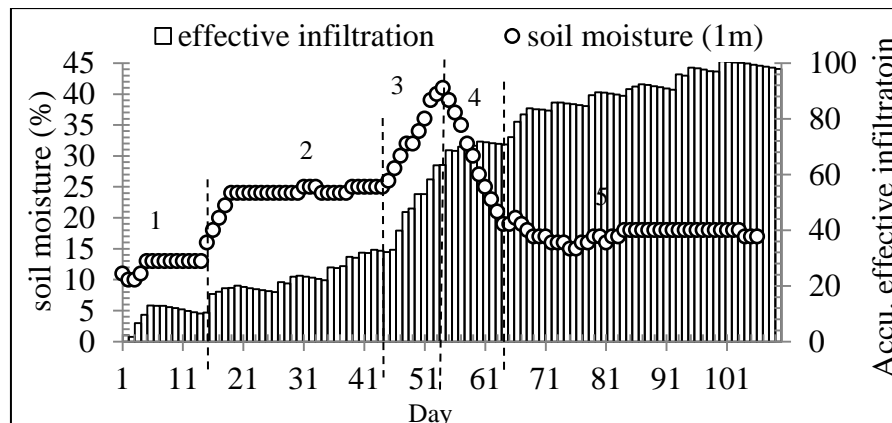
Figure V.5 Soil moisture (at 1m depth) and accumulative effective infiltration at different stages
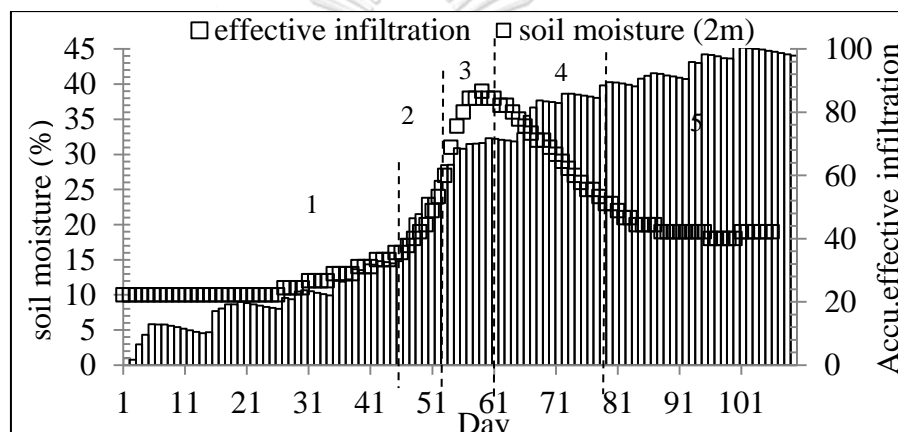
Figure V.6 Soil moisture (at 2m depth) and accumulative effective infiltration at different stages

V.4 Water balance of percolation system

The deep percolation system is derived by using the water balance analysis to check with input, output, and initial-final soil moisture content. Inputs and outputs of water with respect to paddy planting provide information regarding the irrigation events throughout the study period. Changes in deep percolation in different irrigation cycles indicated variation in deep percolation over the rainy season with wetting and drying stages of the soil. Water balance equation was used to know the percolation rate from 0-1m depth, precipitation (Pr), irrigation water (Irr) are input and evaporation (E), transpiration (T) and percolation (Pe_1) are output from the surface (0-1m depth). Then the deep percolation (DPe_1) from 1m depth was affected to 2m depth

as input data to get recharge. The equations for deep percolation system for each depth using water balance analysis are as follows;

$$Pe_1 = (Pr + Irr) - (E + T_0) \qquad (1)$$

$$DPe_2 = Pe_1 - T_1 \qquad (2)$$

Where; Pr is rainfall (cm/day), Irr is irrigation water (cm/day), E is evaporation (cm/day), T_0 is transpiration from 0-1m depth, Pe_1 is percolation rate from 0-1m depth, T_1 is transpiration and DPe_2 is the deep percolation rate from 1-2m depth.

Rainfall (107.8 cm) and irrigation (26.9 cm) of 134.7 cm are input to the deep percolation system during the study period. The total evaporation is 36.1 cm. The transpiration from 0-1m depth is 7.53 cm and the value at 1-2m depth is 19.9 cm. The percolation (land recharge rate) at 2m depth is 56.4 cm. Input-output of each component for water balance analysis of both wetting; drying processes (in bracket) are shown in Figure V.7. The ratio of total percolation and effective infiltration is 0.19 in the rainy season which is in the range with the other study (Lu et al. (2010)).
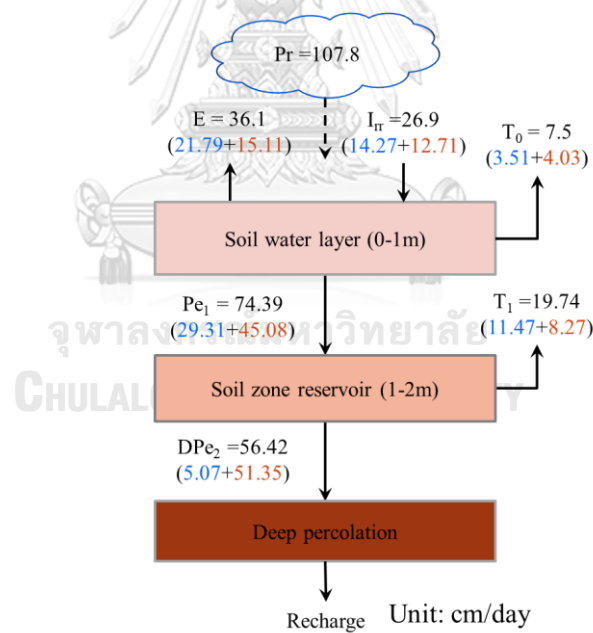
Figure V.7 Input and output components for water balance analysis during study period

Remarks: P is precipitation; E is evaporation; I_{rr} is irrigation water; T_0 is transpiration (0-1m depth); T_1 is transpiration (1-2m depth); P_1 is percolation (0-1m depth); and P_2 is percolation (1-2m depth), in bracket: wetting + drying stages

The monitoring of deep percolation from the field measurement, using the soil moisture sensor system developed, provided more understandings of deep percolation characteristics, percolation rate and overall water balance of deep percolation system in the soil. The study results provide a good basic knowledge to estimate both irrigation demand and groundwater recharge in groundwater modelling in the future.

จุฬาลงกรณ์มหาวิทยาลัย

CHULALONGKORN UNIVERSITY

APPENDIX VI

SEEPAGE METER INSTALLATION FOR RIVER CONDUCTANCE

Seepage meter was constructed in the Plaichumphol Irrigation Project area to measure the flow of surface water and groundwater along the river. The measured data were used to estimate the discharge and recharge from the river seepage. The detail seepage meter construction design and data analysis are explained as follows.

VI.1 Seepage meter instrumentation and design

The seepage meters used in this study was modified slightly from those described by Lee et al. (1978) and consisted of a pan and a collection bag (Figure VI.1). The seepage meter is made by cutting 15-cm-long, end sections from a 0.208m (55 gallon) metal drum. Pans were constructed by cutting 15cm long, top or bottom of a 55gallons cylindrical container. There are two valves in the meter. The first valve is for releasing air inside the meter and the second valve is for letting the water out.

Rubber stopper (rubber band) with a single hole drilled in the center to accept tubing and clear flexible tubing that will fit tightly into the hole in the rubber stopper. The plastic collection bag is connected with the vent tube which insert into the rubber stopper tightly. The size of the plastic collection bag depends on the rate of seepage and the period that measurements are made. A large bag is needed for longer measurement periods and location with larger rates of seepage. Install the collection bag assembly on the seepage meter with the rubber stopper fits in the vent hole that was drilled in the seepage meter.
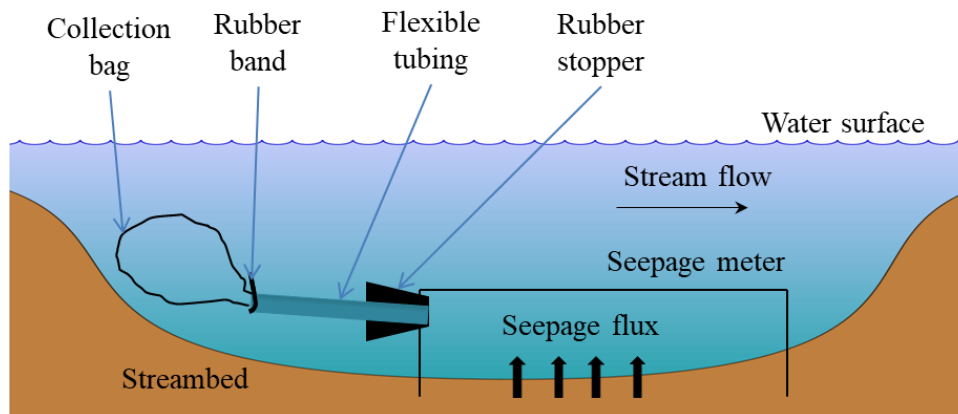
Figure VI.1 Seepage meter instrument design

VI.2 Seepage meter installation and measurement

To make a measurement, seepage meter is normally placed on the riverbed with 10cm depth. Seepage meters were installed 3m far from shore (near shore) and 6m far from shore (Far shore). Laterally, seepage meters were installed 2m each (Figure VI.2). The collection bag was weighted and then connected to the pan. The time recorded since the assembly was installed to determine the rate of flow between groundwater and surface water. After a period of time ranging from 15 to 20 min, the rubber stopper and vent tube assembly were carefully removed from the top of the seepage meter, placing a finger over the end of the tube and then the bag was removed. The water from the bag poured into the graduated cylinder and re-weighted to determine the groundwater seepage rate (i.e., difference in mass of the collection bag, divided by the time interval, pan area, and density of water) then received the final water volume which can be used with the stating water volume and the elapsed time to determine the rate of seepage. In water over 20cm depth, a single tube through the top of the seepage meter works both as a vent for any gas released from the sediment and as a connecting for the measuring bag. A known volume of water is filled into the collection bag using the graduated cylinder. The measured seepage flux data are shown as follows.
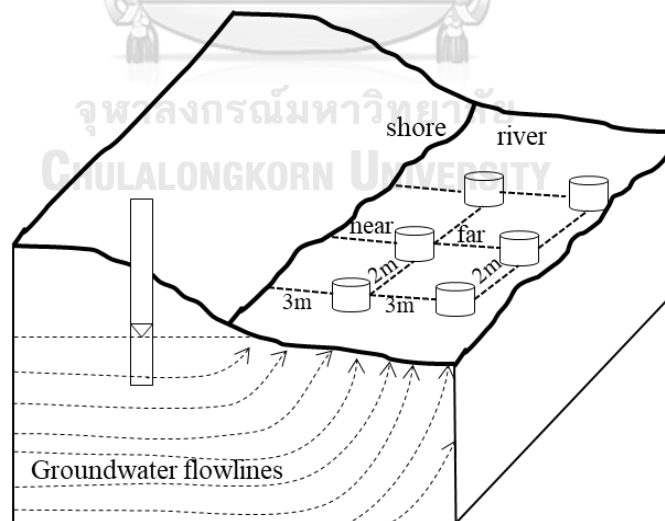
Figure VI.2 Positions of well and seepage meter for field measurememts

VI.3 Seepage flux and river conductance estimation from field measurement

The seepage rate was measured at left (L) and right (R) side of the river bank near shore. The instrument was setup 3m from the shore termed near (N), 6m far from

the shore termed far (F). The seepage meter was measured along the Nan River (up, mid, down streams) and Yom River (mid and downstream). The initial volume was measured before measured and finds the change of volume by measured time. The volumetric seepage flux was calculated by dividing the area of seepage cylinder (0.25 x π x 572 = 2,553 cm^2) gives seepage flux in length per time (m/day). The seepage data from the field measurement was converted to river hydraulic conductance to be used in groundwater modelling. The flow across riverbed is calculated by the equation (13). The head of the river water level (stage) was collected from the each river station and the required groundwater level was measured the near observed water level. The calculated river hydraulic conductance value for each location (up, mid, downstream) for both Nan and Yom river are shown as follow. The calculated river conductance is expressed in section 5.4.2.1.

Table VI.1 Hydraulic conductance calculation from the field measurement

A	B	C	D	E	F	G	H	I
Time		Measured Volume	Volume change	Volume change	Volumetric seepage rate	Seepage flux	Seepage flux	Conductance
	Station	(ml)	(ml)	(cm^3)	(m^3/min)	(m/min)	(m/day)	m/day
(min)			=C-initial	=D*0.00001	=E/A	={F/[(p/4)*(0.57^2)]}	=G*60*24	
Yom River (Midstream), initial volume (250ml)								
20	RN1	1400	1150	0.00115	0.00	2.253E-04	0.324	14.602
20	RN2	1800	1550	0.00155	0.00	3.037E-04	0.437	19.681
20	RN3	1450	1200	0.0012	0.00	2.351E-04	0.338	15.237
20	RN4	950	700	0.0007	0.00	1.372E-04	0.197	8.888
20	RF1	890	640	0.00064	0.00	1.254E-04	0.180	8.126
20	RF2	650	400	0.0004	0.00	7.838E-05	0.112	5.079
20	RF3	1300	1050	0.00105	0.00	2.057E-04	0.296	13.332
20	RF4	410	160	0.00016	0.00	3.135E-05	0.045	2.032
15	RN1	280	30	0.00003	0.00	7.838E-06	0.011	0.508
15	RN2	450	200	0.0002	0.00	5.225E-05	0.075	3.386
15	RN3	480	230	0.00023	0.00	6.009E-05	0.086	3.894
15	RN4	310	60	0.00006	0.00	1.568E-05	0.022	1.016
15	RF1	550	300	0.0003	0.00	7.838E-05	0.112	5.079
15	RF2	850	600	0.0006	0.00	1.568E-04	0.225	10.158
15	RF3	450	200	0.0002	0.00	5.225E-05	0.075	3.386
15	RF4	350	100	0.0001	0.00	2.613E-05	0.037	1.693
15	RN1	600	350	0.00035	0.00	9.144E-05	0.131	5.925

15	RN2	1330	1080	0.00108	0.00	2.822E-04	0.406	18.284
15	RN3	450	200	0.0002	0.00	5.225E-05	0.075	3.386
15	RN4	300	50	0.00005	0.00	1.306E-05	0.018	0.846
15	RF1	850	600	0.0006	0.00	1.568E-04	0.225	10.158
15	RF2	650	400	0.0004	0.00	1.045E-04	0.150	6.772
15	RF3	650	400	0.0004	0.00	1.045E-04	0.150	6.772
15	RF4	500	250	0.00025	0.00	6.531E-05	0.094	4.232
							Average	7.186
Yom River (Downstream), initial volume (200ml)								
15	LN1	750	550	0.00055	3.67E-05	0.0001437	0.206	9.311
15	LN2	600	400	0.0004	2.67E-05	0.0001045	0.150	6.7718
15	LN3	650	450	0.00045	3.00E-05	0.0001176	0.169	7.618
15	LN4	450	250	0.00025	1.67E-05	0.0000653	0.094	4.232
15	LF1	400	200	0.0002	1.33E-05	0.0000523	0.075	3.385
15	LF2	750	550	0.00055	3.67E-05	0.0001437	0.206	9.311
15	LF3	400	200	0.0002	1.33E-05	0.0000523	0.075	3.385
15	LF4	780	580	0.00058	3.87E-05	0.0001515	0.218	9.819
15	LN1	350	150	0.00015	1.00E-05	0.0000392	0.056	2.539
15	LN2	950	750	0.00075	5.00E-05	0.0001959	0.282	12.691
15	LN3	800	600	0.0006	4.00E-05	0.0001568	0.225	10.157
15	LN4	400	200	0.0002	1.33E-05	0.0000523	0.075	3.389
15	LF1	250	50	0.00005	3.33E-06	0.0000131	0.018	0.845
15	LF2	250	50	0.00005	3.33E-06	0.0000131	0.018	0.845
15	LF3	500	300	0.0003	2.00E-05	0.0000784	0.112	5.078
15	LF4	950	750	0.00075	5.00E-05	0.0001959	0.282	12.691
15	LN1	450	250	0.00025	1.67E-05	0.0000653	0.094	4.232
15	LN2	570	370	0.00037	2.47E-05	0.0000967	0.139	6.263
15	LN3	700	500	0.0005	3.33E-05	0.0001306	0.188	8.464
15	LN4	500	300	0.0003	2.00E-05	0.0000784	0.112	5.078
15	LF1	900	700	0.0007	4.67E-05	0.0001829	0.263	11.857
15	LF2	600	400	0.0004	2.67E-05	0.0001045	0.150	6.771
15	LF3	650	450	0.00045	3.00E-05	0.0001176	0.169	7.618
15	LF4	450	250	0.00025	1.67E-05	0.0000653	0.094	4.232
15	LN3	420	220	0.00022	1.47E-05	0.0000575	0.082	3.724
15	LN4	450	250	0.00025	1.67E-05	0.0000653	0.094	4.232
							Average	6.329
Nan River (Upstream), initial volume (200ml)								
20	RN1	520	320	0.00032	0.000016	6.270E-05	0.090	4.063
20	RN2	1550	1350	0.00135	0.000068	2.645E-04	0.380	17.141
20	RN3	920	720	0.00072	0.000036	1.411E-04	0.203	9.141
20	RN4	400	200	0.0002	0.000010	3.919E-05	0.056	2.539
20	RF1	950	750	0.00075	0.000038	1.470E-04	0.211	9.522

20	RF2	240	40	0.00004	0.000002	7.838E-06	0.011	0.507
20	RF3	160	40	0.00004	0.000002	7.838E-06	0.011	0.507
20	RF4	230	30	0.00003	0.000002	5.878E-06	0.008	0.380
15	RN1	1120	920	0.00092	0.000061	2.404E-04	0.346	15.571
15	RN2	450	250	0.00025	0.000017	6.531E-05	0.094	4.234
15	RN3	1500	1300	0.0013	0.000087	3.396E-04	0.489	22.004
15	RN4	450	250	0.00025	0.000017	6.531E-05	0.094	4.232
15	RF1	850	650	0.00065	0.000043	1.698E-04	0.244	11.004
15	RF2	220	20	0.00002	0.000001	5.225E-06	0.007	0.338
15	RF3	270	70	0.00007	0.000005	1.829E-05	0.026	1.185
15	RF4	500	300	0.0003	0.000020	7.838E-05	0.112	5.078
15	RN1	1350	1150	0.00115	0.000077	3.004E-04	0.432	19.468
15	RN2	350	150	0.00015	0.000010	3.919E-05	0.056	2.539
15	RN3	1450	1250	0.00125	0.000083	3.266E-04	0.470	21.161
15	RN4	440	240	0.00024	0.000016	6.270E-05	0.090	4.063
15	RF1	350	150	0.00015	0.000010	3.919E-05	0.056	2.539
15	RF2	170	30	0.00003	0.000002	7.838E-06	0.011	0.507
15	RF3	300	100	0.0001	0.000007	2.613E-05	0.037	1.693
15	RF4	620	420	0.00042	0.000028	1.097E-04	0.158	7.110
15	RN1	500	300	0.0003	0.000020	7.838E-05	0.112	5.078
15	RN2	600	400	0.0004	0.000027	1.045E-04	0.150	6.771
15	RN4	450	250	0.00025	0.000017	6.531E-05	0.094	4.232
15	RF1	240	40	0.00004	0.000003	1.045E-05	0.015	0.677
15	RF3	350	150	0.00015	0.000010	3.919E-05	0.056	2.539
15	RF4	220	20	0.00002	0.000001	5.225E-06	0.007	0.338
							Average	5.754
				Nan River (Midstream), initial volume (200ml)				
5	RN1	350	150	0.00015	0.00003	0.0001176	0.169	7.618
5	RN2	250	50	0.00005	0.00001	0.0000392	0.056	2.539
5	RF1	425	225	0.00022	0.000045	0.0001763	0.253	11.424
5	RF2	520	320	0.00032	0.000064	0.0002508	0.361	16.253
5	RF3	250	50	0.00005	0.00001	0.0000392	0.056	2.534
5	RF4	325	125	0.00012	0.000025	0.0000980	0.141	6.348
5	RN1	450	250	0.00025	0.00005	0.0001959	0.282	12.697
5	RN2	250	50	0.00005	0.00001	0.0000392	0.056	2.539
5	RN3	150	50	0.00005	0.00001	0.0000392	0.056	2.539
5	RF1	525	325	0.00032	0.000065	0.0002547	0.366	16.506
5	RF2	450	250	0.00025	0.00005	0.0001959	0.282	12.697
5	RF3	450	250	0.00025	0.00005	0.0001959	0.282	12.697
5	RF4	350	150	0.00015	0.00003	0.0001176	0.169	7.618
5	RN1	375	175	0.00017	0.000035	0.0001372	0.197	8.888
5	RN2	350	150	0.00015	0.00003	0.0001176	0.169	7.618

5	RN3	400	200	0.0002	0.00004	0.0001568	0.225	10.157
5	RF1	400	200	0.0002	0.00004	0.0001568	0.225	10.157
5	RF2	100	100	0.0001	0.00002	0.0000784	0.112	5.078
5	RF3	400	200	0.0002	0.00004	0.0001568	0.225	10.157
5	RF4	350	150	0.00015	0.00003	0.0001176	0.169	7.618
5	RN1	380	180	0.00018	0.000036	0.0001411	0.203	9.141
5	RN2	270	70	0.00007	0.000014	0.0000549	0.079	3.555
							Average	5.521
Nan River (Downstream), initial volume (200ml)								
20	RN1	1500	1300	0.0013	0.000065	0.0002547	0.366	16.506
20	RN2	1500	1300	0.0013	0.000065	0.0002547	0.366	16.506
20	RN3	700	500	0.0005	0.000025	0.0000980	0.141	6.348
20	RN4	1300	1100	0.0011	0.000055	0.0002155	0.310	13.966
15	RN1	750	550	0.00055	0.000037	0.0001437	0.206	9.311
15	RN2	1500	1300	0.0013	0.000087	0.0003396	0.489	22.008
15	RN3	700	500	0.0005	0.000033	0.0001306	0.188	8.464
15	RN4	250	50	0.00005	0.000003	0.0000131	0.018	0.846
15	RN1	300	100	0.0001	0.000007	0.0000261	0.037	1.693
15	RN2	280	80	0.00008	0.000005	0.0000209	0.030	1.354
15	RN3	450	250	0.00025	0.000017	0.0000653	0.094	4.232
15	RN4	1150	950	0.00095	0.000063	0.0002482	0.357	16.083
							Average	4.888

จุฬาลงกรณ์มหาวิทยาลัย

CHULALONGKORN UNIVERSITY

VITA